Distribution Agreement

In presenting this thesis or dissertation as a partial fulfillment of the requirements for an advanced degree from Emory University, I hereby grant to Emory University and its agents the non-exclusive license to archive, make accessible, and display my thesis or dissertation in whole or in part in all forms of media, now or hereafter known, including display on the world wide web. I understand that I may select some access restrictions as part of the online submission of this thesis or dissertation. I retain all ownership rights to the copyright of the thesis or dissertation. I also retain the right to use in future works (such as articles or books) all or part of this thesis or dissertation.

Signature:

_____ _____

Brigid Moira O'Flaherty Date

Characterizing the Expression and Regulation of MHV68 M1 & Uncovering its Role in Pulmonary Fibrosis

By

Brigid Moira O'Flaherty

Doctor of Philosophy

Graduate Division of Biological and Biomedical Sciences

Microbiology and Molecular Genetics

_____

Samuel H. Speck, PhD

Advisor

_____

Arash Grakoui, PhD

Committee Member

_____

Brian Evavold, PhD

Committee Member

_____

Dan Kalman, PhD

Committee Member

_____

Jake Kohlmeier, PhD

Committee Member

_____

Dave Steinhauer, PhD

Committee Member

Accepted:

_____

Lisa A. Tedesco, PhD

Dean of the James T. Laney School of Graduate Studies

_____

Date

Characterizing the Expression and Regulation of MHV68 M1 & Uncovering its Role in Pulmonary Fibrosis

By

Brigid Moira O'Flaherty
B.S., Towson University, 2007

Advisor: Samuel H. Speck, PhD

An abstract of
A dissertation submitted to the Faculty of the
James T. Laney School of Graduate Studies of Emory University
in partial fulfillment of the requirements for the degree of
Doctor of Philosophy
in
Graduate Division of Biological and Biomedical Sciences
Microbiology and Molecular Genetics

2015

ABSTRACT

Characterizing the Expression and Regulation of MHV68 M1
& Uncovering its Role in Pulmonary Fibrosis

By
Brigid Moira O'Flaherty

Coevolution and adaptation to their hosts has led herpesviruses to encode numerous genes which facilitate infection and establishment of lifelong latency. The focus of this dissertation was to evaluate expression and function of MHV68 unique gene M1, which has previously been shown to play a critical role in control of viral reactivation from peritoneal exudate cells through the activation and expansion of INFγ secreting $V\beta4^+$ $CD8^+$ T cells. To gain insights into M1 function, our first aim was to identify the cellular reservoir of M1 expression *in vivo*. Here we define splenic plasma cells as the predominant source of M1 expression during MHV68 infection. We show that the MHV68 viral replication and transcription activator (Rta), which initiates viral reactivation from latency, synergistically regulates M1 expression with the cellular interferon regulatory factor 4 through protein-protein mediated interaction with the M1 promoter. Furthermore, we identify a novel Rta response element within the M1 promoter, which is conserved in several other MHV68 genes. These findings highlight a mechanism to fine-tune viral gene expression in response to host and viral cues. The second aim of this dissertation was to characterize the role of M1-driven $V\beta4^+$ $CD8^+$ T cell expansion in fibrotic disease. Our lab has shown that M1 expression is required for development of fibrotic disease in IFNγR-/- mice. Here we demonstrate that M1 expression results in heightened levels of inflammation and fibrosis in the lung. Additionally, we find elevated levels of neutrophil and effector $CD8^+$ T cells at 28 days post-infection. We verify the involvement of $CD8^+$ T cells in fibrotic disease through $CD8^+$ T cell depletion which results in protection from fibrosis and lethality. Taken together data raise the possibility that $V\beta4^+$ $CD8^+$ T cells induce fibrosis though cytokine mediated inflammation, which results in altered cellular trafficking and immunopathology. Collectively, these studies provide significant insights into M1 function in MHV68 infection. We link M1 expression with viral reactivation, and provide evidence for the role of $V\beta4^+$ $CD8^+$ T cells as mediators of fibrotic disease.

Characterizing the Expression and Regulation of MHV68 M1 & Uncovering its Role in Pulmonary Fibrosis

By

Brigid Moira O'Flaherty
B.S., Towson University, 2007

Advisor: Samuel H. Speck, PhD

A dissertation submitted to the Faculty of the
James T. Laney School of Graduate Studies of Emory University
in partial fulfillment of the requirements for the degree of
Doctor of Philosophy
in
Graduate Division of Biological and Biomedical Sciences
Microbiology and Molecular Genetics

2015

ACKNOWLEDGEMENTS

First, I would like to thank my mentor, Sam Speck, for the opportunity to train in his lab. His encouragement and support have provided me the opportunities to explore my own scientific interests and develop as an independent scientist.

The Speck lab has been an excellent environment to train in, and I have enjoyed working with members both past and present. I have learned a lot from this talented group of scientists. I would like to thank Katy Gray and Clint Paden for helping me get acclimated to the lab and answering all of my questions. Also, a special thanks to Udaya Rangaswamy and Caline Matar, who have become great friends.

Additionally, I would like to thank my dissertation committee for their suggestions and encouragement along the way.

I would like to thank Beth Moore, for her collaboration on my second dissertation project. She has provided excellent advice and feedback on the project and the fibrosis field, and has always been warm, friendly, and encouraging.

The friends I have met here in Atlanta have meant a lot to me, I don't think I would have had such an enjoyable time without them, especially Shannon Whitmer and Rebecca Iskow Torene.

I would like to thank my family – especially my parents, Virginia and Patrick, and brother, Brendan – for loving and supporting me. Lastly, I would like to thank Nick Fisher, for supporting me through the ups and downs of grad school, and embarking on this adventure with me.

TABLE OF CONTENTS

LIST OF FIGURES AND TABLES

CHAPTER I

INTRODUCTION

Herpesviridae

Herpesviridae comprise a diverse family of large, enveloped, double-strand DNA viruses, which establish infection for the life of their host. Over millennia, these viruses have co-evolved with their hosts and more than 100 herpesviruses have been identified from human and other eukaryotic organisms [1]. A common aspect of herpesvirus biology is the biphasic lifecycle, where the virus transitions between lytic and latent stages of infection. Lytic infection is characterized by a regulated cascade of viral gene expression, genomic replication, and production of functional virions. During lytic infection, the virus is able to disseminate infection within its host, or spread infection to others. Following this initial burst of lytic infection, the virus enters a quiescent state known as latency. In viral latency, gene expression is tightly regulated, resulting in limited viral gene expression. Additionally, the viral genome is maintained as an episome – tethered its host's chromosome – and there is an absence of viral particle production. However, upon the appropriate stimuli the virus can reactivate from latency to facilitate maintenance and spread of infection.

Of the identified herpesviruses, eight commonly infect humans [2]. These include the alpha herpesviruses- herpes simplex virus 1 and 2 (HHV-1 & 2 respectively) and varicella zoster virus (HHV-3); the beta herpesviruses- cytomegalovirus (HHV-5) and roseolo virus (HHV-6 & 7); and the gammaherpesviruses- Epstein Barr virus (HHV-4) and Kaposi's sarcoma associated herpesvirus (HHV-8). The three subfamilies- alpha,

beta, and gamma, are subdivided based on their biological characteristics. Alphaherpesviruses have a broad host range and following a short replication cycle inducing rapid cytopathic effect to host cells. Subsequently, alphaherpesviruses establish latency in the sensory ganglia of their hosts. Beta herpesviruses have a restricted host range, establishing latent infection in the secretory organs after a relatively long replicative cycle. Finally, gammaherpesviruses, with a restricted host range establish latent infection of B and T cells, and are associated with a variety of lymphoproliferative disorders.

Gammaherpesvirinae

The lymphotropic gammaherpesvirus subfamily infects a range of mammalian host species. This subfamily is comprised by the genera lymphocryptovirus (γ1), rhadinovirus (γ2), and the more recently identified macavirus and percavirus [3]. Lymphocryptoviruses, including Epstein-Barr virus (EBV), infect members of the Old and New World primates. Rhadinoviruses, including Kaposi's sarcoma-associated herpesvirus (KSHV), infect a range of hosts including primates, ungulates, and carnivorous species (described in [4]). Macaviruses infect African wildebeest, hippo, sheep, cows, goats and boars, and Percavirus have been identified in horses and badgers [3].

EBV infects individuals in the first decade of life, and its infection rate in the US is estimated to be greater than 95% [5]. However, in the US, a non-endemic area for KSHV, less than 10% of the population is infected [6]. The fact that these viruses are relatively benign in healthy host speaks to their successful adaptation during evolution

with their hosts; however, significant diseases can result from infection in the immunocompromised or immunosuppressed host. KSHV was initially identified from Kaposi's sarcoma lesions in AIDS patients. Additionally, KSHV leads to a number of malignancies including AIDS associated cancer, multicentric Castleman's disease, and primary effusion lymphoma. EBV, identified through its association with Burkitt's lymphoma in equatorial Africa, has been shown to cause Burkitt's lymphoma, nasopharyngeal carcinoma, and oral hairy leukoplakia. These malignancies emphasize the importance of understanding the biology and pathogenesis of gammaherpesvirus infection. However, a significant challenge in the study of gammaherpesviruses is due to its narrow host range and cellular tropism. Until the identification of a rodent gammaherpesvirus, MHV68, study of gammaherpesviruses relied solely on evaluation of patient samples and tissue culture models.

MHV68

Identified from bank voles and yellow-necked field mice in Slovakia [7], MHV68 was found to infect both inbred and outbread mice. MHV68 infection closely mirrors the natural course of infection of EBV. In the laboratory setting, MHV68 infection can be induced following intranasal, intraperitoneal, oral, or intracranial inoculation. Trafficking of MHV68 following intranasal infection is shown (Figure 1). Following intranasal infection, the virus undergoes an initial burst of lytic replication in the lung epithelium which lasts from 4-9 days post infection. Lesser amounts of virus are detected in macrophage and dendritic cells in the lung. Next infected naïve B cells are thought to traffic to the spleen where peak lytic replication lasts from days 9-16 post infection. In the spleen infected naïve B cells undergo a germinal center reaction which facilitates

amplification of virally infected cells. Between days 14-18, ca. 70-90% of virally infected B cells have a germinal center phenotype [8]. Notably, at the peak of splenic infection ca. 10% of infected B cells exhibit a plasma cell phenotype [8], which has been shown to account for the majority of viral reactivation in the spleen – with ca. 50% of plasma cells reactivating upon ex vivo transplant [9]. During the germinal center response cells exit as either plasma cells or memory B cells – the major latency reservoir for MHV68. Between days 16-42 days-post infection levels of latently infected B cells contract precipitously from ca. 1:100 at day 16 to ca. 1:10,000 by day 42 – leaving behind a small pool of latently infected memory B cells.

After its identification, the genome of MHV68 was sequenced and compared with those of the other gammaherpesviruses [10]. Analysis revealed significant homology in both sequence and spatial arrangement with the genomes of EBV, KSHV, and Herpesvirus Siamiri (HVS). Interspersed among the large blocks of conserved genes, were unique genes referred to as the M genes in MHV68. The MHV68 genome contains 14 M genes, M1-M14, which encode proteins that have been shown to aid in infection and manipulation of the host response to infection.

M1 Function

M1, a unique protein encoded in the first open reading frame of MHV68, is a secreted protein that has homology with pox virus serpin proteases. Although protease activity has not been detected, M1 has been shown to play critical roles in MHV68 infection. Initial characterization by Clambey *et al.* revealed functions for M1 in lethality, splenic atrophy and fibrosis in C57Bl/6 interferon gamma receptor deficient mice

(IFNγR-/-) [11]. Further, in the absence of M1 expression, hyper-reactivation of the virus from latently infected peritoneal exudate cells (PEC) was observed [11]. Subsequent studies made key observations linking M1 expression and the characteristic $V\beta4^+$ $CD8^+$ T cell expansion that occurs during MHV68 infection [12]. Until this point, the viral factor responsible for this expansion remained unidentified; Evans *et al.* showed that M1 was absolutely required for this T cell expansion. Recapitulating previous observations, these studies showed that once this population expanded it would remain elevated for up to two years post infection [12,13]. Additionally, Evans and colleagues showed that $V\beta4^+$ $CD8^+$ T cells isolated from infected mice were responsive to intact recombinant M1 protein, secreting both interferon gamma (IFNγ), tumor necrosis factor alpha (TNFα), and interleukin 2 (IL-2) independent of antigen processing and presentation [12]. These observations were consistent with the notion that M1 functions as a novel viral super-antigen.

The predominant source of viral latency and reactivation in the peritoneum is the macrophages [14,15]. Notably, the viral replication and transcription activator (Rta), responsible for driving lytic infection and reactivation from latency, has been shown to be controlled through IFNγ in a Stat1 dependent manner [15-17]. Taken together with its role in $V\beta4^+$ $CD8^+$ T cell expansion, the following model was hypothesized for M1 function – (i) secreted M1 stimulates $V\beta4^+$ $CD8^+$ T cell activation and expansion, (ii) these cells then traffic through the blood stream to various sites of infection where they secrete IFNγ, (iii) thus suppressing Rta transcription in a IFNγ dependent manner and blocking viral reactivation from latently infected macrophages (Figure 2).

The role for M1 in MHV68 induced fibrosis in IFNγR-/- C57Bl/6 mice was posited to depend on the absence of IFNγ signaling – leading to uncontrolled virus reactivation from latently infected macrophages (and possibly other cell types). This persistent replication would be expected to result in continued expression of M1 causing continued activation of cytokine producing $V\beta4^+$ $CD8^+$ T cells. These cells, either directly or indirectly, would induce tissue damage or potentially initiate bystander T cell activation, contributing to an ongoing process of tissue damage and repair resulting in fibrosis.

Recently, a novel function for M1 protein has been identified in viral latency. In the absence of M1 expression, increased levels of viral latency were observed in naïve (IgD-) B cells in the spleen and PEC of both C57Bl/6 and Balb/c mice at 3-5 months post infection [18]. Given that $V\beta4^+$ $CD8^+$ T cells expansion occurs at low levels of in Balb/c mice [13], these results suggest a function independent of $V\beta4^+$ $CD8^+$ T cell expansion. Furthermore, Krug *et al.* observed increased viral persistence from the lung of long term M1-null infected C57Bl/6 mice. This raises interesting questions regarding the function of M1. What role is M1 playing in naïve B cell infection? Is viral persistence observed in both mouse strains, or is it limited to C57Bl/6 mice where M1 is known to control viral reactivation from other latently infected populations? What cell types are responsible for the persistent infection in the lung, and are they controlled by the $V\beta4^+$ $CD8^+$ T cell produced cytokines? Further evaluation of M1 function in different genetic backgrounds may facilitate the uncoupling of Vβ4 expansion from other M1 dependent functions.

M1 Expression

A better understanding of how M1 carries out its function may be provided by an understanding of where it is expressed in vivo, and what regulates its expression. Much of the available data pertaining to M1 expression is based on global analyses of MHV68 viral gene expression. A caveat to these findings is the reliance on detection methods that are not strand specific, and therefore not stringent enough to discriminate between bona fide M1 transcription and transcripts originating from the anti-sense strand. Nevertheless, these studies provide some clues into M1 expression, and are discussed here.

Herpesviral genes, categorized as immediate-early (IE), early, and late, can be distinguished by their expression patterns in the presence of DNA and protein synthesis inhibitors. Viral IE genes do not require ongoing protein synthesis or DNA replication, and are readily expressed in presence of their inhibitors. Early genes require IE protein synthesis, and therefore are susceptible to protein synthesis inhibitors such as cyclohexamide; whereas late genes are dependent on viral DNA replication, and are susceptible to DNA synthesis inhibitors such as cidofovir.

M1, a lytic gene in MHV68 [10], has been defined as an early-late gene [19-22]. To evaluate global viral gene expression *in vitro*, infected BHK-21 cells were analyzed by membrane array at various times post infection using ^{32}P labeled probes [21]. This study found very low levels of M1 expression which peaked at 24 hours post infection. Another study identified M1 transcript at 18 hours post infection from 3T12 cells infected at an MOI of 10 [22].

In vivo detection of M1 transcripts has identified the lung as a reservoir for expression. M1 was detected in lung tissue at 5 days post infection [23,24], while levels were nearly absent by 14 days post infection [23]. In the spleen, detection methods failed to show M1 expression at 10 or 21 days post infection [24]. To identify specific cellular reservoirs of viral gene expression, Marques *et al.* used fluorescence activated cell sorting to isolate various cellular populations from the Balb/c spleen prior to gene expression analysis by real time PCR. The highest levels of M1 expression were detected from dendritic cells, and follicular (Fo) B cells; followed by newly formed (NF) B cells and macrophages; the lowest levels of expression were in germinal center B cells and marginal zone (MZ) B cells [23]. A confounding issue to these observations is the ability of gammaherpseviruses to manipulate expression of CD21 and CD23 (unpublished data C.M. Collins and S.H. Speck, and [25-28]). This complicates interpretation of gene expression from the MZ, NF, and Fo B cell populations. Additionally, as plasma cells play an important role in gammaherpesvirus biology and reactivation [9,29-34], another shortcoming of this study was the failure to include the plasma cell population. Studies in chapter II of this dissertation identify cellular reservoirs of M1 expression *in vivo*, and identify the transcriptional regulators controlling M1 expression.

Genetic Requirements

Suggestive of genetic requirements for M1 expression is the failure to see $V\beta4^+$ $CD8^+$ T cell expansion in certain knock strains of mice. The absence of B cells has been shown to provoke numerous changes in MHV68 infection including altered latency and reactivation. Although MHV68 is capable of initiating and maintaining infection in B cell deficient (μMT) mice, numerous changes including absence of lytic virus in the spleen,

lack of splenomegaly, and absence of $V\beta4^+$ $CD8^+$ T cell expansion have been observed [14,35,36]. $CD4^+$ T cell help has been shown to play an important role in $V\beta4^+$ $CD8^+$ T cell expansion, as CD40L-/- and $CD4^+$ T cell depleted mice fail to show expansion during the course of a 53 day infection [35]. Additionally, at 21 days post infection, CD4-/-, MHCII-/-, and CD4+ T cell depleted mice fail to show this expansion [37]. Interpretation of this data is cautioned by the finding that CD4-/- mice have a delayed $V\beta4^+$ $CD8^+$ T cell expansion during MHV68 infection which correlates to delayed splenic B cell activation [37], here Flano *et al.* note a delayed expansion at days 35-45 post infection, underscoring the importance of CD4-B cell interactions in this process. Alteration of the immune composition of mice no doubt alters MHV68 infection – nevertheless, these studies provide important clues regarding M1 expression.

Functional Homologs to M1

Within the gammaherpesvirus subfamily several proteins which share some homologous function to M1 have been identified, suggesting that the role for M1 in MHV68 infection might be a conserved among other gammaherpesviruses. EBV encodes a structural protein, gp350, which like LMP-1 and LMP-2A has been shown to transactivated an endogenous human retrovirus superantigen, HERV-K18, leading to $V\beta13^+$ T cell expansion [38-40]. The consequence of this expansion remains to be explored, but the similarities certainly suggest that this may be a common strategy to control aspects of viral infection. Similarly HVS encodes a viral super-antigen, immediate-early gene ie14/vsag, which stimulates T cell proliferation and is necessary for cellular transformation and viral persistence [41]. Like M1 ([24] and shown in chapter II), ie14/vsag is not essential for viral replication, and is linked to viral reactivation –

showing elevated expression in the presence of phorbol ester treatment [41]. These similarities leave us to question the function of viral super-antigens in gammaherpesvirus infection. What role do these proteins play in regulating infection or immune response? It is unlikely that these genes would be maintained if they did not play some important role in the gammaherpesvirus biology.

Fibrosis

Chapter III of this dissertation explores a small animal model of pulmonary fibrosis, where the role of M1 is addressed. An overview of fibrotic disease and the relevant murine models are presented here. Fibrotic disorders encompass a wide spectrum of progressive diseases affecting multiple organ systems. Fibrosis may be limited to a particular organ such as the lung, liver, or kidney; or may affect multiple organ systems, in the cases of systemic sclerosis, multifocal fibrosclerosis, nephrogenic systemic fibrosis, and sclerodermatous graft versus host disease in transplant recipients [42]. Though the driving mechanism and etiology differ among these disorders, a common feature is the excessive deposition of extracellular matrix (ECM), leading to disruption of normal tissue architecture and eventual loss of organ function.

Pulmonary Fibrosis

Pulmonary fibrosis or interstitial lung disease (ILD) encompasses a heterogeneous group of more than 200 chronic disorders affecting the interstitium, the space surrounding the air sacs of the lung. ILD results in progressive inflammation and scarring of the lung that is generally irreversible. Diagnostic criteria include distinct clinical, phsysiologic, and radiographic findings. Shared features of ILD include impaired gas

exchange, restriction of pulmonary function and identification of bilateral infiltrates on chest imaging [43].

One of the most severe ILD, idiopathic pulmonary fibrosis (IPF), has no known etiology. This disease results in progressive scaring of the lung, respiratory decline and eventual mortality. The natural history of disease is unpredictable and variable; while some patients remain stable, the majority experience gradual decline over many years, yet others experience rapid decline [44]. Further complicating disease progression is the fact that some individuals experience acute exacerbations resulting in rapid decline despite previous stability in their condition [44,45]. Generally affecting individuals over the age of 65, this unrelenting disease has a median survival of 2-5 years post diagnosis [46]. Currently only two FDA approved drugs are available for IPF treatment, and though these slow disease progression, there is no cure [47,48]. Furthermore, in addition to its association with numerous environmental, genetic, and infectious factors, IPF has several comorbidities that may influence the progression and severity of disease [43,49].

Diagnostic criteria for IPF were recently outlined by the ATS/ERS/JRS/ALAT in 2011, these criteria include “[the] exclusion of other known causes of interstitial lung disease (ILD)...presence of a usual interstitial pneumonia (UIP) pattern on high-resolution computed tomography (HRCT) in patients not subjected to surgical lung biopsy...[and] specific combinations of HRCT and surgical lung biopsy pattern in patients subjected to surgical lung biopsy.” UIP refers to specific phenotypic changes observed in the lung, which include marked fibrosis with architectural distortion, presence of subpleural or paraseptal honeycombing, patchy fibrosis in the lung parenchyma, presence of fibrotic foci, as well as a number of exclusionary features [44].

Role of Infections

Viral infections have been hypothesized to play an important role in progression of IPF. Microscopic damage of alveolar epithelial cells in the lung, in conjunction with dysregulated tissue repair, may contribute to development of IPF [50]. Further, it has been proposed that occult viral infections may act as a cofactor contributing to disease pathogenesis [51]. To elucidate the role of infection, numerous studies have evaluated IPF patients for presence of viral DNA, antigen, and humoral immune response and are discussed here (also reviewed in [51-53]).

Hepatitis C Virus

A study in Japan implicated hepatitis C virus (HCV) in IPF, finding 28.2% of IPF patients, and only 3.7% of controls being sero-positive for HCV [54]. Subsequent evaluations failed to show that HCV was contributing specifically to IPF. Meliconi *et al.* found seroconversion rates of 13% in IPF patients, 0.3% for non-IPF controls, and 6.1% in patients with non-interstitial lung disease, suggesting a more general role for HCV in lung disease [55]. However, Irving and colleagues evaluated sera of 62 IPF patients for presence of HCV by ELISA, identifying a single serum reactive patient [56]. In a retrospective evaluation of HCV positive patients over a mean observation period of 8 years, elevated incidence of IPF with 0.3% and 0.9% incidence of IPF at 10 and 20 years respectively was observed [57]. Notably, none of the hepatitis B virus positive control patients in this study developed fibrosis.

Torque Teno Virus & Adenovirus

Additional candidate viruses contributing to IPF include Torque Teno virus (TTV) and adenovirus. One study detected the presence of TTV in 36.4% of patients and noted a reduced 3 year survival rate [58]. Subsequent observations from this group identified TTV in patients with IPF (94.3%), lung cancer (97.2%), and IPF and lung cancer (100%); notably viral titers were higher in those with IPF and lung cancer, compared to individuals with either disease alone [59]. Another study to assess the role of viral infection in acute exacerbations of IPF found TTV in 14/43 patients by microarray analysis. Although TTV infection rates were significantly higher in individuals with acute exacerbations compared to stable controls, rates were similar to those with other acute lung injuries [60]. Its prevalence in the population complicates interpretation of these findings and further studies will be required to appreciate the contribution of TTV in IPF. *In vitro* studies have shown that adenoviral gene product E1A upregulates profibrotic factor TGFβ and induces epithelial to mesenchymal transition [61]. Despite these observations, researchers have failed to find a correlation between adenovirus and IPF [62,63].

Influenza Virus

A case report of an individual experiencing acute exacerbation of IPF following vaccination for pandemic H1N1 was reported [64]. A subsequent report noted elevated viral output in infected alveolar type II cells isolated from individuals with fibrotic lungs [65]. This study suggests that the fibrotic lung may be more permissive to infection, what

consequence this may have on development of disease and it progression remains to be seen.

Herpesviruses

Some of the most compelling evidence linking herpesvirus infection with IPF was shown in a study by Tang and colleagues [66]. Here lung tissue from 33 IPF patients and 25 control subjects was evaluated by PCR for HHV-7, HHV-8, EBV, and human cytomegalovirus (HCMV). Strikingly, one or more virus was detected in 97% of patients, compared to 36% of controls. CMV, EBV, and HHV-8 were found more frequently in IPF patients compared to controls, and two or more viruses were detected in 57% of IPF patients vs 8% of controls.

Cytomegalovirus

The role of CMV in IPF has been addressed in a number of other studies. Notably, higher CMV IgG and complement fixation titers were observed in IPF patients compared to healthy controls, or those with other lung disease (sarcoidosis and chronic obstructive pulmonary disease) [63]. In evaluating the role of microvascular injury in IPF, Margo and colleagues identified 9 CMV positive patients by serology, these patients showed CMV RNA in pulmonary cells indicating an active infection [67]. Another study evaluating acute exacerbation in IPF patients found 10% of patients with nonspecific interstitial pneumonia, and 25% of patients with organizing pneumonia patters, to be CMV infected by immunohistochemistry [68]. Contradictory evidence was shown in a study evaluating bronchoalveolar lavage fluids and blood for CMV, which showed no

difference in infection among IPF patients and controls [69]. Further studies will be necessary to clarify the role of CMV in IPF.

Epstein-Barr virus

The strongest link between viral infection and IPF has been shown with EBV. The association was first noted in 1984 where 13 IPF patients were shown to have elevated EBV antibody response compared to control subjects [70]. Several reports have found elevated levels of EBV DNA in the lung [71,72], with evidence of viral replication indicated by WZhet rearrangement [72]. Increased viral capsid antibody titers have been shown in the bronchoalveloar lavage fluids for 60% of IPF patients compared to 22% of controls [73]. EBV replication has been detected in the type II alveolar epithelial cells from the lower respiratory tract of IPF patients [74] and *in vitro* findings indicate EBV infection of type II AEC results in increased levels of TGFβ [75]. Interestingly, *in vitro* expression of EBV protein, LMP-1, in the presence of low levels of TGFβ has been shown to increase mesenchymal markers and concurrently decrease epithelial cell makers – an indication of epithelial to mesenchymal transition [76]. Furthermore, EBV has been shown to modulate expression of CD21 [25-27]; and notably, primary type II AEC treated with IL4, which express CD21, have been shown to be more permissive to EBV infection [77]. Taken together these findings highlighting how the Th2 cytokine environment, observed in IPF patients, may impact viral infection and disease. Additionally, Lawson and colleagues have shown a correlation between EBV infection, unfolded protein response (UPR) and endoplasmic reticulum (ER) stress [78]. This study finds elevated levels of ER stress and UPR activation in patients with familial IPF, associated with a mutated surfactant protein C gene, highlighting how EBV might disrupt

the balance in a genetically predisposed individual. Though some studies have failed to find a correlation between EBV and IPF [79,80], much of the evidence points to a role for EBV in IPF pathogenesis and disease progression.

Case Reports, Pulmonary Fibrosis in Animals

In addition to its presence in humans, pulmonary fibrosis (PF) has been identified in a number of mammalian genera including felines, canines, and equines. First described in 1999, pulmonary fibrosis has been shown to afflict domesticated canines [81-84]. Evidence of spontaneous feline IPF has also been noted. Initial reports of disease were made in 2004, and since then feline PF has been radiologically and histologically characterized [85-88]. However, little effort by the veterinary community has been made classify forms of fibrotic lung disease in companion animals, and the etiologic agent(s) responsible for canine and feline PF remain unknown [89]. Equine multinodular pulmonary fibrosis (EMPF) initially described in 2007, has been shown to have a strong association with gammaherpesvirus infection [90-95]. Histologic features bear a striking similarity to those of human IPF, with interstitial fibrosis, cuboidal epithelial cells lining the alveolar walls, and neutrophilic and macrophage infiltrates [90]. Strikingly, Williams and colleagues revealed a strong correlation between Equine herpesvirus 5 (EHV-5) infection and EMPF, where 19/24 (79.2%) affected horses and only 2/23 (8.7%) of control horses lung tissue were positive for EHV-5 [90].

MHV68 Induced Fibrosis in IFNγRKO Mice

Limitations to study of pulmonary fibrosis have led to the development of numerous small animal models to characterize the underlying mechanisms driving PF.

Rodent models broadly include use of (i) respiratory irritants, (ii) cytokine overexpression, (iii) genetic mutation, (iv) tissue injury, (v) age related fibrosis, and (vi) viral infection, and are thoroughly described by Moore *et al.* [96]. Additionally, several model systems have evaluated the role of MHV68 infection, as well as other viruses as exacerbating agents in traditional models of pulmonary fibrosis such as bleomycin and FITC (Reviewed in [53,89,97,98]. However, for the sake of brevity, we will focus on MHV68 infection of interferon gamma receptor deficient mice (IFNγR-/-) and describe the resulting pathology and mechanistic findings.

Atrophy and Fibrosis of the Spleen

Initial discovery of a spontaneous fibrotic disorder initiated by MHV68 infection was shown in IFNγR-/- 129Sv/Ev [99]. Here, MHV68 infection was shown to cause a dramatic reduction in spleen cellularity between 15 and 20 days post infection, which stabilized at ca. $1x10^7$ cells/mouse spleen through day 70 post infection. This initial characterization showed granulocytic infiltrate in the white pulp of the spleen, increased fibroblasts, and collagenous matrix deposition disrupting the white and red pulp. Strikingly, depletion of $CD8^+$ T cells through the course of infection was shown to prevent fibrosis, restoring spleen size and level of MHV68 infective centers. Subsequent analyses have worked to uncover the mechanism contributing to this fibrotic disease and have revealed that MHV68 infection of IFNγR-/- results in multi-organ fibrosis, these studies will be discussed below.

Dal Canto *et al.* revealed the importance of viral replication in this model, showing that MHV68 infection resulted in ca. 80% lethality, yet with administration of

cidofovir at 24 days post infection, lethality was reduced to ca. 40% [100]. Furthermore, treatment led to a significant reduction in fibrotic lesions in the spleen. In a series of elegant adoptive transfer experiments, Ebrahimi and colleagues revealed the driving mechanism for splenic fibrosis and atrophy [101]. Dramatic alteration in the chemokine and cyokine profiles resulted in altered lymphocyte trafficking [101]. Notable changes include elevated levels of IFNγ, TNFα, TNFβ, IL1β, TGFβ1, LTN, MIP1; and reduced levels of IP10, MIG1 in the spleen. Ebrahimi *et al.* also described the fibrosis and atrophy of the spleen and mediastinal lymph node, and fibrosis of the lung and liver. An unexpected finding of these studies was the apparent resolution of atrophy and fibrosis occurring between 21-45 days post infection. This reason for this observation is unclear as previous reports failed to show this apparent resolution.

Infiltration of macrophage populations over the course of disease progression has been observed [102]. The migration of “ameboid like” macrophages into the germinal center, marking positive for TR9 and MOMA1 were noted, and markers of alternative macrophage activation (Arg1 and FIZZ1) were shown to coincide with development of fibrosis. Consistent with presence of alternative macrophages were elevated levels of IL13, IL21, and IL5. Levels of TIMP1 and MMP12, mediators of extracellular matrix turn over were also increased, along with fibronectin and FXIIA.

Notably, in the absence of MHV68 unique protein M1, splenic fibrosis and atrophy failed to occur in IFNγR-/- C57Bl/6 mice [11,12]. Evans *et al.* proposed a mechanism in which the $V\beta4^{+}$ $CD8^{+}$ T cell population played a critical role in driving disease and pathogenesis through Vβ4 induced immunopathology and possible bystander T cell activation [12].

Hepatic Fibrosis

Another finding of the IFNγR-/- 129Sv/Ev MHV68 infections was hepatic fibrosis. Gangadaharan *et al.* described fibrosis in ca. 30% of infected mice [103]. Proliferation of the intrahepatic bile duct with chronic mononuclear cell infiltration was observed during the course of infection, along with epithelial cell expression of Arg1.

Pulmonary Fibrosis

As the second aim of this dissertation focuses on the role of M1 in pulmonary fibrosis, we discuss relevant background in pulmonary cellular immune response and pathology here. Studies to address the role of M1 in MHV68 induced fibrosis of IFNγR-/- mice are presented in Chapter III.

Mora and colleagues first described a pulmonary fibrotic disease in MHV68 infected IFNγR-/- mice reminiscent of human IPF [104]. Infection of IFNγR-/- mice resulted in severe inflammation of the subpleura areas surrounding the airways and blood vessels. Notably these changes and the presence of pulmonary infiltrates primarily made up of lymphocytes, plasma cells, neutrophils, and eosinophils persisted throughout chronic infection, with evidence of subpleural fibrosis observed at 150 days post infection. Collagen deposition was patchy and most evident in subpleural areas adjacent to large alveolar macrophages. Additional features included decreased tidal volume, increased expression of TGFβ in the lung, and MHV68 detection in the type II AEC.

During the early stages of infection, elevated IL5, IL10, and IL4 have been detected in the bronchoalveolar lavage fluids [104]. Levels of MIP1α and MCP1in

fibrotic mice were elevated in the bronchoalveolar lavage fluid and serum [105]. Additionally, markers of alternative macrophage activation were indicated by Ym1/2, Arg1, and FIZZ1 [105].

Subsequent studies have provided insights into the underlying mechanisms driving pulmonary fibrosis in this model system. Consistent with Dal Canto's observation that cidofovir treatment led to improved survival and reduction in splenic fibrosis [100]; cidofovir treatment was shown improve survival, and dramatically reduce lung pathology and collagen deposition [106]. Cidofovir treatment led to reduction in IFNγ, IL13, MIP1α, Arg1, Ym1/2, and TGFβ expression, as well as reduced gelatinase activity and levels of MMP2 and 9 [106], highlighting the role of alternative macrophage activation in pathogenesis. Another notable feature of MHV68 infection of IFNγR-/- mice was the persistence of virus in the lung at 90 days post infection [107,108]. Infection of IFNγR-/- with a NFκB dominant negative mutant virus was shown to dramatically reduce development of fibrosis [108]. Coincident with the decreased fibrosis were decreased levels of virus in the lung, decrease levels of mesenchymal markers, and decreased presence of alternatively activated macrophages [108].

Fidelity of this Model System for IPF

Many features of this model are consistent with many the physiologic and pathological changes observed human IPF. In parallel to elevated collagen deposition mice experience decrease in tidal volume; furthermore, increased levels of TGFβ, myofibroblast transformation, Th2 cytokine production, type II cell hyperplasia, and alteration in MMP-7 are observed [104]. Genetic mutation of SFTPC is observed in some

cases of familial IPF [49], consistent with this is the observation that MHV68 infection of IFNγR-/- mice result in altered synthesis of surfactant proteins [104]. This highlights an interesting ability of gammaherpesviruses to manipulate host cell biology. Furthermore, like EBV, MHV68 viral protein was detected in type II alveolar epithelial cells. Mirroring the observation of EBV infection of lower lung alveolar epithelial cells, Mora and colleagues showed MHV68 antigen present in type II AEC [104]. A number of salient features of this model recapitulate the histological findings of IPF outlined in the ATS/ERS/JRS/ALT diagnostic criteria [44] and are outlined in Table 1.

Summary

MHV68 provides a unique model system where we can probe various aspects of gammaherepsvirus biology and pathogenesis. We hope that through a better understanding of M1 regulation and function, we may gain insights into the role of viral super-antigens in gammaherpesvirus infection. This dissertation aims explore MHV68 M1 protein through two different arms of investigation. The first of these aims is to understand the site and regulation of M1 expression (Chapter II). By gaining a more complete picture of M1 expression and regulation, we gain insights into how M1 carries out its function during infection. The second aim of these studies is to understand the role of M1 during fibrotic disease (Chapter III). Unlike M1, many of the previously identified MHV68 mutants which fail to induce fibrosis, play critical roles in establishment and maintenance of MHV68 infection. Our investigation into the role of M1 in MHV68 induced fibrotic disease explores its immunomodulatory functions in the context of an immunocompromised host and provides insights into the role of $CD8^+$ T cells in gammaherpesvirus associated pulmonary fibrotic disease.

FIGURES

Figure 1.

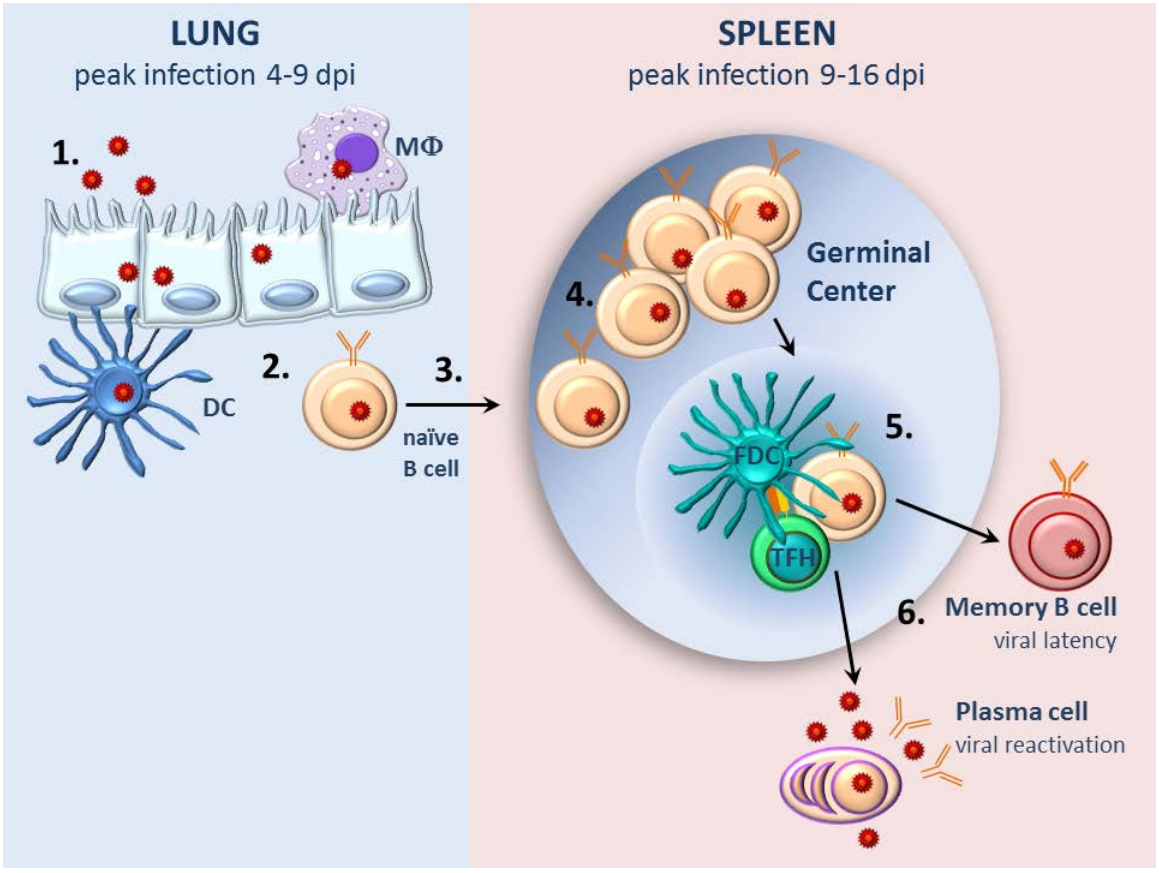

Figure. 2

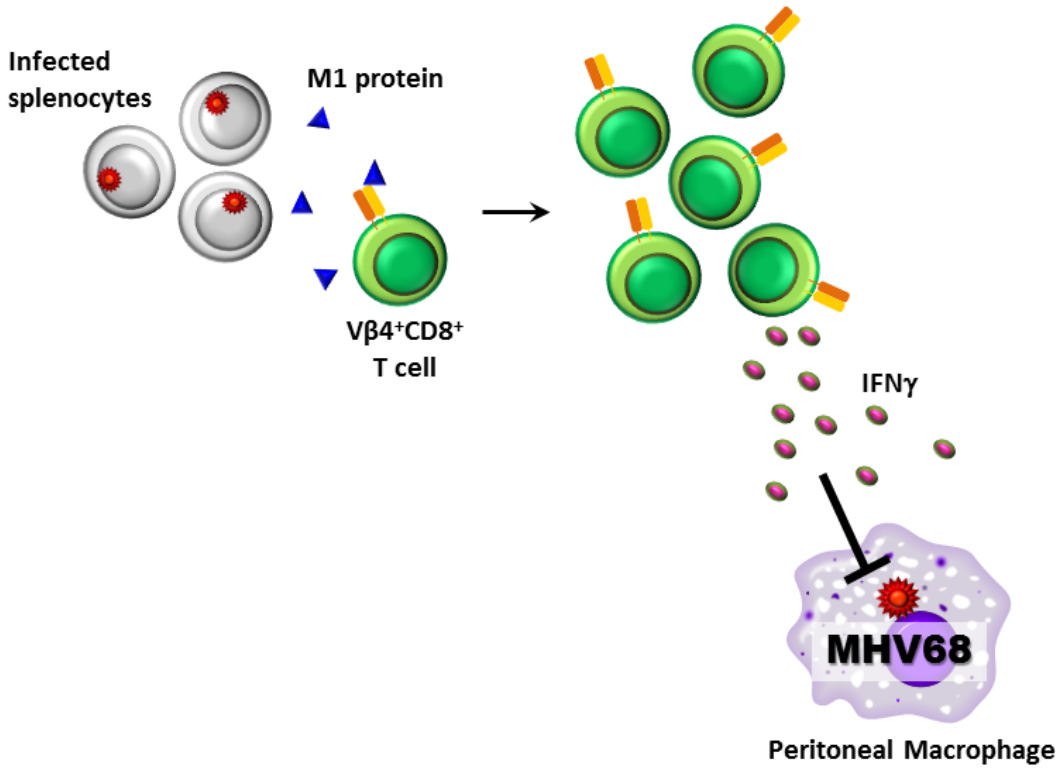
Infected
splenocytes
M1 protein
Vβ4⁺CD8⁺
T cell
IFNγ
MHV68
Peritoneal Macrophage

FIGURE LEGENDS

Figure 1: Trafficking and replication of MHV68 following intranasal infection. Following intranasal MHV68 infection the virus undergoes lytic replication in the respiratory epithelium (1), subsequently the virus infects naïve B cells, and to a lesser extent dendritic cells and macrophages (2) which traffic to the spleen (3). In the spleen these infected cells enter a germinal center reaction where the infected B cell population proliferates, and at this stage cells undergo somatic hyper-mutation (4). Subsequently, infected B cells exit the dark zone and move to the light zone where B cell maturation and Ig class switch occurs (5). Upon completion of the germinal center reaction, cells exit as memory B cells (the long term latency reservoir of MHV68) or plasma cells (a predominant site or viral reactivation) (6).

Days post infection (dpi), Macrophages (MΦ), Dendritic Cell (DC), Follicular dendritic cell (FDC), T follicular helper (TFH), immunoglobulin (Ig)

Figure 2. Expression and function of M1 protein in MHV68 infection. During MHV68 infection, the stimulatory ligand for $V\beta4^+$ $CD8^+$ T cell activation is expressed from infected splenocytes [109], Evans and colleagues identified this stimulatory ligand as MHV68 M1 [12]. During infection, M1 is expressed as a secreted protein capable of inducing $V\beta4^+$ $CD8^+$ T cell activation and expansion independent of antigen processing and presentation. This population of cells traffics to different sites in the mouse including peripheral blood, lung, spleen, and peritoneum. These activated T cells produce high levels of interferon gamma (IFNγ), as a result of M1 stimulation, which is capable of

suppressing the MHV68 ORF50 (Rta) promoter in a Stat 6 dependent manner in the peritoneal macrophage population. Blocking the ORF50 promoter prevents Rta mediated transactivation, thus allowing the virus to maintain latency.

Figure modified from Evans et al. [12]

TABLES

Table 1. Similarities between IPF and MHV68 infection of IFNγR-/- mice.

Phenotype	**IPF**	**MHV68 Infection**
Marked fibrosis	Yes	Yes
Architectural distortion	Yes	Yes
Presence of subpleural or paraseptal honeycombing	Yes	No
Patchy fibrosis in the lung parenchyma	Yes	Yes
Presence of fibrotic foci	Yes	Yes

CHAPTER II

The murine gammaherpesvirus immediate-early Rta synergizes with IRF4, targeting expression of the viral M1 superantigen to plasma cells

Brigid M. O'Flaherty[1,2], Tanushree Soni[1,2], Brian S. Wakeman[1,2], Samuel H. Speck[1,2,*]

[1] Department of Microbiology and Immunology, Emory University School of Medicine, Atlanta, Georgia 30322 U.S.A. [2] Emory Vaccine Center, Emory University School of Medicine, Atlanta, Georgia 30322 U.S.A.

All figures were generated by Brigid Moira O'Flaherty.

Figure 1-3. M1st-YFP and M1p-YFP viruses were generated by Tanushree Soni.
Figure 6. 1025bp M1p plasmid generated by Lisa Gargano.
Figure 10A. M2p plasmid a generous gift of Shariya Terrell.
Figure 10 B&C. ORF50ppRREm plasmid generated by Brian Wakeman, N4/N5p previously described in [110].

PLoS Pathog. **2014; 10(8): e1004302.**

CHAPTER II

The Murine Gammaherpesvirus Immediate-Early Rta Synergizes with IRF4, Targeting Expression of the Viral M1 Superantigen to Plasma Cells.

ABSTRACT

MHV68 is a murine gammaherpesvirus that infects laboratory mice and thus provides a tractable small animal model for characterizing critical aspects of gammaherpesvirus pathogenesis. Having evolved with their natural host, herpesviruses encode numerous gene products that are involved in modulating host immune responses to facilitate the establishment and maintenance of lifelong chronic infection. One such protein, MHV68 M1, is a secreted protein that has no known homologs, but has been shown to play a critical role in controlling virus reactivation from latently infected macrophages. We have previous demonstrated that M1 drives the activation and expansion of $V\beta4^+$ $CD8^+$ T cells, which are thought to be involved in controlling MHV68 reactivation through the secretion of interferon gamma. The mechanism of action and regulation of M1 expression are poorly understood. To gain insights into the function of M1, we set out to evaluate the site of expression and transcriptional regulation of the M1 gene. Here, using a recombinant virus expressing a fluorescent protein driven by the M1 gene promoter, we identify plasma cells as the major cell type expressing M1 at the peak of infection in the spleen. In addition, we show that M1 gene transcription is regulated by both the essential viral immediate-early transcriptional activator Rta and cellular interferon regulatory factor 4 (IRF4), which together potently synergize to drive M1 gene expression. Finally, we show that IRF4, a cellular transcription factor essential for plasma

cell differentiation, can directly interact with Rta. The latter observation raises the possibility that the interaction of Rta and IRF4 may be involved in regulating a number of viral and cellular genes during MHV68 reactivation linked to plasma cell differentiation.

INTRODUCTION

MHV68 is a naturally occurring murid gammaherpesvirus that has significant genetic and functional homology to the human gammaherpesviruses Epstein-Barr virus (EBV) and Kaposi's sarcoma-associated herpesvirus (KSHV). Among herpesviruses, there are a large number of genes involved in virus replication that are conserved – both in sequence and spatial arrangement in the viral genome. However, every herpesvirus, having co-evolved with its host during speciation, has acquired unique genes - many of which function to modulate and/or evade the host immune response. Coevolution of with their hosts has led to some divergence of host-pathogen interactions; however, unique genes may reveal homologous functions required for chronic infection of the host. One such gene is the MHV68 M1, which is found in a cluster of unique genes at the left end of the MHV68 genome.

Initial functional studies of M1, utilizing an M1-null virus revealed a hyper-reactivation phenotype from latently infected peritoneal exudate cells (PEC) [11]. Subsequent studies found that this hyper-reactivation phenotype was strain specific – occurring in C57Bl/6 mice, but not Balb/c mice [12]. In addition to the strain specific reactivation phenotype, a strain specific expansion of $V\beta4^+$ $CD8^+$ T cells had previously been observed in response to MHV68 infection [13]. This pronounced T cell expansion and activation is a hallmark of MHV68 infection in many inbred mouse strains and is observed in peripheral lymphoid organs, as well as the blood, reaching peak levels after the virus has established latency [13,111]. Notably, the $V\beta4^+$ $CD8^+$ T cells remain elevated during the course of chronic MHV68 infection, and do not adopt an exhausted phenotype [13]. Analysis of M1-null mutants revealed that a functional M1 gene is

required for the Vβ4$^+$ CD8$^+$ T cell expansion [12]. Furthermore, M1 was shown to be a secreted protein capable of stimulating Vβ4$^+$ CD8$^+$ T cells to produce IFNγ and TNFα [12]. These analyses suggested that M1 may exert control over MHV68 reactivation from peritoneal macrophages through the induction of IFNγ from Vβ4$^+$CD8$^+$ T cells [12], this is supported by the observations that: (i) IFNγ-/- mice exhibit hyper-reactivation from PECS [112]; and (ii) the demonstration that IFNγ can suppress MHV68 replication in macrophages [12,15,17].

Early experiments to evaluate the expansion in thymectomized mice suggested that Vβ4$^+$ CD8$^+$ T cells are maintained through continued stimulation by a stimulatory ligand, which is now known to be M1 [113]. Interestingly, B cells appear to play a critical role in the expansion of Vβ4$^+$ CD8$^+$ T cells, as no expansion is observed upon MHV68 infection of mice lacking B cells [35,36]. Other studies provide some clues to the timing and site of M1 expression during MHV68 infection, where B220$^+$ splenocytes at 14 days post-infection were found to be capable of stimulating Vβ4$^+$ CD8$^+$ T cell hybridomas [109].

Though no homolog to M1 has been found in other gammaherpseviruses, HVS has been shown to encode a viral superantigen, immediate early gene ie14/vsag [41]. Like M1, ie14/vsag, is not essential for viral replication; and interestingly, ie14/vsag expression is elevated in phorbol ester treated cells, indicating a link with viral reactivation. In EBV, structural protein gp350, as well as latent membrane proteins LMP-1 and LMP-2A have been shown to activate expression of an endogenous human retroviral superantigen, HERV-K18, which results in a Vβ13$^+$ T cell expansion [38-40]. Due to limitations in study of non-human primate and human patients it has been difficult to assess the role of these superantigens and the consequence of their resulting T cell

expansion. We are therefore left to speculate what benefit they provide to their host. Do they aid in infection or the establishment of latency? Do they divert the immune response? Are they involved in control of infection? We hope that a better understanding of the expression and role of M1 in MHV68 infection may shed light into the conserved use of viral superantigens by gammaherpseviruses.

Though numerous studies to define the transcriptional program of MHV68 *in vitro* have identified M1 as an early through late gene [19,20,22] relatively little is known about when and where M1 is expressed during infection. Furthermore, while a number of transcriptome based analyses have detected transcripts extending through the M1 locus during *in vivo* infection, much of this data relies on methods that are not strand specific and therefore not definitive [21,23,24,114]. Due to the dearth of information about M1expression *in vivo*, we set out to characterize M1 expression using a novel approach wherein a fluorescent reporter virus would allow detection of M1 promoter activity during infection. This approach led to the identification of splenic plasma cells as the primary cell type expressing M1 *in vivo*. Furthermore, factors regulating M1 transcription were previously uncharacterized. The current studies have elucidated key cis-elements and transcription factors controlling the expression of M1 in plasma cells. Overall, these findings provide insights into the role of M1-mediated regulation of MHV68 pathogenesis. Moreover, we reveal a novel and potentially conserved mechanism which controls the timing and site of viral gene expression in response to reactivation in the B cell.

MATERIALS & METHODS

Ethics statement: This study was carried out in strict accordance with the recommendations in the Guide for the Care and Use of Laboratory Animals of the National Institutes of Health. The protocol was approved by the Emory University Institutional Animal Care and Use Committee and in accordance with established guidelines and policies at Emory University School of Medicine (Protocol Number: YER-2002245-031416GN).

Mice and virus infections: Six to eight week old female C57Bl/6 mice were obtained through Jackson Laboratory (Bar Harbor, ME) and housed at Emory University in accordance with university guidelines. Prior to infection mice were sedated with isofluorane and intranasally infected with $5x10^5$pfu in 20ul of DMEM.

Cell Lines: Cells were grown under normal conditions at 37°C with 5% CO2. A20-HE2 cell were grown in complete RPMI-1640 (supplemented with 10% FCS, 100U/mL penicillin, 100mg/mL streptomycin, 2mM L-glutamine, and 50mM β-mercaptoethanol); P3X63Ag8 (ATCC TIB-9) were grown in compete RPMI-1640 with the addition of 10mM non-essential amino acids, 1mM sodium pyruvate, and 10mM HEPES; and 293T cells (a generous gift from Dr. Edward Mocarski) were grown in complete DMEM (supplemented with 10% FCS, 100U/mL penicillin, 100mg/mL streptomycin, and 2mM L-glutamine).

Generation of recombinant viruses: To generate the M1 promoter driven YFP virus a 500bp homology arm immediately upstream of M1 ORF was amplified with LFA_MluI_1521-1573 (5'-TCCCCAATGACGCCAAAGTCTAAGTCCCTGTACAGGCTTAACTTTTTTAGAAT-3') and LFA_SpeI_2005-2022 (5'-GGTCGCCGCTGCTCAATG-3') and cloned into pCR Blunt-eYFP vector (a kind gift from Dr. Chris Collins) using MluI and SpeI to generate pCR Blunt-eYFP M1 LFA Flank. Next a 495bp homology arm immediately downstream of the M1 ORF was PCR amplified using RFA_NotI_3286-3307 (5'-GCCTGAATACATGTTTACTGGG-3') and RFA_NsiI_3758-3780 (5'-AACCTACGCGGCCACTCAACAGA -3') was cloned into pCR Blunt-eYFP using NotI and NsiI to create pCR Blunt-eYFP M1 LFA RFA flank. The eYFP flanked by left and right homology arms for the M1 locus was then PCR amplified to include BglII and NsiI restriction sites and was cloned into pGS284. The resulting plasmid pGS284-eYFP M1 LFA RFA flank was then electroporated into λPir electro-competent bacteria for allelic exchange with WT MHV68 BAC in GS500 RecA+ *Escherichia coli*. To generate the M1st-eYFP virus, GS500 containing M1st. BAC [12] were crossed with λPir containing pGS284-XL9CD-CMV-YFP-F for allelic exchange. Following allelic exchange virus preparation was performed as previously described [8].

Flow cytometry: Single cell suspensions of splenocytes were prepared and resuspended in PBS supplemented with 2% fetal bovine serum. Samples were stained using standard procedures. Following initial FC receptor block (CD16/32), samples were stained with a master mix containing: CD138-PE, CD3e-PerCP, CD95-PE, GL7-APC, B220-APC-Cy7,

CD19-Pacific Blue. 1-2x10^6 events were recorded on BD LSRII flow cytometer and results were analyzed using FloJo software (Tree Star Inc).

Rapid amplification of cDNA ends (RACE) analysis: A20-HE2 cells were stimulated with 20ng/mL tetradecanoylphorbol acetate (TPA) for 48 hours prior to RNA isolation. NIH3T12 were infected with an MOI of 1.5 for 18 hours prior to RNA isolation. RNA was extracted using Trizol Reagent (Invitrogen Life Technologies) according to manufacturer's instructions and RNA concentration was determined. Prior to RACE analysis RT-PCR was performed to detect M1 and pol transcripts using primers described previously [10]. 5' and 3' RACE analysis was performed using GeneRacer Kit L1502-02 (Invitrogen Life Technologies) according to manufacturer's specifications. Gene specific primers were generated for detection of M1 transcript. For the first round of PCR M1ORF_Rd1_Fwd (5'-GGCCATTATGTGGACGTG AAGAGAATTGTAGGTAT-3') was used to amplify the 3' region and M1ORF_Rd1_Rvs (5'-CCTTGGTATCATCCTCAGGAAATGGGTAGGTTTCA-3') was used to amplify the 5' region. For the second round of PCR M1ORF_Rd2_Fwd (5'-GGAAAACTCTCCAGAGCTGCTGTCGTG GGGGATGAT-3') was used to amplify the 3' region and M1ORF_Rd2_Rvs (5'-GCCAG TGAGCTATGCTTTGGCCCAGTATGCAGGAA-3') was used to amplify the 5' region.

Generation of plasmids: M1 promoter luciferase constructs were cloned into pGL4.10 (Promega) using BglII and KpnI restriction sites. With the exception of the M1pIRF4mut1, M1pIRF4mut2, and G50ppRREm binding site mutants, inserts were

generated by PCR amplification of regions upstream of the M1 ORF, using WT BAC DNA as template, with primers listed in table 1. The M2 promoter construct was the generous gift from Dr. Shariya Terrell.

To generate M1pIRF4mut1 and 2 Overlapping PCR was used to introduce IRF4/IRF8 binding site mutations into the 197bp M1 promoter region corresponding to nt. 1960-1961 and nt. 1961-1963 in the viral for mutants 1 and 2 respectively. Amplification of a 118bp left flaking arm was done using 197bp forward primer (table 1) and reverse primers: (5'-TCTTTCTTGGTGTGTTCACTTCTAAACATG-3') and (5'-TCTTTCTTGGTGGGACCACTTC TAAACATG -3') for mutants 1 and 2 respectively. Amplification of a 70bp right flanking arm was done using 197bp reverse primer (table 1) and forward primers: (5'-CATGTTTAGAAGTGAACA CACCAAGAAAGA-3') and (5'-CATGTTTAGAAGTGGTCCCACCAAGAAAGA-3') for mutants 1 and 2 respectively. The left and right flanking arms were used as template and allowed to anneal for 6 rounds of the PCR cycle prior to the addition of the 197bp forward and reverse primers. The resulting amplicon was then cloned into pGL4.10.

To generate the ORF50ppRREm MHV68 WT BAC DNA was used as a template for overlapping PCR. In the first PCR round left and right flanking arms were generated using ProxPromF (5'-GATCGCTAGCTCTTTATAGGTACCAGGGAA-3') with ProxRREmR (5'-tcactctgttcaagaagttgcctgaggttcataaa-3'), and ProxPromR (5'-TAGCAGATCTGGTCACATCTG ACAGAGAAA-3') with ProxRREmF (5'-ttcattttcaggccatttatgaacctcaggcaact-3')respectively. These products were used as a template for a second round PCR amplifcation with primers ProxPromF and ProxPromR, and amplicons were cloned into pGL4.10

Expression constructs were cloned into pCDNA 3.1 (+) (Invitrogen) using NotI and XhoI restriction sites using primers listed in table 1. Both flag-tagged and non-tagged unspliced Rta were amplified from WT BAC DNA corresponding to viral genomic coordinates (66,761-69,374). Murine IRF4 was amplified from pMSCV-IRF4-IRES-GFP (a kind gift from Dr. Xiaozhen Liang).

All PCR amplification was carried out using high fidelity Phusion DNA polymerase (New England Biolabs), and sequence analysis confirmed completed plasmid constructs (Macrogen).

In vitro promoter assays: $5x10^5$ 293T cells were seeded into 6 well plates, the following day cells were transfected with 2.5µg firefly luciferase and protein expression plasmids and 10ng of pRL-TK (Promega) using TransIT 293T (Mirus). $1x10^6$ P3X63Ag8 cells were nucleofected with 5µg firefly luciferase plasmids using Ingenio Electroporation Solution (Mirus) using setting X-01 on the Amaxa nucleofector. Reactions were done in triplicate for each condition, and 2-4 independent experiments were conducted. 48 hours later cells were lysed using passive lysis buffer (25 mM Tris-phosphate pH 7.8, 2 mM DTT, 2 mM DCTA, 10% glycerol, 1% Triton X-100). P3X63Ag8 cells were assessed for firefly luciferase activity using 10µl lysate and 50µl luciferase assay reagent (LAR) (75 mM HEPES pH 8, 4mM MgSO4, 20 mM DTT, 100 µM EDTA, 53.0 µM ATP, 270 µM Coenzyme A, and 470 µM beetle Luciferin). A dual luciferase assay for firefly and renilla luciferase activity was performed on 293T cells using 10µl cell lysate and 50µl LAR, followed by the addition of 50µl Stop & Glo reagent (Promega). Light units were read on a TD-20/20 luminometer.

Nuclear extract and electrophoretic mobility shift assay: Nuclear extracts of P3X63Ag8 cells grown under normal conditions were made as previously described [115]. Briefly, cells were washed with PBS, pelleted cells, resuspended in ice cold hypotonic lysis buffer and incubated on ice for 15 minutes. 10% Nonidet P-40 was added at 1/20 final volume and nuclei were spun down. Nuclei were then washed in hypotonic lysis buffer, resuspended in high salt buffer, and incubated with vigorous shaking for 2-3 hours at 4°C. Supernatants were collected following centrifugation and aliquoted on dry ice and stored at -80°C. Following isolation protein content in nuclear extract was quantified using DC Protein Assay (BioRad), and western blot was performed to confirm presence of IRF4.

Electrophoretic mobility shift assay was performed using nuclear extracts as previously described [116]. Briefly, a binding reaction containing 10µg of nuclear extract, 0.2ng ^{32}P-labeled double stranded oligonucleotide probe containing IRF4 consensus binding sequence (underlined) (sense-5'-TTGGTGGTTTCACTTCTAAACA-3'), and 2µg poly (di-dC) was made up in binding buffer (10mM Tris-HCl (pH 7.5), 10mM HEPES, 50mM KCl, 1.1mM EDTA, and 15% glycerol, with 1.25mM DTT) and incubated on ice for 30 minutes. Supershift assays included 1µg of IRF4 antibody (clone M17, Santa Cruz Biotech.) or isotype control pSTAT1 antibody (clone Tyr 701, Santa Cruz Biotech.) incubated with nuclear extracts slow shaking at 4°C for 1 hour. Competition experiments were performed with 2X and 20X unlabeled oligonucleotides containing WT or mutated (underlined) IRF4 consensus binding sequence (sense 5'-TTGGTGGGACCACTTCTAAACA-3'). Nucleoprotein complexes were run on 5% native polyacrylamide gel in 0.5X Tris Buffered EDTA at 180V for 1 hour. Gel was dried

under vacuum and analyzed with PhosphorImager analysis (Typhoon 9410; Amerisham Bioscience)

Co-Immunoprecipitation: 10cm dishes were seeded with $4x10^6$ 293T and were transfected the next day using TransIT-293T (Mirus). 48 hours later cells were washed 2 times with ice cold PBS, and lysed while rocking at 4°C, in 1mL Triton X Lysis Buffer (50mM Tris HCl pH 7.4-7.5, 150mM NaCl, 1mM EDTA, 0.1% Triton; supplemented with 1mM NaF, 1mM activated Na3V04, and Roche EDTA free protease inhibitor cocktail tablet for 50mL volume). Following lysis, membranes were pelleted and lysates were transferred to pre-chilled tubes. Protein concentration was determined using DC Protein Assay (BioRad). 1mg of cell lysate was precleared with prepared protein G beads (Pierce), then 8µg of IRF4 antibody (clone M17, Santa Cruz Biotech) or flag antibody (clone M2, Sigma) was added and lysates were incubated overnight at 4°C. Lysates were transferred to freshly prepared protein G beads for binding and were incubated at 4°C for 2 hours. Following wash, protein was eluted and samples were electrophoresed on 10% polyacrylamide gels, and transferred onto nitrocellulose membranes for western blot. The following detection antibodies were used: IRF4 (clone H140, Santa Cruz Biotech.) and Flag (clone M2, Sigma).

RESULTS

M1 is expressed in a subset of MHV68 infected splenocytes

To identify cellular reservoirs in which the M1 gene is expressed *in vivo,* we generated a series of recombinant viruses that express yellow fluorescent protein (YFP) to mark infected cells. For detection of M1 promoter activity, the M1 coding sequence was replaced with that encoding YFP, creating a M1 promoter-driven YFP mutant (Figure 1A). This strategy allows detection of the cellular reservoirs in which M1 is expressed during infection. Additionally, two important controls were used: MHV68-YFP, in which the YFP transgene under the control of the HCMV IE promoter was cloned into a neutral locus in the viral genome (efficiently marking MHV68 infected B cells and plasma cells) [8]; and (ii) MHV68-M1st.YFP, which contains the M1 translational stop mutation (M1-null virus) in the context of the YFP transgene cloned into the neutral locus (Figure 1B). As M1 has previously been identified as a non-essential for both virus replication and for the establishment of latency *in vivo* [117], we did not anticipate that the M1pYFP recombinant would change the cellular reservoirs infected by MHV68. However, to formally address this issue, we have included analyses of the MHV68-M1st.YFP virus – which like the M1pYFP lacks a functional M1 gene.

Analysis of MHV68 infection of splenocytes at day 14 post-infection revealed robust marking of splenocytes by both the MHV68-YFP and MHV68-M1stYFP viruses (Figure 2). We have previously noted that there is significant mouse to mouse variation in the frequency of infected splenocytes for a given virus [118], and have recently determined that this directly correlates with the frequency of the $CD4^+$ T follicular helper (T_{FH}) response [119]. For these analyses we observed on average ca. 0.5% and 1.0% of

splenocytes were YFP^+ for the MHV68-YFP and MHV68-M1stYFP viruses, respectively (Figure 2). The latter result confirms that M1 function is dispensable for the establishment of latency in splenocytes. In contrast, only ca. 0.04% of splenocytes were YFP^+ with the M1pYFP virus, indicating that the M1 promoter is active in only ca. 5-10% of infected splenocytes.

The majority of M1 expression is detected in MHV68 infected plasma cells

We have previously shown that the majority (ca. 70-90%) of virally infected B cells, as indicated by YFP expression, exhibit a germinal center phenotype [8,9]. Individual mice were assessed for YFP marking and, consistent with previous observations, we found a similar frequency of virus infected (YFP^+) B cells with a germinal center phenotype for mice infected with either the MHV68.YFP or MHV68-M1st.YFP viruses, both showing an average of ca. 70% (Figure 3). These results further substantiate that a functional M1 gene is dispensable for establishment of MHV68 latency in B cells. In contrast, few infected germinal center B cells were marked by the M1pYFP virus (an average of ca. 20% of YFP^+ cells) – indicating that the majority of M1 expressing cells do not have a germinal center B cell phenotype. Based on the ca. 10-fold lower frequency of splenocytes marked by the M1pYFP virus (see Figure 2), we estimate that M1 promoter activity is only detectable in ca. 5% of infected germinal center B cells. Based on these results it is clear that M1 is predominantly expressed in some other MHV68 infected cellular reservoir.

The other major cell population in the spleen that is infected by MHV68 are plasma cells ($CD138^{hi}$, $B220^{low}$) [8,9]. During infection, virus infection (YFP marking) of splenic

plasma cells reaches peak levels at day 14 post-infection (ca. 10-20% of virus infected splenoctyes) and begins to wane by day 18 post-infection (ca. 5-10% of virus infected splenocytes) [8]. We observed marking of splenic plasma cells for both MHV68-YFP and MHV68-M1st.YFP infected mice at day 14 post-infection consistent with previous observations, with ca. 10% YFP^+ cells exhibiting a plasma cell phenotype (no significant difference between these 2 groups) (Figure 4). Strikingly, when assessing YFP marking of the splenic plasma cell population by the M1pYFP virus, the vast majority of YFP^+ cells exhibited a plasma cell phenotype (on average >75% of YFP^+ cells) (Figure 4). Thus, this strongly argues that M1 gene expression is largely limited to the infected plasma cell population. Notably, MHV68 reactivation from latently infected splenocytes is tightly linked to plasma cell differentiation [9], which suggests that M1 expression is coupled to virus reactivation from B cells. Finally, when considering the frequency of M1pYFP marked cells with the frequency of MHV68-YFP and MHV68-M1st.YFP marked splenic plasma cells, it appears that the majority of virus infected plasma cells express M1.

Identification and initial characterization of the M1 gene promoter

Having identified the reservoir where M1 is expressed *in vivo,* we sought to characterize the structure of the M1 transcript and to identify the M1 promoter. Rapid amplification of cDNA ends (RACE) was done to identify the transcript initiation and termination sites in two cell lines: (i) infected NIH3T12 fibroblasts; and (ii) reactivated A20-HE2 cells. A20-HE2 cells are a stable lymphoblast B cell line which carry the MHV68 genome where viral reactivation can be induced by tetradecanoylphorbol acetate

(TPA) [120]. RNA and protein were collected from both cell lines and lytic gene expression was confirmed prior to analysis (data not shown). Transcript analysis revealed four initiation sites and a single termination site from an unspliced transcript (Figure 5A, 5B). Though all transcript initiation sites were found in infected 3T12 cells, only transcripts starting at bp 2003 and bp 2013 were detected from reactivated A20-HE2 cells. The sizes of the predicted unspliced M1 transcripts were confirmed by northern analyses of RNA prepared from: (i) TPA stimulated A20-HE2 cells (a MHV68 latently infected B cells); and (ii) MHV68 infected NIH 3T12 fibroblasts (data not shown).

To identify the regulatory elements controlling M1 gene expression we next set out to characterize the M1 promoter. Serial truncations of the putative M1 promoter region were cloned into a luciferase reporter vector and tested for promoter activity in a variety of cell lines. Notably, minimal activity was detected in the murine B cell lines A20, WEHI, NSO, and BCL1-3B3 (data not shown) – perhaps consistent with the failure to observe significant M1 promoter-driven YFP activity in most splenic B cell populations with the MHV68-M1pYFP virus in mice. In addition, we failed to detect significant activity from these reporter constructs in the murine macrophage cell line RAW264.7 (data not shown). However, when these reporter constructs were transfected into the P3X68Ag8 murine plasmacytoma cell line significant basal promoter activity was observed (Figure 6). Similar levels of M1 promoter-driven luciferase activity were observed for the longer M1 promoter constructs (M1p/-1025bp, M1p/-525bp, and M1p/-245bp), while truncation of sequences upstream of -100bp significantly decreased activity (Figure 6). Activity was further decreased to near background levels when sequences upstream of -50bp were deleted (Figure 6).

The region upstream of the M1 transcription initiation sites was screened for the presence of candidate transcription factor binding sites [University of Pennsylvania Transcription Element Search System (TESS)]. TESS and manual sequence analyses identified a number of candidate transcription factor binding sites for NFκB, GATA3, IRF8/IRF4, and RBPJκ. Because M1 promoter activity was detected in plasma cells *in vivo*, interferon regulatory factor 4 (IRF4), a transcription factor upregulated in plasma cells which plays a critical role in plasma cell differentiation as well as immunoglobulin class switch recombination ([121-123] and reviewed in [124]), was of particular interest.

To characterize IRF4 binding to the candidate IRF site in the M1 promoter, an electrophoretic mobility shift assay (EMSA) was carried out (Figure 7A). EMSA was performed using nuclear extracts from P3X63Ag8 cells grown under normal conditions, along with a [^{32}P]-labeled oligonucleotide probe containing the candidate M1 promoter IRF4 binding site. As expected we observed shifted complexes, which could be competed away using unlabeled double stranded DNA probes containing the M1p IRF4 binding site, but not with a competitor containing an IRF binding site mutation which has previously been shown to disrupt IRF8 binding with DNA [125] (Figure 7A). Furthermore, binding of IRF4 was confirmed by supershift analysis using an antibody against IRF4 (Figure 7A). This analysis was extended by generating M1 promoter-driven luciferase reporter constructs in which mutations were introduced into the IRF binding site. Two mutations in the core interferon response sequence, which have previously been shown to ablate IRF8 DNA:protein interaction [125], were introduced into the M1 promoter. Notably, either mutation led to a significant loss in basal M1 promoter activity (ca. 8-fold decrease in promoter activity) (Figure 7B).

Viral Rta and cellular IRF4 synergize to activate transcription from the M1 promoter

Several studies have established a link between gammaherpesvirus reactivation from latency and plasma cell differentiation [9,29-34]. Given that our data shows: (i) M1 promoter expression is detected from plasma cells during *in vivo* infection; (ii) basal M1 promoter activity requires a functional IRF4 site; and (iii) viral reactivation is linked with plasma cell differentiation, we set out to evaluate whether the M1 promoter is responsive to the MHV68 viral lytic transactivator Rta. Expressing increasing amounts of Rta with an M1 promoter-driven reporter construct in the P3X63Ag8 plasmacytoma cell line resulted in a dosage dependent increase in M1 promoter activity (Figure 8A). Moreover, the ability of Rta to efficiently transactivate the M1 promoter in the P3X63Ag8 cell line was dependent on the presence of an intact IRF4 binding site (Figure 8B). To further assess whether Rta functionally synergizes with IRF4 to activate the M1 promoter, we chose a cell line (293T cells) which lacks expression of Rta and IRF4. In 293T cells we observed that either factor alone led to very modest increase in M1 promoter activity (ca. 5-10 fold) (Figure 8C). However, when the two factors were co-expressed there was a significant increase in promoter activity (ca. 250-fold) (Figure 8C). Importantly, disruption of the IRF4 binding site dramatically impaired the ability of IRF4 and Rta to synergistically activate the M1 promoter (Figure 8C).

Based on the synergy between Rta and IRF4 in activating the M1 promoter, we assessed whether these factors can physically interact with each other. A co-immunoprecipitation was performed with cell lysates from transfected 293T cells. Immunoprecipitation with anti-IRF4 antibody, followed by anti-Flag detection of Rta,

resulted in detection of a 90 kD band corresponding to Rta that was present only when Rta and IRF4 were co-expressed in 293T cells (Figure 8D). Following detection of Rta the blot was stripped and probed for IRF4 to confirm expression of the 52kD band corresponding to IRF4. IRF4 was detected in whole cell lysates and immunoprecipitated samples containing IRF4. The reciprocal blot using anti-flag for immunoprecipitation and anti-IRF4 for detection showed a 52kD band corresponding to IRF4. Additionally, Rta was detected from whole cell lysates and immunoprecipitated samples containing Rta. These results are consistent with a physical interaction between Rta and IRF4 that likely facilitates that observed synergy of these factors in activating M1 gene expression.

Several investigators have identified Rta responsive elements in viral promoters for both KSHV and MHV68 [126-130]. To date, the known Rta responsive genes are either regulated through: (i) direct interaction of Rta and DNA through a core Rta binding sequence; or (ii) Rta DNA binding is facilitated through protein-protein interactions – in the case of KSHV Rta, through interaction with the cellular transcription factor RBPJκ (reviewed in [131]). In MHV68 gene 57 promoter, it appears that both types of Rta response elements may be utilized – although a role for RBPJκ in MHV68 Rta activation has not been formally demonstrated [126,127]. Interestingly, neither of the binding sites identified in the MHV68 gene 57 promoter are present in the M1 promoter, suggesting a novel Rta interaction motif. To identify the Rta response element(s) in the M1 promoter, a series of promoter truncations were generated and tested in the P3X63Ag8 plasmacytoma cell line. A candidate Rta response element was identified by evaluating promoter constructs which lost the ability to be transactivated by Rta. Using this approach we identified a putative Rta response element between -88 and -76 bp in the M1

promoter (Figure 9A). This 12bp sequence (5'-GGTCAGAAGGCT-3') failed to show homology to any known Rta response element identified in the gammaherpesvirus family. However, a screen of the MHV68 genome identified a number of candidate sites upstream of other MHV68 replication-associated genes which share significant homology with the core 5'-TCAGAAG-3' sequence in the putative M1 promoter Rta response element (Figure 9B). Mutations of the three most central residues of the predicted Rta response element (see M1pRREm in Figure 9B) resulted in an ca. 10-fold reduction in transactivation in the plasma cell line (Figure 9C), as well as an ca. 6-fold reduction in Rta and IRF4 synergistic transactivation of the M1 promoter in 293T cells (Figure 9D).

The novel Rta response element in the M1 promoter is conserved in other viral promoters

With the identification of a novel Rta response element, we next wanted to evaluate whether this element was functional in other viral promoters that appear to contain this RRE (see Fig 9C). Reporter constructs for the putative promoter regions of the M2 gene (encoding an adaptor protein involved in B cell signaling), ORF8 (encoding glycoprotein B), ORF22 (encoding glycoprotein H), ORF63 (encoding a tegument protein), and ORF73 (encoding the MHV68 Latency Associated Nuclear Antigen (LANA) homolog) were generated. In addition, the gene 50 proximal, distal, and N4/N5 promoter constructs previously described in Wakeman *et al.* [110] were evaluated for response to Rta expression. We observed varying levels of promoter response, with the strongest responses from ORF50pp, ORF8p, ORF22p, ORF63p, intermediate responses from the M1p, ORF50dp and ORF50 N4/N5p, and weak responses from M2p and ORF73p

(Figure 10A). To further investigate the role of the Rta response element in the observed transactivation, we engineered the same three nucleotide mutation used in the M1p (Figure 9B) into the proximal ORF50 promoter (Figure 10B). Notably, mutation of this sequence resulted in a 38-fold reduction in Rta transactivation (Figure 10C). With the exception of the M1 promoter, all of the other reporter constructs we failed to show any syngeristic activation by the co-expressoin of Rta and IRF4 (data not shown).

DISCUSSION

Here we described the characterization of a recombinant MHV68 in which a gene encoding a fluorescent protein (YFP) has been introduced into the viral genome in place of a non-essential viral gene. This approach allows identification of the site and timing of viral gene expression *in vivo* for viral genes that are dispensable for replication and/or dissemination of virus. For viral genes that play an important role in either replication or dissemination, other approaches - such as the generation of fusion gene products - may be required. Information obtained from such studies can provide significant insights into viral gene function and their mode of action. In the case of M1, these analyses led to identification of the predominant cellular reservoir in which M1 is expressed, and subsequent identification of transcription factors involved in regulating M1 gene transcription.

Coppola *et al.* have previously demonstrated the ability of either $B220^+$ cells, or T cell depleted splenocytes, isolated from MHV68 infected mouse spleen to stimulate $V\beta4^+$ $CD8^+$ T cell hybridomas [109]. However, they also found that B cell depleted splenocytes from MHV68 infected mice retained $V\beta4^+$ $CD8^+$ T cell stimulatory activity – which they interpreted as the presence of other non-B cells populations in the spleen that are infected by MHV68. However, based on our findings that M1 expression is largely restricted to plasma cells, it seems unlikely that either the isolation or depletion of $B220^+$ cells would efficiently capture or eliminate, respectively, all MHV68 infected plasma cells. As such, one would anticipate $V\beta4^+$ $CD8^+$ T cell stimulatory activity in both the enriched and depleted fractions. This interpretation is consistent with the complete failure to observe any expansion of $V\beta4^+$ $CD8^+$ T cells in MHV68 infected B cell-deficient mice [35,36] –

even though we have previously shown robust MHV68 infection in the spleens of B cell-deficient mice under some experimental conditions (intraperitoneal inoculation of virus) in the absence of any detectable $V\beta4^+$ $CD8^+$ T cell expansion [14,36].

As we have previously shown, MHV68 reactivation in the spleen is tightly linked to plasma cell differentiation [9]. The observation that M1 is predominantly expressed in plasma cells thus suggested that M1 expression is linked to virus reactivation/replication. This was substantiated by demonstration that Rta can strongly transactivate the M1 promoter in a plasma cell line (see Figure 8A). We propose that during infection, in response to viral reactivation and the transition from germinal center or memory B cell to plasma cell, M1 expression is activated by the synergistic effects of viral Rta and cellular IRF4. M1 protein is secreted from infected plasma cells and, by an undefined mechanism, stimulates $V\beta4^+$ $CD8^+$ T cell activation and expansion. It is likely that M1 activates $V\beta4^+$ $CD8^+$ T cells via a mechanism similar to classic viral super-antigens [12]. Activation does not require classical MHC class I molecules [109,132], but does require an intact M1 protein - we have previously shown that proteolytic digestion, or denaturation of recombinant M1 renders it unable to activate $V\beta4^+$ $CD8^+$ T cell hybridomas [12].

$V\beta4^+$ $CD8^+$ T cells have been shown to traffic throughout the body, and can be detected in the blood, spleen, liver, lung, and peritoneal cavity [12,13,113]. These cells show cytolytic activity [113] and adopt an effector memory phenotype where upon re-stimulation with recombinant M1 protein *ex vivo* they degranulate and produce INFγ and TNF α ([12], unpublished observations). As IFNγ has been shown to regulate MHV68 reactivation from macrophages in the peritoneum, but not reactivation from splenic B cells [15], we would predict that the $V\beta4^+$ $CD8^+$ T cells traffic to sites in which infection

is less tightly controlled, to suppress MHV68 reactivation through the secretion of IFNγ in a paracrine fashion. We find it noteworthy that MHV68 M1-null infected mice exhibit hyper-reactivation in the peritoneal cavity and persistent viral replication in the lung [11,12,18], further underscoring the importance of M1 expression in controlling viral infection.

Our findings demonstrate that the M1 promoter is regulated by MHV68 Rta, a viral transcription factor that is essential for induction of viral reactivation. Rta activation of the M1 promoter synergizes with IRF4, a transcription factor that plays a critical role in both plasma cell differentiation and immunoglobulin class switch recombination. Furthermore, we show that this interaction is likely mediated through both DNA-protein interactions with the M1 promoter sequence, as well as protein-protein interactions between Rta and IRF4. We propose that during MHV68 latency, the viral latency-associated gene product M2 is expressed in a sub-population of latently infected germinal center and memory B cells [23] leading to expression of high levels of IRF4 [133]. M2 appears to play an important role in virus reactivation from latency: (i) MHV68 M2 null mutants exhibit a profound reactivation defect from B cells, but not latently infected macrophages [134,135]; (ii) exogenous expression of M2 in primary B cells results in acquisition of a pre-plasma memory phenotype [136]; (iii) M2 can drive B cell differentiation of a B lymphoma cell line *in vitro* [9]; (iv) M2 is required for efficient immunoglobulin class switch in infected B cells *in vivo* [9]; and (v) plasma cells are the primary source of viral reactivation from the spleen [9]. Taken together these data suggest that MHV68 is capable of driving plasma cell differentiation, and concurrent with this differentiation, viral reactivation. As a result of this transition, the increased

expression of the transcription factors Rta and IRF4 lead to induction of M1 expression in plasma cells (Figure 11).

That M1 is responsive to viral Rta and cellular IRF4 highlights the importance of tightly regulated gene expression in response to host and viral cues. This promotes cell type specific expression coordinated with viral reactivation. Furthermore, the interaction with Rta and IRF4 suggests a conserved strategy for gene regulation in MHV68, allowing for better control of Rta responsive gene expression. In fact numerous lytic genes in MHV68 appear to share the Rta response element identified in the M1 promoter (Figure 9B).

Though our efforts to find other viral genes that are similarly responsive to the concerted effects of Rta and IRF4 were unsuccessful, we find it attractive to speculate that the partnership of Rta and IRF4 or other cellular transcription factors may mediate their gene expression in a cell type specific manner. However, many of the genes we evaluated showed response to the novel Rta response element. Our analysis was limited to the putative promoter regions of ORF50, ORF8, ORF22, ORF63, ORF73, and M2. However, many of these genes play critical role in the biology of the virus, either as structural genes- ORF8 and ORF 22 are both surface glycoproteins, or as genes involved initiating infection- ORF63 is a tegument protein; so it is not surprising to find a significant response to Rta but lack of synergy with IRF4. Furthermore, some of the candidate genes are known to be involved in viral latency, ORF73- or murine latency associated nuclear antigen (mLANA) a homolog of EBV and KSHV LANA, has many functions including: viral replication, episomal maintenance, transcriptional regulation, and dysregulation of cell cycle and cell division (reviewed in [137]). M2, a latency

associate protein appears to play roles in both maintenance and establishment of latency, as well as in viral reactivation [133,136,138]. We therefore find it plausible that these genes would have less stringent requirements for cell specific expression, and that other unidentified genes, might be regulated by Rta and IRF4. Additionally, due to the differing functions of these genes in MHV68 biology, we were not surprised that in our studies we found differing levels of Rta responsiveness. Future studies using genome wide analyses will be necessary to identify genes which are temporally regulated by viral and host factors including Rta and IRF4.

Our identification of a partnered interaction between Rta and IRF4 suggests a conserved method for regulating MHV68 viral gene expression. Moreover, this mechanism appears throughout the gammaherpesviruses family as several studies have shown that Rta is capable of binding DNA through orchestration of complex protein-protein interactions. In KSHV, kRta has been shown to directly interact with cellular Oct1 and RBPJκ to regulate the KSHV bZip promoter [129]. This interaction with RBPJκ is maintained through a tetrameric protein complex of kRta flanking RBPJκ, and is mediated through a core "CANT" DNA repeat element found in the Mta promoter sequence [128]. Notably, kRTA has also been found to interact with viral IRF4 (vIRF4), one of several viral IRF homologs encoded by KSHV which in the case of vIRF4 is involved in counteracting innate antiviral defenses mediated by interferons to regulate vIRF1, vIRF4, PAN, and ORF57 gene expression [130].

In summary, the data reported here defines the timing and location of M1 expression during *in vivo* infection using a recombinant reporter virus – demonstrating that M1 is predominantly expressed from plasma cells. Furthermore, M1 gene

transcription in plasma cells is driven by the viral immediate-early Rta in conjunction with cellular IRF4 – which potently synergize with each other to activate M1 gene transcription. Whether other viral (and perhaps cellular genes) are co-regulated by Rta and IRF4 remains to be determined, and will be the topic of future work. However, we find it interesting to speculate that this might be an effective strategy to target viral replication-associated gene expression in plasma cells.

ACKNOWLEDGEMENTS

We would like to thank Hongyan Guo, Laurie T. Krug, and Alexis Santana for their technical guidance and suggestions, Lisa Gargano for technical help, and the members of the Speck lab for their helpful comments and suggestions.

FIGURES

Figure 1.

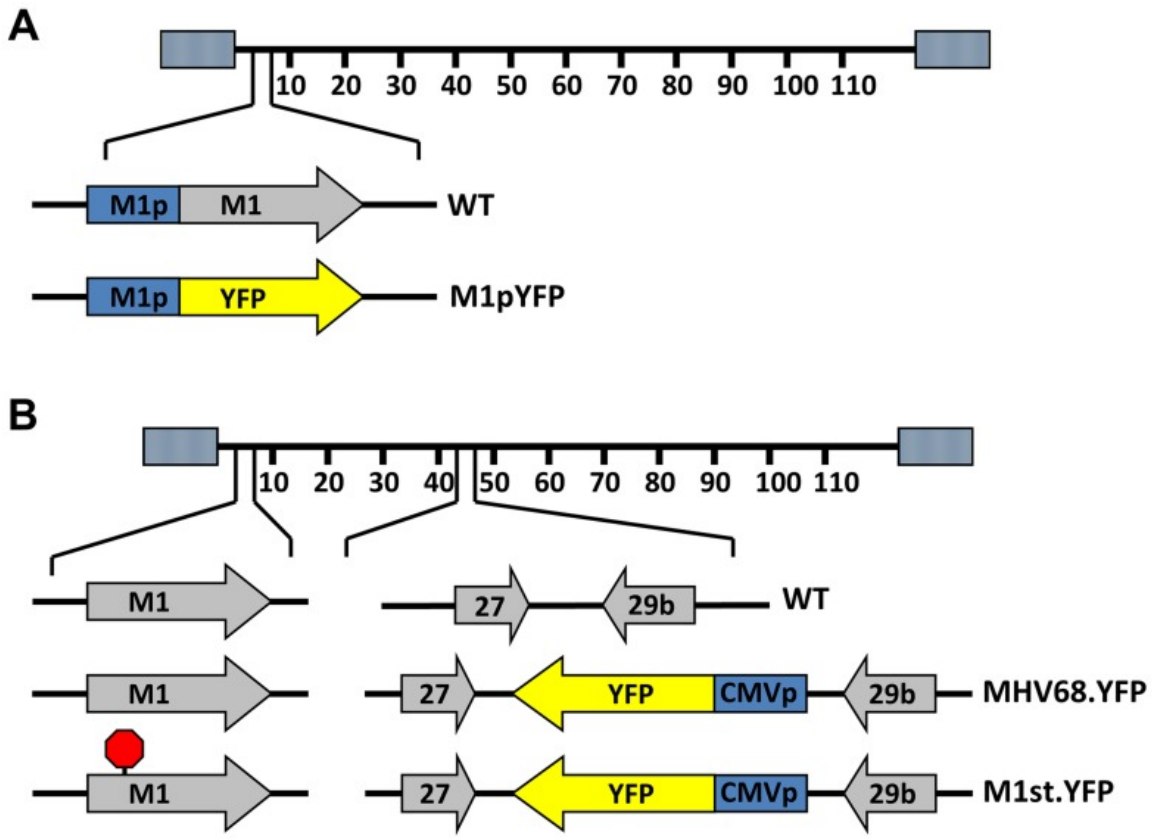

Figure 2.

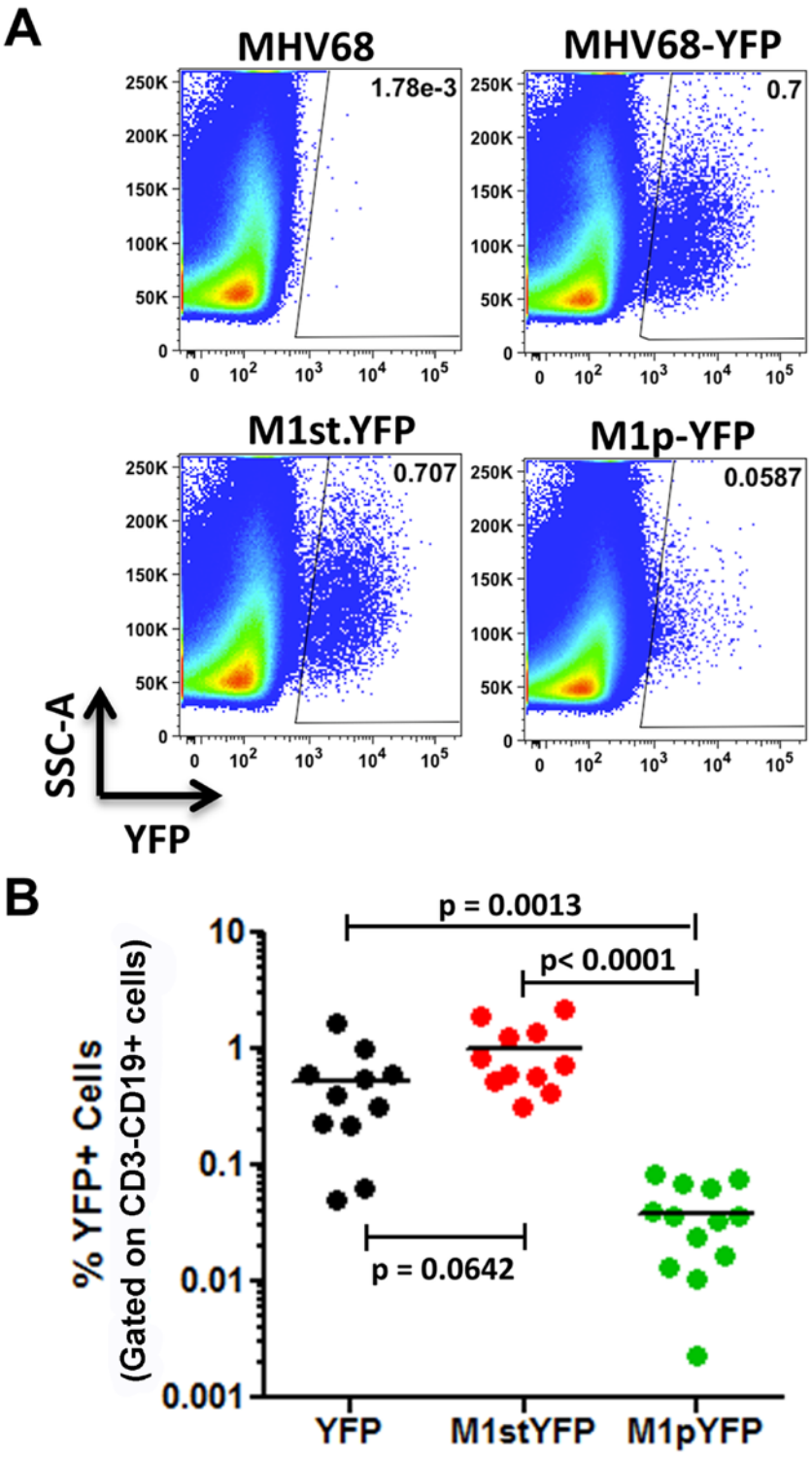
A
MHV68
1.78e-3
MHV68-YFP
0.7
M1st.YFP
0.707
M1p-YFP
0.0587
SSC-A
YFP
B
p = 0.0013
p< 0.0001
p = 0.0642
% YFP+ Cells
(Gated on CD3-CD19+ cells)
YFP
M1stYFP
M1pYFP

Figure 3.

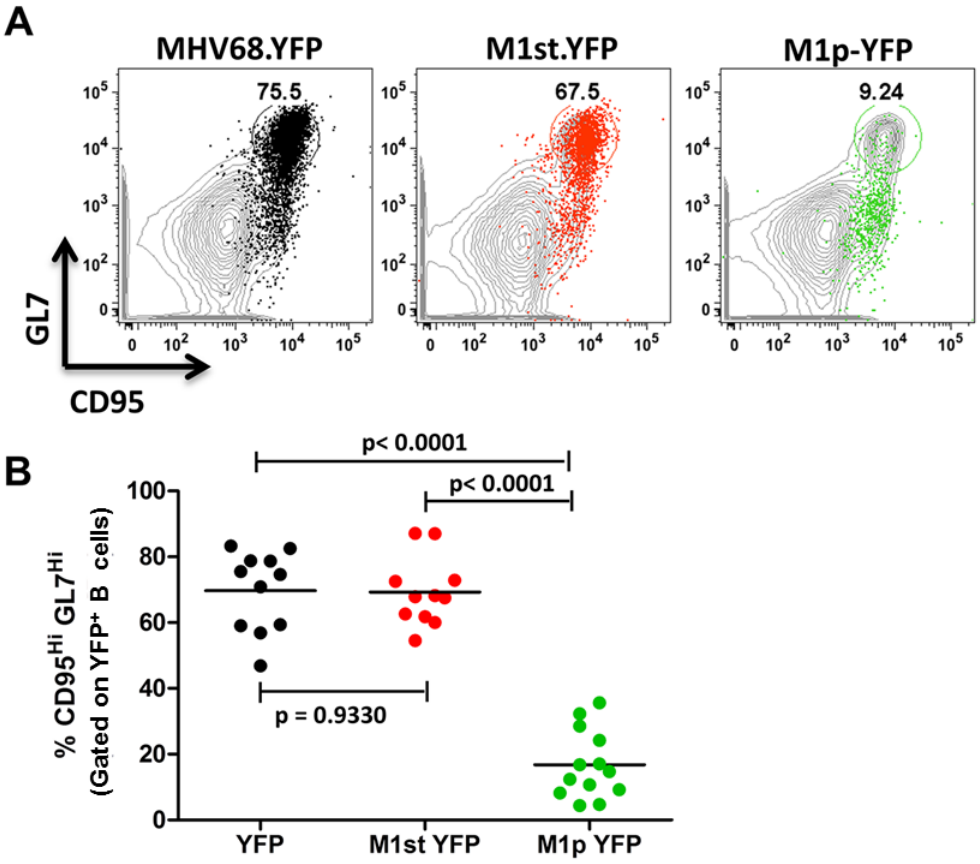
A
MHV68.YFP
M1st.YFP
M1p-YFP
75.5
67.5
9.24
GL7
CD95
B
p< 0.0001
p< 0.0001
p = 0.9330
% CD95Hi GL7Hi
(Gated on YFP+ B cells)
YFP
M1st YFP
M1p YFP

Figure 4.

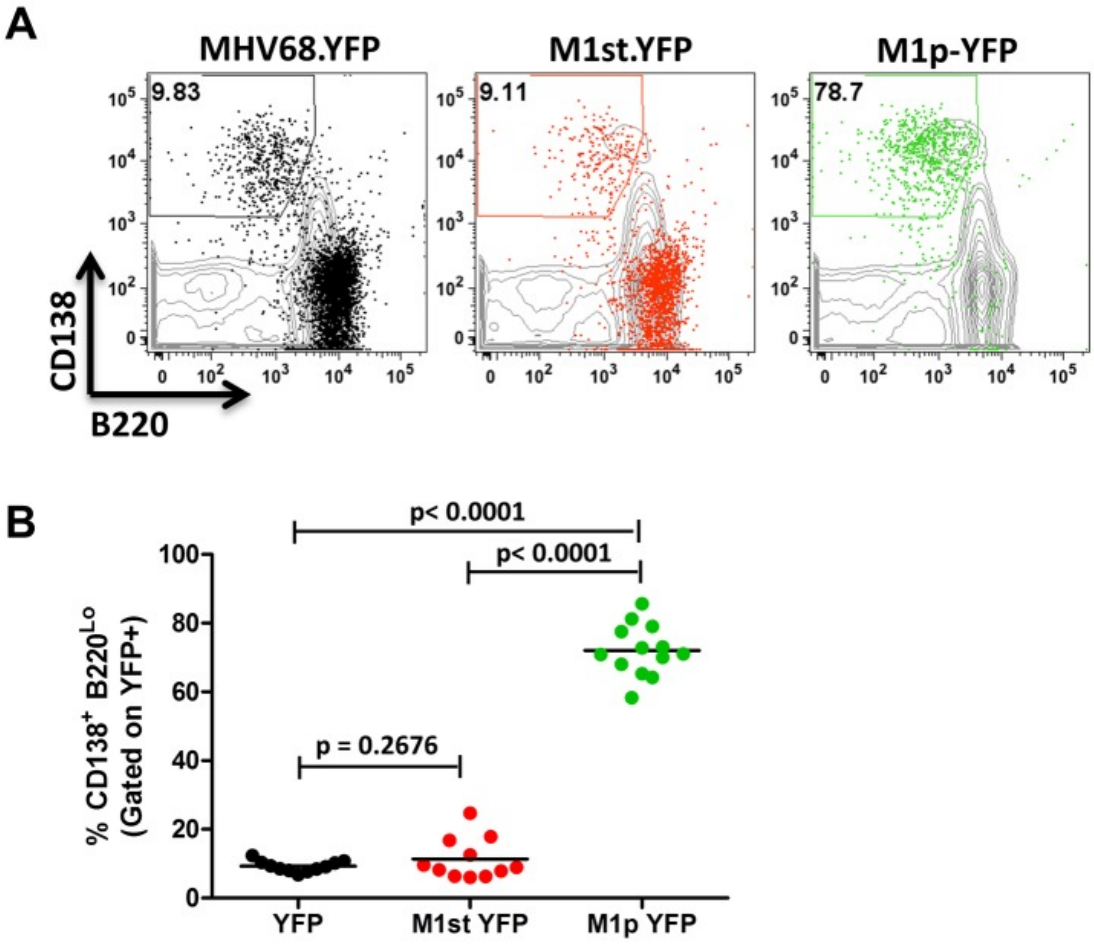
A
MHV68.YFP
M1st.YFP
M1p-YFP
9.83
9.11
78.7
CD138
B220
B
p< 0.0001
p< 0.0001
p = 0.2676
% CD138+ B220Lo
(Gated on YFP+)
YFP
M1st YFP
M1p YFP

Figure 5.

A

Transcript Start Site (genomic coordinate)	Lytic Infection NIH-3T12	Reactivation A20-HE2
1853	9	0
2003	15	4
2013	11	17
2069	1	0

B

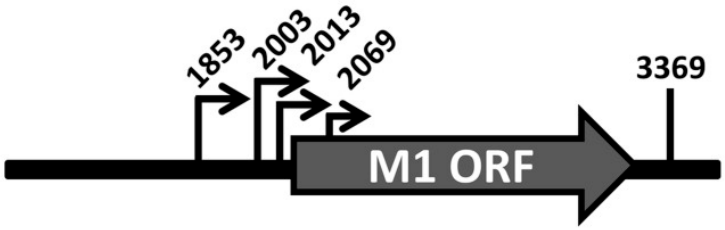

Figure 6

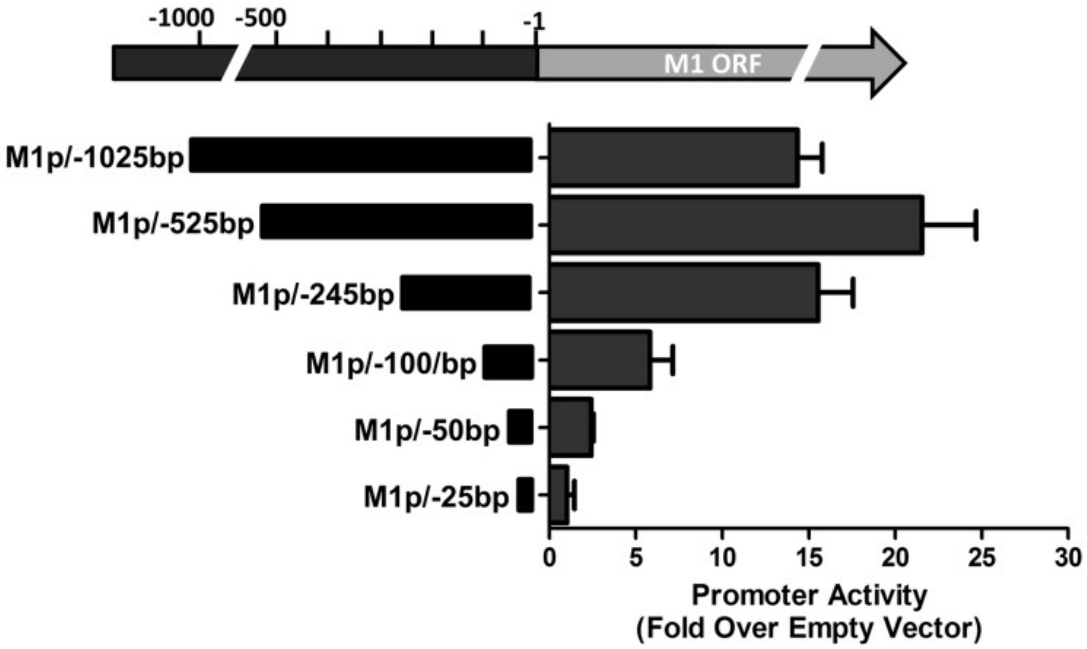
-1000
-500
-1
M1 ORF
M1p/-1025bp
M1p/-525bp
M1p/-245bp
M1p/-100/bp
M1p/-50bp
M1p/-25bp
0
5
10
15
20
25
30
Promoter Activity
(Fold Over Empty Vector)

Figure 7.

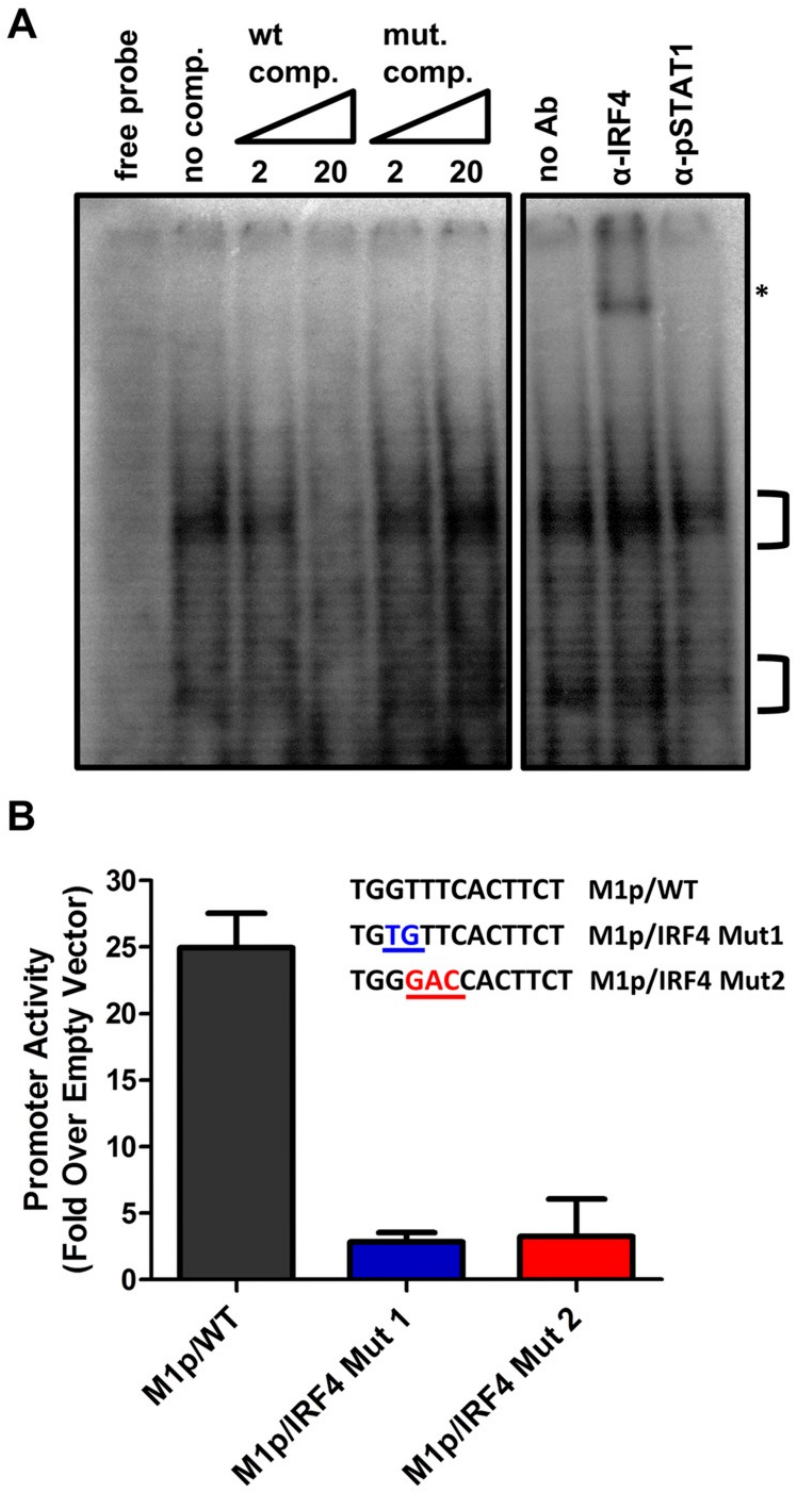
A
free probe
no comp.
wt comp.
2
20
mut. comp.
2
20
no Ab
α-IRF4
α-pSTAT1
*
B
Promoter Activity (Fold Over Empty Vector)
30
25
20
15
10
5
0
TGGTTTCACTTCT M1p/WT
TGTGTTCACTTCT M1p/IRF4 Mut1
TGGGACCACTTCT M1p/IRF4 Mut2
M1p/WT
M1p/IRF4 Mut 1
M1p/IRF4 Mut 2

Figure 8.

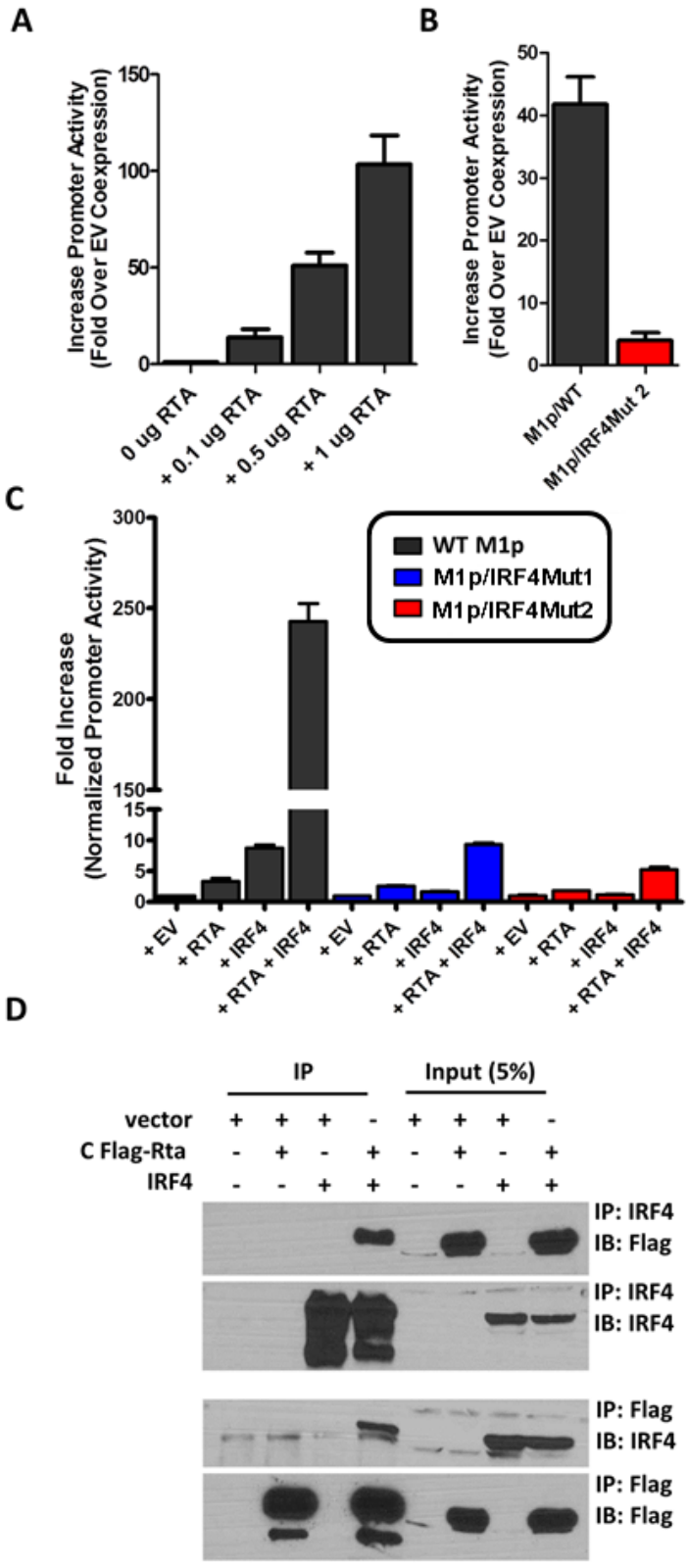
A
Increase Promoter Activity (Fold Over EV Coexpression)
150
100
50
0
0 ug RTA
+ 0.1 ug RTA
+ 0.5 ug RTA
+ 1 ug RTA
B
Increase Promoter Activity (Fold Over EV Coexpression)
50
40
30
20
10
0
M1p/WT
M1p/IRF4Mut 2
C
Fold Increase (Normalized Promoter Activity)
300
250
200
150
15
10
5
0
WT M1p
M1p/IRF4Mut1
M1p/IRF4Mut2
+ EV
+ RTA
+ IRF4
+ RTA + IRF4
D
IP
Input (5%)
vector
C Flag-Rta
IRF4
IP: IRF4
IB: Flag
IP: IRF4
IB: IRF4
IP: Flag
IB: IRF4
IP: Flag
IB: Flag

Figure 9.

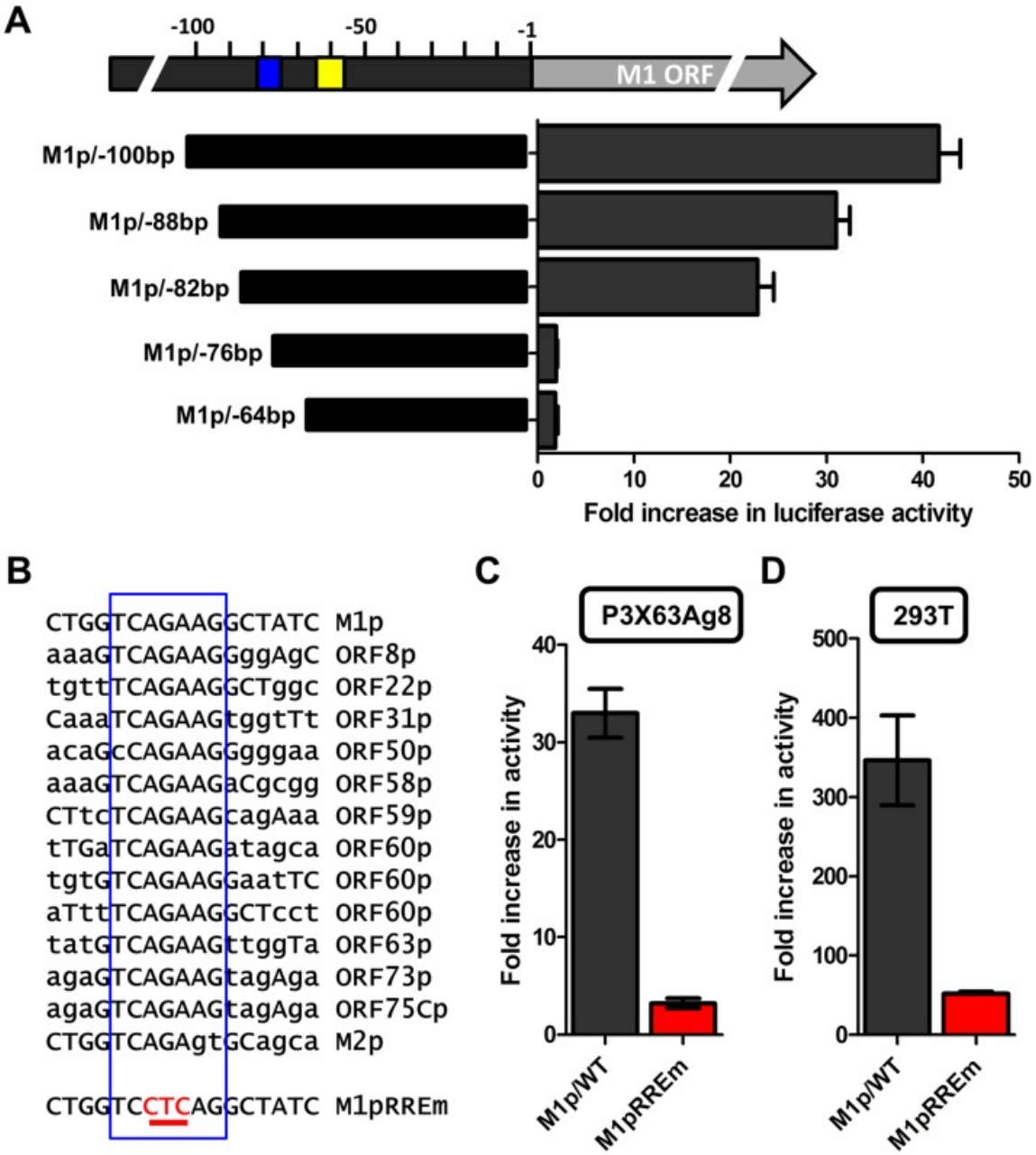
A
-100
-50
-1
M1 ORF
M1p/-100bp
M1p/-88bp
M1p/-82bp
M1p/-76bp
M1p/-64bp
0
10
20
30
40
50
Fold increase in luciferase activity
B
CTGGTCAGAAGGCTATC M1p
aaaGTCAGAAGGggAgC ORF8p
tgttTCAGAAGGCTggc ORF22p
CaaaTCAGAAGtggtTt ORF31p
acaGCCAGAAGGgggaa ORF50p
aaaGTCAGAAGaCgcgg ORF58p
CTtcTCAGAAGcagAaa ORF59p
tTGaTCAGAAGatagca ORF60p
tgtGTCAGAAGGaatTC ORF60p
aTttTCAGAAGGCTcct ORF60p
tatGTCAGAAGttggTa ORF63p
agaGTCAGAAGtagAga ORF73p
agaGTCAGAAGtagAga ORF75Cp
CTGGTCAGAgtGCagca M2p
CTGGTCCTCAGGCTATC M1pRREm
C
P3X63Ag8
Fold increase in activity
40
30
20
10
0
M1p/WT
M1pRREm
D
293T
Fold increase in activity
500
400
300
200
100
0
M1p/WT
M1pRREm

Figure 10.

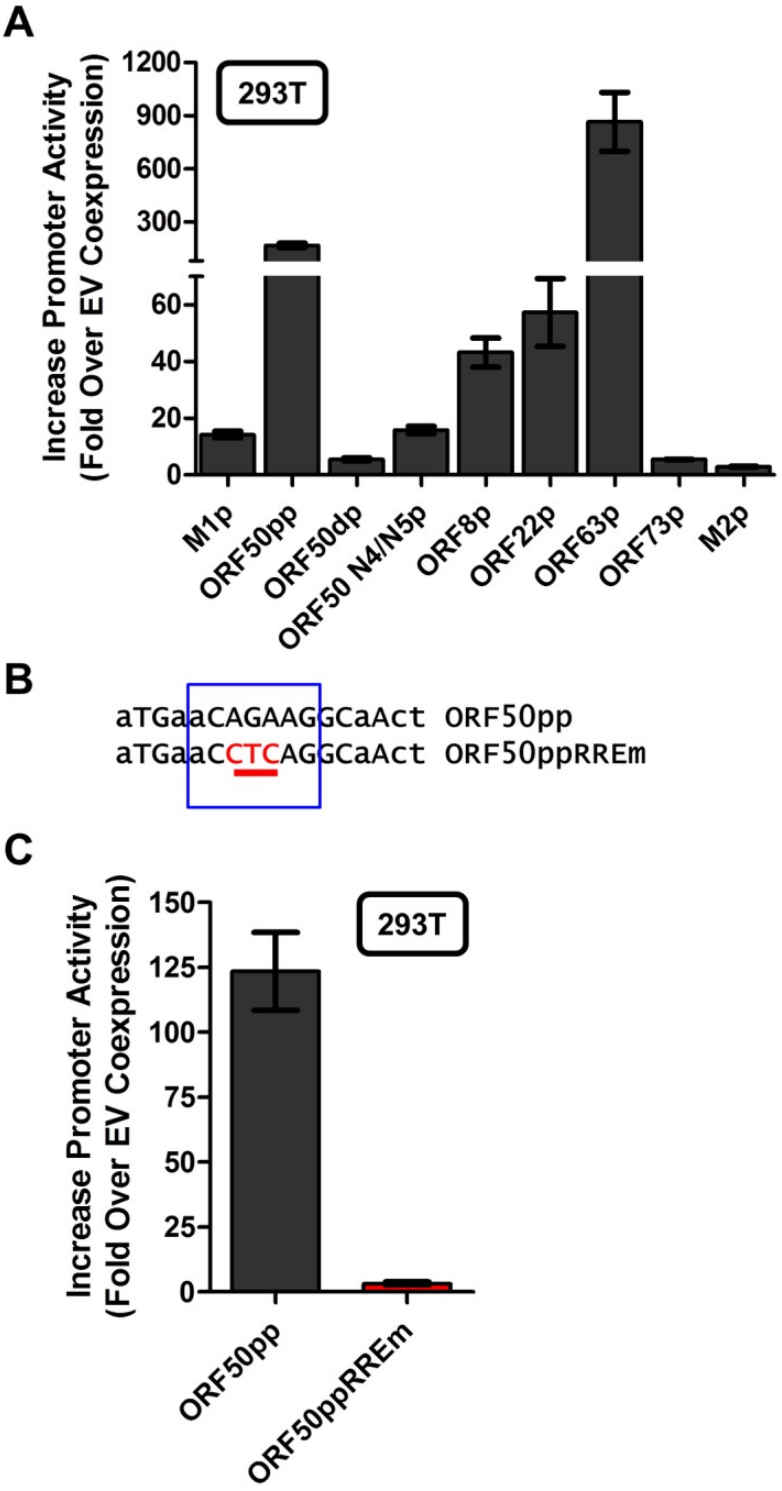
A
293T
Increase Promoter Activity
(Fold Over EV Coexpression)
1200
900
600
300
60
40
20
0
M1p
ORF50pp
ORF50dp
ORF50 N4/N5p
ORF8p
ORF22p
ORF63p
ORF73p
M2p
B
aTGaaCAGAAGGCaAct ORF50pp
aTGaaCCTCAGGCaAct ORF50ppRREm
C
293T
Increase Promoter Activity
(Fold Over EV Coexpression)
150
125
100
75
50
25
0
ORF50pp
ORF50ppRREm

Figure 11.

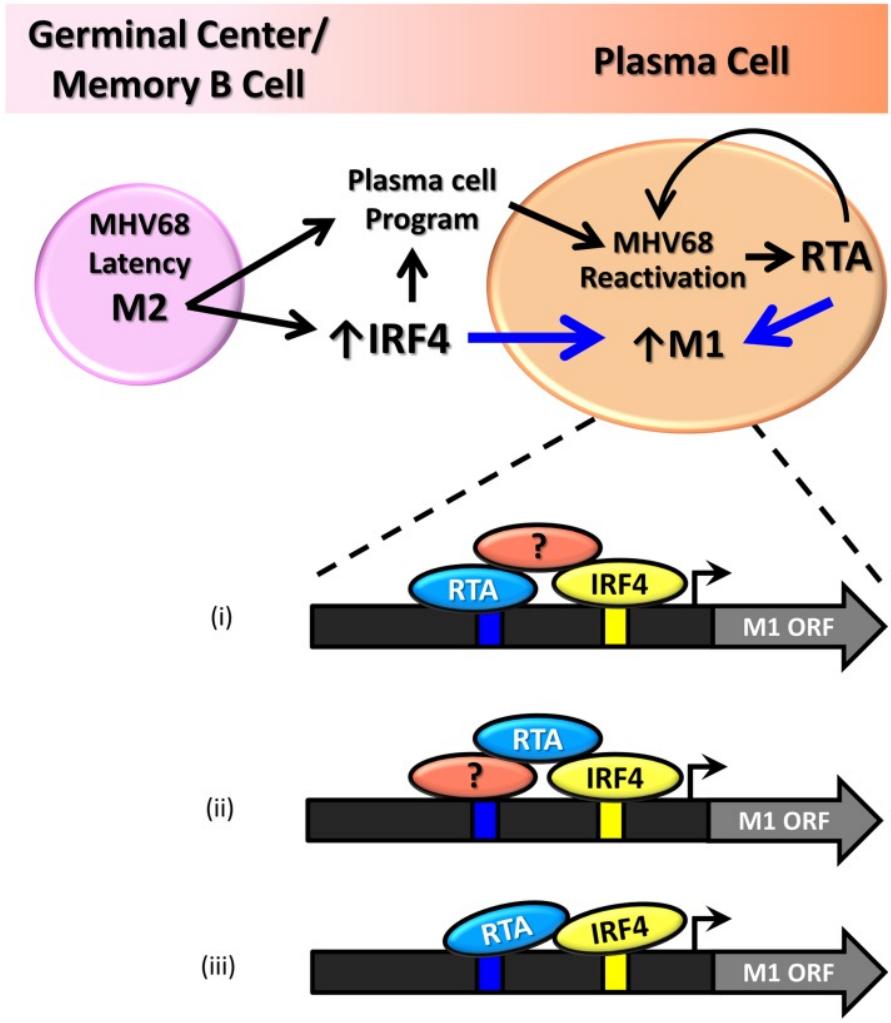
Germinal Center/
Memory B Cell
Plasma Cell
MHV68
Latency
M2
Plasma cell
Program
↑IRF4
MHV68
Reactivation
RTA
↑M1
?
RTA
IRF4
M1 ORF
(i)
RTA
?
IRF4
M1 ORF
(ii)
RTA
IRF4
M1 ORF
(iii)

FIGURE LEGENDS

Figure 1. Generation of YFP reporter viruses. C57Bl/6 mice were intranasally infected with 5×10^5 pfu of the indicated virus and spleens were harvested at 14 days post infection. (A) To assess M1 promoter activity, a YFP cassette was cloned in place of the M1 open reading frame, allowing marking of infected cells where M1 promoter was active. (B) To determine MHV68 infection in the absence of M1 expression, a translational stop codon was introduced into the M1 open reading frame (ORF) of the MHV68-YFP BAC [23] by allelic exchange as previously described [2].

Figure 2. M1 promoter activity is detected in a subset of MHV68 infected splenocytes. C57Bl/6 mice were intranasally infected with 5×10^5 pfu of the indicated virus and spleens were harvested at 14 days post infection. Splenocytes were gated on the $CD3^-$ negative fraction to eliminate auto-fluorescing cells, as previously described [23]. (A) Representative plots show YFP marking of infected splenocytes. YFP-positive gates were based on mice infected with wild type MHV68 lacking a YFP expression cassette. (B) Complied results from 3 experiments, with 3–5 mice per group, show the frequency of YFP^+ cells in spleens of infected mice.

Figure 3. Low levels of M1 promoter activity are detected in germinal center B cells. C57Bl/6 mice were intranasally infected with 5×10^5 pfu of the indicated virus and spleens were harvested at 14 days post infection. B cells were defined by $CD19^+$ $CD3^-$ population. (A) Representative plots show YFP marking (colored) overlayed on total B cell population (gray) and are gated for germinal center B cells defined by $GL7^{Hi}$ $CD95^{Hi}$.

(B) Complied results from 3 experiments, with 3–5 mice per group, show the frequency of YFP^+ cells with a germinal center B cell phenotype.

Figure 4. The majority of M1 promoter activity is detected in splenic plasma cells. C57Bl/6 mice were infected with 5×10^5 pfu/IN of the indicated virus and spleens were harvested at 14 days post infection. Cells were gated on $CD3^-$ population for analysis. (A) Representative plots show YFP marking (colored) overlayed on total $CD3^-$ population (gray) and are gated for plasma cells defined by $CD138^+$ $B220^{Lo}$. (B). Compiled results from 3 experiments, with 3–5 mice per group, show the frequency of YFP^+ cells with a plasma cell phenotype.

Figure 5. M1 transcript mapping identifies initiation and termination sites which result in a 1.3 and 1.5. (A) 5′ and 3′ rapid amplification of cDNA ends (RACE) was performed using RNA isolated from infected NIH3T12 fibroblasts and stimulated MHV68 infected A20-HE2 cells. The number of RACE clones that were identified for transcript initiation and termination sites are summarized. (B) A diagram of the transcript initiation and termination sites is shown with the genomic coordinates.

Figure 6. M1 promoter exhibits basal activity in a plasmablast cell line. Serial truncations of the M1 promoter region were cloned into a luciferase reporter vector and tested for luciferase activity in the P3X63Ag8 cell line from ATCC. P3X63Ag8 cells were nucleofected and 48 hours later luciferase activity was detected. M1 promoter activity is represented as fold over luciferase acivity of empty vector (pGL4.10).

Experiments were done with triplicate samples and repeated in two independent experiments.

Figure 7. Basal activity of the M1 promoter is dependent on IRF4 binding. (A) To identify DNA-protein interaction an electrophoretic mobility shift assay was performed using radiolabeled probe with P3X nuclear extracts. A competition assay to determine the specificity of DNA-protein complexes used 2 and 20 fold molar excess of unlabeled competitor DNA containing either the WT or mutant IRF4 binding sequence. An antibody supershift assay was performed by preincubating samples with anti-IRF4, or an isotype control antibody (anti-pSTAT1) prior to electrophoresis. The asterisk denotes the anti-IRF4 supershifted complex. (B) Point mutations in the M1 promoter were made in the IRF4 binding site and assessed in the P3X63Ag8 plasmacytoma cell line.

Figure 8. Efficient RTA transactivation of M1 promoter is dependent on a functional IRF4 binding site. (A) To evaluate the ability of Rta to transactivate the M1 promoter, a dosage response using increasing amounts of Rta expression vector were performed in P3X63Ag8 cells. (B) Mutations to the IRF4 binding motif were then generated and tested for the ability to respond to Rta in P3X63Ag8 cells. (C) Synergistic effects of RTA and IRF4 on WT and mutated M1 promoter were evaluated by expressing Rta or IRF4 alone or in combination (normalized with pCDNA empty vector) in 293T cells. (D) Lysates from 293T cells transfected with Rta or IRF4 alone or in combination were used for co-immunoprecipitation with IRF4 or Flag antibody. Membranes were probed with the anti-Flag or anti-IRF4 for detection. The data shown for the reporter gene

assays (panels A–C) were done with triplicate samples, and were repeated in 2–3 independent experiments. Standard error of the mean is shown.

Figure 9. Identification of a novel RTA response element in the M1 promoter. (A) To identify the Rta response element serial truncations of the M1 promoter were tested for RTA transactivation in the P3X63Ag8 plasmacytoma line which constitutively expresses IRF4. The blue box indicates the putative RTA response element; the yellow box denotes the location of the IRF4 binding site. (B) The nucleotide sequence of the putative Rta response element found in the M1 promoter is shown, along with nucleotide sequences sharing the core sequence with the M1 Rta response element (RRE) (denoted by the open blue rectangle) that are located upstream of a number of other MHV68 genes. In addition, the mutation (M1pRREm) introduced into the M1 Rta response element is shown. (C and D) Activity of the M1 promoter-driven reporter construct containing a mutation (indicated in red) in the putative Rta response element (RREm) was assessed in the P3X63Ag8 plasmacytoma cell line for Rta transactivation (panel C) and in 293T cells for IRF4+Rta synergy (panel D). Transient transfection reporter gene assays were conducted in triplicate and three independent assays were performed. Standard error of the mean is shown.

Figure 10. Novel RRE involved in Rta activation of the gene 50 proximal promoter. (A) Analysis of Rta transactivation of MHV68 promoters that contain the core sequence present in the novel RRE identified in the M1 promoter. The indicated promoter-driven luciferase reporter constructs were transfected into 293T cells in the presence and

absence of an Rta expression plasmid. (B) Mutation introduced into the putative RRE present in the gene 50 proximal promoter (ORF50pp described in [46]). (C) Analysis of Rta transactivation of the WT and RRE mutant gene 50 proximal promoter transfected into 293T cells.

Figure 11. Model of M1 gene regulation upon differentiation of latently infected B cells to plasma cells and ensuing virus reactivation. During infection MHV68 M2 regulates the expression of cellular IRF4, a critical transcription factor in plasma cell differentiation. M2 has also been shown to be critical for viral reactivation in the plasma cell reservoir. Increased levels of Rta and IR4 during viral reactivation in infected plasma cells lead to increased expression of M1, which is mediated through protein:protein interactions between Rta and IRF4, as well as binding through cis-elements within the M1 promoter. Shown are 3 possible mechanism for how Rta synergizes with IRF4 to activate transcription of the M1 gene: (i) Rta binds to the novel RRE and interaction with IRF4 is mediated by a cellular and/or viral factor that binds both Rta and IRF4; (ii) Rta interacts with a cellular and/or viral factor bound to the RRE and also directly binds to IRF4; and (iii) Rta binds to the RRE and interacts directly with IRF4.

TABLES

Table 1. Oligonucleotide primer sequences.

M1p 1025 bp–forward	gatcggtacccttccagctaagatagcatgtgccg
M1p 1025 bp–reverse	ctagagatctggtcgccgctgctcaatgatg
M1p 525 bp–forward	gctcggtacccccagaagaccatgtctgggaat
M1p 525 bp–reverse	gctagatctggtcgccgctgctcaatg
M1p 245 bp–forward	gcgggtacccctacccctttgctccac
M1p 245 bp–reverse	gctagatctggtcgccgctgctcaatg
M1p 197 bp–forward	gcgggtacccaaaacaagaacagttgc
M1p 197 bp–reverse	gctagatctggtcgccgctgctcaatg
M1p 100 bp–forward	gcgggtaccgtttcaaacactggtcag
M1p 100 bp–reverse	gctagatctggtcgccgctgctcaatg
M1p 100 bp RREm–forward	gcgggtaccgtttcaaacactggtcctcaggctatc
M1p 100 bp RREm–reverse	gctagatctggtcgccgctgctcaatg
M1p 88 bp–forward	gcgggtaacggtcataaggctatc
M1p 88 bp–reverse	gctagatctggtcgccgctgctcaatg
M1p 82 bp–forward	gccggtaccaaggctatctttctt
M1p 82 bp–reverse	gctagatctggtcgccgctgctcaatg
M1p 76 bp–forward	gcgggtaccatctttcttggtggt
M1p 76 bp–reverse	gctagatctggtcgccgctgctcaatg
M1p 64 bp–forward	gcgggtaccggtttcacttctaaa
M1p 64 bp–reverse	gctagatctggtcgccgctgctcaatg
M1p unspliced Rta–forward	ggcgcggccgcatggcctctgactcggattccc
M1p unspliced Rta –reverse	ggcctcg ggcctcgagttatgactccaggctgtttggg
M1p unsplice C-flag RTA–forward	ggcgcggccgcatggcctctgactcggattccc
M1p unspliced C-flag RTa–reverse	cggctcgagctacttatcgtcgtcatccttgtaatctgactccaggctgtttg
M1p mIRF4–forward	ggcgcggccgcatgaccttggagacgggcagc
M1p mIRF4–reverse	ggcctcgagtcactcttggatggaagaatgac
M1p ORF8p–forward	ccgggtaccccaaaattgttgcggccctaag
M1p ORF8p–reverse	gccagatctcaacactggctgaatcggttc
M1p ORF22p–forward	ccgggtaacctgcgacccgagtcaaggagag
M1p ORF22p–reverse	gccagatctttgtgcttggctatttattactac
M1p ORF63p–forward	ccgctcgagcagccagcacattagcttcatgg
M1p ORF63p–reverse	gccagatcttatgtcagaagttggtaaatat
M1p ORF73p–forward	ccgggtaccataggacaatgatgagttttc
M1p ORF73p–reverse	gccctcg gccctcgagtatctgaaagagataaagtacac
M1p 50 sense	gctgggtaccacatgggccattaaaagggagggaattggcatcattgagcagcggcgaccagatctgtcg
M1p 50 antisense	cgacagatctggtcgccgctgctcaatgatgccaattccctccctttttaatggcccatgtggtacccagc
M1p 25 sense	gctgggtaccttggcatcattgagcagcggcgaccagatctgtcg
M1p 25 antisense	cgacagatctggtcgccgctgctcaatgatgccaaggtacccagc

CHAPTER III

$CD8^+$ T cell response to gammaherpesvirus infection mediates inflammation and fibrosis in interferon gamma receptor-deficient mice

Brigid M. O'Flaherty[1,2], Caline G. Matar[1,2], Brian S. Wakeman[1,2], Anapatricia Garcia[3], Carol A. Wilke[4], Cynthia L. Courtney[3], Elizabeth J. Elrod[1,2], Arash Grakoui[1,2], Bethany B. Moore[4], and Samuel H. Speck[1,2,*]

[1]Department of Microbiology and Immunology, Emory University School of Medicine, Atlanta, GA, USA; [2]Emory Vaccine Center, Emory University School of Medicine, Atlanta, GA, USA; [3]Division of Pathology, Yerkes National Primate Research Center, Emory University, Atlanta GA, USA; [4]Department of Internal Medicine, Division of Pulmonary and Critical Care Medicine, University of Michigan, Ann Arbor, MI, USA.

All figures were generated by Brigid Moira O'Flaherty exceptions noted below.

Figure 1A&B. Tissue sections were performed by Yerkes Pathology lab, imaging was performed by Dr. Cindy Courtney, and scoring was performed by Dr. Anapatricia Garcia.
Figure 4 A&B. Lung titers were performed by Brian Wakeman.
Figure 4 C. Viral persistence assay was performed by Caline Matar.
Figure 7. Hydroxyproline analysis was performed by Carol Wilke.
Figure 8 B&C. Tissue sections were performed by Yerkes Pathology lab and scoring was performed by Dr. Anapatricia Garcia.
Figure 9 D-F. Tissue sections were performed by Yerkes Pathology lab and scoring was performed by Dr. Anapatricia Garcia.

CHAPTER III

$CD8^+$ T cell response to gammaherpesvirus mediates inflammation and fibrosis in interferon gamma receptor deficient mice

ABSTRACT

Idiopathic pulmonary fibrosis (IPF), one of the most severe interstitial lung diseases, is a progressive fibrotic disorder of unknown etiology; however, there is growing appreciation for the role of viral infection in disease induction and/or progression. A small animal model in which murine gammaherpesvirus (MHV68) infection of interferon gamma receptor deficient (IFNγR-/-) mice results in multi-organ fibrosis, has been utilized to model the association of gammaherpesvirus infections and lung fibrosis. Notably, several MHV68 mutants which fail to induce fibrosis have been identified. Our current study aimed to better define the role of the unique MHV68 gene M1 in development of pulmonary fibrosis. We have previously shown that the M1 gene encodes a secreted protein which possesses superantigen-like function to drive the expansion and activation of cytokine producing $V\beta4^+$ $CD8^+$ T cells. Here we show that M1-dependent fibrosis is correlated with heightened levels of inflammation in the lung. We observe an M1-dependent cellular infiltrate of innate immune cells with most striking differences at 28 days-post infection. Furthermore, in the absence of M1 protein expression we observe reduced $CD8^+$ T cells and MHV68 epitope specific $CD8^+$ T cells to the lungs – despite equivalent levels of viral replication between M1st and WT MHV68. Notably, backcrossing the IFNγR-/- onto the Balb/c background, which has previously been shown to exhibit weak MHV68-driven $V\beta4^+$ $CD8^+$ T cell expansion,

eliminated MHV68-induced fibrosis – further implicating the $V\beta4^+$ $CD8^+$ T cell population in the induction of fibrosis. We further addressed the role that $CD8^+$ T cells play in the induction of fibrosis by depleting $CD8^+$ T cells throughout the course of infection. We show that depletion protects mice from fibrotic disease. Taken together these findings provide evidence for the role of $V\beta4^+$ $CD8^+$ T cells as mediators of fibrotic disease in IFNγR-/- mice.

INTRODUCTION

Fibroproliferative disorders are a class of diseases which result from dysregulated wound repair mechanisms, lead to excessive scaring and can affect multiple tissues and organ systems. Interstitial lung diseases (ILD), systemic and local scleroderma, liver cirrhosis, progressive kidney disease, cardiovascular disease, and macular degeneration are some of the fibrotic diseases affecting major organ systems [139]. Idiopathic pulmonary fibrosis (IPF), one of the most severe ILD, has unknown etiology and results in progressive scaring of lung tissue, respiratory failure, and eventual mortality. IPF affects middle-aged and elderly adults, occurring more frequently in males, and disease pathogenesis has been associated with a variety of environmental, genetic, and infectious factors (reviewed in [49,140,141]). Following clinical trials, two therapies (perfinidone and nintedanib) were recently FDA approved [47,48]; however, these therapies only delay functional decline. IPF has a median survival rate of 2-5 years post diagnosis (reviewed in [46]), thus a better understanding of the mechanisms driving disease is critical for developing better therapies.

To gain insights into the mechanisms driving fibrosis, researchers have focused on well-defined animal models of disease. Numerous small animal models exist for exploration of the mechanisms driving pulmonary fibrosis (Reviewed in [96,97]). MHV68 infection of IFNγR-/- has previously been shown to result in multi-organ fibrosis [99,101], and has been highlighted as a potential model to study the role of gammaherpesvirus infections in development and exacerbation of IPF, due to pathologic and immunologic similarities [104]. Key findings in this model have revealed roles for alternative macrophage activation, and the ability of MHV68 to induce epithelial to

mesenchymal transition in the lung [105,142]. Most strikingly, Mora and colleagues identified viral replication and reactivation as a critical driver of disease [106]. This study showed that inhibition of viral replication with a nucleoside analog, cidofovir, led to reduction in pathology and reversal of fibrosis. Further underscoring the importance of viral replication and persistence in disease, several latency compromised MHV68 mutant viruses which failed to induce fibrotic disease in IFNγR-/- mice have been described [107,108].

We had previously identified the requirement for the unique, non-essential [117], MHV68 M1 gene product for the induction of multi-organ fibrosis in IFNγR-/- mice [11,12]. M1 is thought to function as a novel viral superantigen, inducing the activation and expansion of $V\beta4^+$ $CD8^+$ T cells independent of antigen presentation [12]. During MHV68 infection, M1 plays an important role in suppressing viral reactivation from latently infected peritoneal macrophages, through activation and expansion of IFNγ producing $V\beta4^+$ $CD8^+$ T cells. As M1-null infected mice failed to develop fibrotic disease, we postulated that the $V\beta4^+$ $CD8^+$ T cell population induced during infection may contribute to lung pathology and fibrosis. Additional support for this hypothesis was lent by the observation that $CD8^+$ T cells play a critical role in MHV68-induced fibrosis [99].

Herein, we describe the immunologic changes observed during MHV68 infection of IFNγR-/- mice, comparing WT and M1st viruses. We show a strong correlation between inflammation and fibrosis, with heighted levels of inflammation and fibrosis observed in the M1 expressing virus infections. Additionally, we find striking M1-dependent changes to the cellular infiltrates in the lung, where elevated neutrophil and

effector $CD8^+$ T cell levels are observed in the presence of M1 expression. These data suggest that M1-dependent alteration in cellular trafficking likely contributes to immunopathology. Notably we show that depletion of $CD8^+$ T cells during the course of infection prevents fibrotic disease. Taken together, our data suggest a role for M1-induced $V\beta4^+$ $CD8^+$ T cells as mediators of fibrotic disease, where this population induces inflammation and altered recruitment to the lung resulting in immunopathology and fibrosis.

MATERIALS & METHODS

Ethics statement: This study was carried out in strict accordance with the recommendations in the Guide for the Care and Use of Laboratory Animals of the National Institutes of Health. The protocol was approved by the Emory University Institutional Animal Care and Use Committee and in accordance with established guidelines and policies at Emory University School of Medicine (Protocol Number: YER-2002245-031416GN).

Mice: Six to eight week old female C57Bl/6 and Balb/c mice were obtained through Jackson Laboratory (Bar Harbor, ME) and IFNγR-/- C57Bl/6 and Balb/c mice were bred in-house. Mice were infected at eight to twelve weeks of age. Prior to infection mice were sedated with isofluorane and intranasally infected with $5x10^5$pfu in 20ul of DMEM. Mice used in T cell depletion studies were sedated with isofluorane, and injected intraperitoneally with 100µg Rat anti-CD8 (clone YTS 169.4) or Rat IgG2b (clone LTF-2) as an isotype control, according to experimental schedule described in Fig. 9.

Pathology: Tissues were collected and fixed in 10% buffered neutral formalin for up to 7 days prior to processing for hematoxylin and eosin or Masson's trichrome staining. Samples were sent for evaluation by pathologists, blinded samples were scored by AG and imaging was performed by CLC. Pathology scores are as follows 0= Normal, 1= 1-2 foci, 2= 3-4 foci, 3= Multifocal, 4= Diffuse.

Tissue preparation: Following euthanasia, tissues were collected in cold complete medium. Spleens were processed mechanically, and lung tissue was minced and digested using type IV Collagenase and DNAse I to produce a single cell suspension. Subsequently, single cell suspensions were treated with red blood cell lysis buffer and cells were enumerated.

Flow Cytometry: Single cell suspensions were resuspended in PBS supplemented with 2% fetal bovine serum and 2mM EDTA. Samples were blocked with CD16/32 and stained using standard procedures, antibodies used for these studies are described in table 1. Events were recorded on BD LSRII flow cytometer and results were analyzed using FloJo software (Tree Star Inc).

Viral Titers: Plaque assays were performed as previously described [143]. NIH 3T12 cells were plated in six-well plates 1 day prior to infection at 2×10^5 cells per well. Organs were subjected to 4 rounds of mechanical disruption of 1 min each by using 1.0mm zirconia-silica beads (Biospec Products, Bartsville, OK) in a Mini-Beadbeater-8 instrument (Biospec Products). Serial 10-fold dilutions of organ homogenate were plated onto NIH 3T12 monolayers in a 200-µl volume. Infections were performed for 1h at 37°C with rocking every 15 min. Immediately after infection plates were overlaid with 1.5% methylcellulose in complete DMEM. After 10 days, cells were stained with 0.12% (final concentration) Neutral Red. The next day, methylcellulose was aspirated, and plaques were enumerated. The sensitivity of the assay is 50 PFU/organ.

Viral Persistence: A highly sensitive limiting dilution assay to determine viral persistence previously described [18] was used. Briefly, the left lung was homogenized in 1ml of complete DMEM media using 1.0mm Zirconia/Silicon beads (BioSpec products) 4 times (1 min homogenization, followed by 1 minute resting on ice). The single cell homogenate was lysed with 0.5mm Zirconica/Silicon beads using the same homogenization program. The final homogenate was then plated on Mouse Embryonic Fibroblasts (MEFs) in 2 fold dilutions, up to a total of 8 dilutions. Wells were incubated in a low evaporation incubator (37°C, 5% CO2) for a total of 14 days. Each well was then evaluated for cytopathic effect (CPE). Data is presented as percent of wells displaying CPE at each plated dilution.

Assessment of active TGFβ: Mink lung epithelial cell line (MLEC clone 23) stably transfected with plasminogen activator inhibitor-1 fused to a luciferase reporter gene, a generous gift of Dr. Dan Rifkin, were plated at $5x10^5$ cells/well for infection in a 12 well plate. Cells were infected with MHV68-YFP or MHV68-M1st-YFP at different multiplicities of infection. At 42 hours post infection, cell lysates were collected and assessed for luciferase activity using a TD-20/20 luminometer.

Western Blot: Lung tissues from infected C57Bl/6 mice were collected and homogenized using 200ul of Sigma CelLytic MT Mammalian Tissue Lysis/Extraction reagent per 40mg lung tissue. Following lysis membranes were pelleted at 14,000xg for 10 minutes and samples were stored at -80°C. 30µg of cell lysate was loaded on a

denaturing 12% SDS polyacrylamide gel and detected with TGFβ1 antibody (Ebioscience clone A75-2), membranes were stripped and probed for β-actin.

Hydroxyproline Assay: Mice were euthanized and right and accessory lobes of the lung were collected and frozen at -80°C until further processing as previously described [144]. Briefly, lung tissue was homogenized in 1mL of PBS, and hydrolyzed by the addition of 1ml of 12N hydrochloric acid (HCl). Samples were then baked at 110° C for 12 h. Aliquots (5µl) were then assayed by adding chloramine T solution for 20 min followed by development with Erlich's reagent at 65°C for 15 min. Absorbance was measured at 550 nm, and the amount of hydroxyproline was determined against a standard curve generated using known concentrations of hydroxyproline standard (Sigma).

Simulation for T cell Effector Function: WT or IFNγR-/- mice on the C57Bl/6 or Balb/c background were infected with $1x10^5$pfu WT or M1st MHV68 intranasally. Mice were sacrificed at 28 days post infection and single cell suspensions of lung or spleen cells were prepared as described above. Cells were either unstimulated or stimulated with 20ng/ml PMA & 1µg/ml ionomycin, 10µM viral peptides p56 (AGPHNDMEI) or p79 (TSINFVKI) a generous gift of Dr. Mandy Ford, or recombinant M1 or M1st protein containing supernatants previously described in [12]. Cells were cultured in the presence of 1µl/ml BD-GolgiPlug (brefeldin-A) and respective stimuli for 4-6 hours at 37°C. Cells were subsequently surface stained, fixed and permeablized using BD Cytofix/Cytoperm, and stained for intracellular cytokines. For antibodies used, refer to table1.

Analysis of Vβ Repertoire: Naïve WT or IFNγR-/- mice were sacrificed and single cell suspensions of splenocytes were prepared using standard methodology. Cells were then blocked with CD16/32 and stained using BD-Pharmingen Mouse Vβ TCR Screening Panel in FITC along antibodies listed in table 1.

RESULTS

MHV68 mediated lethality in IFNγR-/- mice is associated with heightened inflammatory response to the virus. Lethality and multi-organ fibrosis are well characterized outcomes of MHV68 infection in IFNγR-/- C57Bl/6 mice. We have previously identified M1 as a critical viral factor involved in induction of fibrosis and lethality in this strain [11,12]. Here we recapitulate this observation, showing that in the absence of M1 expression mice are rescued from weight loss and subsequent lethality (Fig 1A&B). Protection from lethality appears to be associated with a reduction in pulmonary infiltrates (Fig. 2A). M1-dependent pathology in IFNγR-/- mice includes dramatic changes to the lung architecture, including thickening of the alveolar septa, type II pneumocyte hyperplasia, and extracellular matrix deposition (Fig. 2A&B). Histological analyses revealed reduced levels of inflammation, fibrosis, hyperplasia, and edema in the M1st infected animals (Fig. 2B). Notably, fibrotic foci were often associated with inflammatory infiltrates suggesting a causal role in lung damage and subsequent repair. This observation led to the identification of a striking correlation between inflammation and fibrosis in the lung (R=1, P=0.0167) (Fig. 2C).

To characterize the inflammatory response in the lungs of infected IFNγR-/- mice, we utilized a panel of makers described by Misharin *et al.* [145], to identify innate cell populations by flow cytometry. As a result of infection, both M1st and WT viruses resulted in increased lung cellularity at 28 days post- infection, suggesting increased recruitment of leukocytes to the lung. However, we note that WT infected mice showed a more striking increase in cellularity when compared to the moderate increase observed in M1st infection (Fig. 3A). To identify cellular subsets in the lung, cells were first gated for

leukocytes ($CD45^+$ cells), we observe similar frequencies of leukocytes among the different infection conditions (Fig. 3B). Leukocytes were classified as macrophages, dendritic cells, eosinophils, neutrophils, and monocytes based on surface marker expression. Here we observed a striking M1-dependent increase in the frequency of neutrophilic infiltrates and a reduction in alveolar macrophages (Fig. 3C). Over the course of infection differences in the M1-dependent infiltrating populations were shown to be most striking between 18 and 28 days post-infection (Fig. S1). Consistent with previous observations [105], we find an increase in absolute numbers of alveolar macrophages during the MHV68 infection (Fig. S2A). As alternative macrophage activation (M2) has been described as a potential driver of fibrotic disease, we were surprised to note that M1st and WT infected IFNγR-/- mice had similar numbers of alveolar macrophages with an M2 phenotype (marking $Fizz1^+$ and $CD206^+$). We did observe a slight elevation in the number of interstitial macrophages with an M2 phenotype by 28 days post-infection in WT, but not M1st, infected mice - although this failed to reach statistical significance (Fig. S2B).

Failure to control viral persistence is not sufficient to induce inflammation and fibrosis. Although M1 expression is dispensable for the establishment of latency in wild type C57Bl/6 mice [117], our data raised the possibility that the reduction in M1st virus immunogenicity in IFNγR-/- mice could simply be due to a defect in virus replication. To address this possibility we evaluated acute titers in the lung and spleen at various times post-infection. As anticipated, we find that M1 is dispensable for acute replication in the lungs and spleen of IFNγR-/- mice (Fig. 4A & B). However, since it has previously been

noted that viral reactivation and persistent replication are critical for development of MHV68-induced fibrotic disease [108], we next assessed persistent virus replication in the lungs at a late time point in WT and M1st infected IFNγR-/- mice (Fig. 4C). We observed higher levels of persistent virus replication at 90 days post-infection in the lungs of IFNγR-/- mice infected with M1st than in those infected with WT MHV68. This strongly argues that persistent virus replication alone is not sufficient to induce a fibrotic response (Fig. 4C). It should be noted that the levels of viral persistence were measured from surviving mice; as such these values may under-represent the amount of persistent virus in the WT infected mice – which experienced ca. 50% lethality.

Absence of M1 expression does not alter expression of the profibrotic mediator TGFβ in lung. Numerous fibrotic diseases are mediated by the cellular growth factor and cytokine transforming growth factor beta (TGFβ) (reviewed [146]). MHV68 infection has been shown to induce TGFβ production from a variety of cell types *in vivo* [147], and like EBV [75], MHV68 infection of alveolar epithelial cells *in vitro* and *in vivo* results in TGFβ production [148]. To determine whether the lack of a fibrotic response in M1st infected mice was due to a defect in TGFβ induction, we evaluated the ability of WT and M1st MHV68-YFP viruses to induce active TGFβ in mink lung epithelial cells stably transfected with a plasminogen activator inhibitor-1 (PAI1) luciferase reporter [149]. In this cell line the TGFβ responsive PAI1 promoter is fused to a firefly luciferase gene, and presence of TGFβ results in expression of luciferase. Testing various multiplicities of infection, we find that the M1st virus induced levels of TGFβ similar to the WT virus (Fig. 5A). To verify that the M1st virus was capable of inducing equivalent levels of

TGFβ *in vivo*, we evaluated lung homogenates from mice at 28 days post-infection. We find roughly equivalent levels of latent and active TGFβ in M1st and WT infection – although notably these were not significantly different from the levels observed in lungs homogenates recovered from mock infected animals (Fig. 5B).

Absence of fibrosis is associated with reduced $CD8^+$ T cell responses during infection. Viral specific T cell response during MHV68 infection is characterized by a heterogeneous population of epitope specific $CD8^+$ T cells which have two dominant patterns of expansion and contraction [150-152]. These CTL arise rapidly after acute replication in the lung, with peak splenic response between 6-10 days post-infection [153]. The H-$2D^b$ epitope restricted "pattern 1" responders, exemplified by p79 (ORF61), arise and decline rapidly following acute replication and require viral reactivation for optimal response [150,154]. The H-$2K^b$ epitope restricted "pattern 2" responders, exemplified by p56 (ORF6), arise rapidly but have a gradual decline, and relatively high frequencies are maintained into viral latency [150]. To evaluate both viral antigen-specific T cell response and $V\beta4^+$ $CD8^+$ T cell expansion, we assessed these populations at 28 days post-infection. As a measure of efficiency of $CD8^+$ T cell response during infection, we measured levels of epitope specific $CD8^+$ T cells and response to their cognate peptides. Our analyses show a significant reduction in overall $CD8^+$ T cells levels in the absence of M1 expression (Fig. 6A). More strikingly, we noted reduced epitope specific $CD8^+$ T cell numbers in M1st infected mice, using tetramer staining for p56 and p79 specific T cells (Fig. 6B&C), suggesting that these cells are less efficiently recruited to the lung. We find decreased levels responsiveness in p56 but not p79 specific

T cells in the M1st infection compared with WT infection (Figur 6B&C), perhaps reflecting the different kinetics of these T cell populations. However, a notable increase in cytokine production is observed in the presence of M1 expression, with p56 responsive cells producing more TNFα and p79 responsive cells producing more IFNγ and TNFα – suggesting that there is no inherent defect in ability to produce cytokines, and that they may produce these cytokines even more efficiently (Fig. 6B&C). The latter observation could be driven by higher levels of persistent virus replication in the lungs of M1st infected IFNγR-/- mice, as shown in Figure 4 C.

Concomitant with the establishment of MHV68 latency is the M1-dependent $V\beta4^+$ $CD8^+$ T cell expansion which occurs between 21 and 28 days post-infection [13]. This population of cells is thought to control MHV68 viral reactivation in C57Bl/6 mice, through the secretion of IFNγ [11,12]. Following expansion $V\beta4^+$ $CD8^+$ T cells remain elevated though the life of infection, requiring continued stimulation by the stimulatory ligand, M1, in a MHC independent manner [12,13,109]. As anticipated, elevated levels of $V\beta4^+$ $CD8^+$ T cells were observed in WT but not M1st MHV68 infected mice that were capable of producing IFNγ and TNFα in response to the recombinant M1 protein (Fig. 6D).

To better understand the timing and development of pulmonary fibrosis in IFNγR-/- C57Bl/6 mice, we analyzed the extracellular matrix content in lung tissue following infection using the hydoxyproline assay. Lung tissue was collected at days 4, 9, 28, and 90 days post-infection and assayed for collagen content. Consistent with our previous observations, we show that fibrotic scaring, as indicated by extracellular matrix (ECM) deposition, does not occur in the absence of M1 expression. Interestingly, we note that

timing of collagen deposition in the lung roughly mirrors that of the Vβ4$^+$ CD8$^+$ T cell expansion suggesting an association between these phenomenon (Fig. 7) [13].

IFNγR-deficient mice which fail to develop an M1-dependent Vβ4$^+$ CD8$^+$ T cell expansion are protected from MHV68 induced fibrosis. The level of M1-mediated Vβ4$^+$ CD8$^+$ T cell expansion that occurs during MHV68 infection varies in different mouse strains. C57Bl/6 mice have high levels of expansion, with an ca. 9-12-fold increase above naïve Vβ4$^+$ CD8$^+$ T cell levels; whereas Balb/c mice have very minimal expansion resulting in a 2-4-fold or lower increase in Vβ4$^+$ CD8$^+$ levels [13]. To evaluate the impact of Vβ4$^+$ CD8$^+$ T cell activation and expansion in MHV68 infection-induced fibrosis, we generated IFNγR-/- mice on the Balb/c background and infected these mice with either WT or M1st virus (Fig. 8).

An unexpected finding, following the generation of the IFNγR-/- Balb/c mice, was the loss of Vβ4$^+$ T cells in approximately 50% of naïve mice (Fig. S3). This loss of Vβ4$^+$ T cells occurred in both the CD4$^+$ and CD8$^+$ T cell populations (Fig. S3 A&B), and appeared to occur during thymic selection as exiting single positive cells showed loss of Vβ4 (data not shown). To determine whether this loss resulted in other changes in the T cell repertoire, T cell receptor repertoire analysis was carried out to assess the frequencies of other Vβ subsets in mice that lost or maintained their Vβ4$^+$ T cells. We found that the loss of Vβ4 expression in CD4$^+$ T cells resulted in a compensatory increase in Vβ8.1/8.2, Vβ8.3, Vβ10b, and Vβ13 positive cells (Fig. S4). Loss of Vβ4 expression in CD8$^+$ T cells, led to a compensatory increase in Vβ8.1/8.2, and Vβ8.3, and Vβ10b positive cells

(Fig. S4). Due to this finding, mice were screened prior to infection to ensure the presence of $V\beta4^+$ T cells for subsequent experiments.

As expected we observed a weak $V\beta4^+$ $CD8^+$ T cell expansion, resulting in an ca. 2-fold increase compared to naïve levels in the IFNγR-/- Balb/c mice (Fig. 8A). Importantly, the modest M1-dependent $V\beta4^+$ $CD8^+$ T cell expansion in Balb/c mice fails to elicit cytokine production in response to recombinant M1 protein (Fig. S5). To assess fibrotic effects induced by MHV68 infection of IFNγR-/- Balb/c mice, spleen and lung were collected and assessed for pathological changes. We failed to observe splenic atrophy in MHV68 infected mice in this background (data not shown). Histological analysis of Masson's trichrome stained tissue sections revealed an absence of fibrosis in this background for both WT and M1st infected mice (Fig. 8B &C).

Depletion of CD8 T cells prevents fibrotic disease. The CD8 T cell response plays an important role in clearance of MHV68 infection from the lung of wild type C57Bl/6 mice [150]. Additionally, the role of $CD8^+$ T cells in fibrotic disease has been highlighted in IFNγR-/- mice. Depletion of $CD4^+$ or $CD8^+$ T cells was shown to reduce splenic pathology in IFNγR-/- 129/Sv/Ev mice [99]. These studies showed that depletion of $CD8^+$ T cells led to restoration of spleen appearance, increased cellularity, and an overall reduction in MHV68 infectious centers [99]. However, it is worth noting that a striking difference between the 129/Sv/Ev and C57Bl/6 backgrounds; IFNγR-/- mice in the 129/Sv/Ev background undergo an apparent resolution of fibrosis at ca. 45 days post-infection [101] whereas C57Bl/6 mice fail to resolve disease. Nonetheless, the studies by Dutia and colleagues highlight an important role for T cells in development of fibrotic

disease in IFNγR-/- mice [99]. As the M1st virus mutant lacks expansion of $V\beta4^+$ $CD8^+$ T cells, and exhibits reduced numbers $CD8^+$ T cells and viral antigen specific $CD8^+$ T cells in the lungs of infected IFNγR-/- C57Bl/6 mice (Fig. 6), we wanted to evaluate what role $CD8^+$ T cells (including $V\beta4^+$ $CD8^+$ T cells) play in development of fibrosis. A technical limitation for to $V\beta4^+$ $CD8^+$ T cell depletion had been noted in previous attempts to deplete this population [12,113]. The single commercially available Vβ4 antibody, clone KT4, failed to deplete $V\beta4^+$ T cells *in vivo* and instead simply masked detection by flow cytometry [12]. Due to this shortcoming, we were unable to delete $V\beta4^+$ $CD8^+$ T cells independently and instead utilized a global $CD8^+$ T cell depletion. Mice were injected starting at day -2 before infection using a rat monoclonal anti-CD8 antibody (or an isotype control) (Fig. 9A).

To measure the efficiency of depletion, weekly blood samples were collected and assessed by flow cytometry (Fig. 9B). We observed a striking elimination in the $CD8^+$ T cell population within the first week following treatment, but ultimately these cells partially recovered - remaining ca. 50% below isotype treated levels (Fig. 9B). Surprisingly, activated $CD8^+$ T cells ($CD62L^{lo}$ $CD44^{hi}$) appeared to resist depletion while naïve populations ($CD62L^{hi}$ $CD44^{lo}$) were susceptible (data not shown). Due to this limitation, and the effector memory phenotype of $V\beta4^+$ $CD8^+$ T cells [12], we were failed to deplete the $V\beta4^+$ $CD8^+$ T cells that accumulate during infection. Despite this shortcoming, we were able to make important observations about the role of other $CD8^+$ T cells in this model.

We observed striking phenotypic changes as a result of the $CD8^+$ T cell depletion. Compared to the isotype treated group, body condition was greatly improved.

Additionally, gross anatomic changes were apparent. For example, the atrophied spleen (Fig. 9C) and the irregular liver surface containing multifocal confluent raised nodules (data not shown), was prevented in the $CD8^+$ T cell depleted group. Histological evaluation revealed reduced fibrosis, hemosiderosis, and cellular depletion in the spleen (Fig. 9D); reduced inflammation, fibrosis, hyperplasia, and edema in lung (Fig. 9E); and reduced inflammation, fibrosis, necrosis, hemorrhage, and hemosiderosis in the liver (Fig. 9F) following $CD8^+$ T cell depletion. Overall, these data point to a critical role of $CD8^+$ T cells in mediating the pathology observed in the lung, spleen and liver.

DISCUSSION

An association between human herpesvirus (HHV) infection and IPF development and exacerbation is supported by a significant body of work. Some of the most compelling evidence for this association was reported in 2003 by Tang *et al.*, where 97% of lung tissues from IPF patients were shown to have one or more HHV compared to 36% of control samples. Further, two or more herpesviruses (CMV, EBV, and HHV-8) were identified in 57% of IPF patients compared to 8% of controls [66]. Associations for EBV infection in IPF are supported by the observation of elevated levels of EBV DNA in the lung [71], presence of the EBV lytic spliced gene product WZhet in lung biopsies [72], and increased viral capsid antibody titers [73] (reviewed in [53]). Further, EBV infection of type II alveolar epithelial cells and has been shown to induce TGFβ production [75], while EBV protein LMP-1 has been shown to play a role in epithelial to mesenchymal transition [76]. However, not all studies have shown a correlation between EBV and IPF [79,80]. Risk factors for IPF are numerous involving genetic, environmental, and infectious agents, and these risk factors need not all be present to result in disease [53,155]. HHV are perhaps just one of the factors setting the stage for fibrotic disease.

Many similarities between the MHV68 model system in IFNγ unresponsive mice and human IPF have been described, including infection and apoptosis of alveolar epithelial cells, type II pneumocyte hyperplasia, epithelial to mesenchymal transition, and M2 macrophage differentiation in the lung [104,105,142]. Furthermore, IPF patients have been shown to shed equivalent levels of EBV from saliva and lower airways, while non IPF controls show a 10-fold reduction in titers from the lower airway [156]. This chronic

infection in the lung is mirrored by the high levels of persistent MHV68 in IFNγR-/- C57Bl/6 lung as late as 90 days post infection, shown here and in previous studies [106,107]. It is likely that viral persistence has many deleterious effects on the host. During this chronic stage of infection, repeated insult to the lung epithelium likely contributes to the ongoing damage and repair cycles. It was therefore noteworthy that we observed elevated levels of viral persistence with the fibrosis impaired M1-null mutant MHV68 (Fig. 4C). We suggest that a cumulative influence, where viral persistence alone is not sufficient to induce fibrotic response in the absence of a strong inflammatory response.

A frequently disputed aspect of pulmonary fibrosis is the role of inflammation. Often, inflammation is not observed in lung biopsies from IPF patients (Reviewed [157]). Human trials utilizing anti-inflammatory treatments, such as corticosteroids, have shown no survival benefit, and chronic use is associated with increased co-morbidities [158,159]. Further, the use of azathioprine, an immunosuppressant which blocks T and B cell proliferation as well as reducing levels of circulating monocytes and granulocytes, has failed to result in a survival benefit [159]. The strongest evidence contradicting the role of inflammation as a driver of fibrotic disease was revealed in the recent PANTHER-IPF study, in which anti-inflammatory treatment was actually harmful to IPF patients. In this study the triple treatment arm using N-acetyl cysteine, prednisone, and azathioprine had to be discontinued due to a 10% increase in mortality – largely due to respiratory causes, and ca. 3-fold increase in hospitalization and adverse effects [160]. This disparity between inflammation and disease is a confounding feature, and is mirrored in many small animal models for IPF. Certainly bleomycin treatment, one of the most commonly

used models for lung fibrosis, is initiated by a strong inflammatory response. These data have led to the hypothesis that an initiating inflammatory insult leads to epithelial damage and initiation of the tissue repair process, while 'multiple hits' may be required to induce fibrotic disease (discussed in [141,155]).

Conflicting view regarding the role of T cells in IPF are present in the field; however, T cells are a well-documented finding in the lungs of IPF patients, and are frequently found in areas of interstitial fibrosis in the lung [161-164]. Some researchers have shown an association between CD8 T cells and worsening clinical symptoms or disease progression [165-167]; while other studies have indicated CD4 T cells [168] and their activation [169] negatively impact disease status. Contradicting the aforementioned data, a recent report from Herazo-Maya and colleagues indicated that markers of T cell activation and signaling corresponded to a better prognosis [170]. However, there is a paucity of data showing a direct role of T cells in IPF. One issue to these studies is the fact that evaluation of human samples can only provide correlative insights at a snapshot during the course of disease (discussed [171]). Luzina *et al*. described T cells as an important component cell type of inflammation – likely affecting fibrosis through a diverse set of mechanisms, but not a driving force of IPF [171], suggesting that T cells might modulate the severity of fibrosis. Further adding to the complexity, small animal studies have also shown conflicting roles for T cells in pulmonary fibrosis. SCID or nude mice, both lacking T cells, have been shown to develop fibrosis in the bleomycin model [172,173]. Models of pulmonary fibrosis utilizing asbestos have suggest a protective role of T cells in pulmonary fibrosis, where SCID and nude mice develop higher levels of fibrosis compared to WT mice, and immune reconstitution with T cells reduces fibrotic

response [174]. Studies in CD28 knock out mice showed attenuated fibrosis, and adoptive transfer of $CD28^+$ T cells restored normal fibrotic response [175]. Furthermore, in a model utilizing CCL18 overexpression, prolonged perivascular and peribronchial T cell infiltrate associated with collagen deposition is observed in the lung [176]. Collectively, these data suggest that T cells may wear many hats, functioning as profibrotic or antifibrotic mediators depending on the host environment.

Here we describe an immunological characterization of MHV68 infection of IFNγR-/- C57Bl/6 mice which results in fibrotic disease. This chronic infection leads to multi-organ fibrosis and has been utilized to evaluate the role of gammaherpesviruses in the development of pulmonary fibrosis. Through examination of a fibrosis-deficient virus, MHV68 M1st, our study has been able to highlight the role of $CD8^+$ T cells in the development of pulmonary fibrosis. We have shown that this viral mutant, which fails to elicit expansion and activation of $V\beta4^+$ $CD8^+$ T cells, has reduced levels of viral antigen specific $CD8^+$ T cells in the lungs. We suggest that the absence of the $V\beta4^+$ $CD8^+$ T cell population results in reduced inflammation and cellular infiltrate in the lung, protecting mice from subsequent immunopathology and fibrosis. Furthermore, we are able to show that depletion of $CD8^+$ T cells during acute infection with the WT virus prevents the development of fibrosis, directly implicating $CD8^+$ T cells in the fibroproliferative process. Future studies will be necessary to clarify the role of $CD8^+$ T cells. It will be of interest to evaluate how depletion of this cellular subset impacts viral replication and cellular infiltrates in the lung. Additionally, understanding which CD8 subsets are required for disease – including epitope specific, bystander activated, and Vβ4 – may shed light on the disease process.

We find it notable that a striking immunologic change revealed by these analyses was the increased levels of neutrophils in the lungs of WT infected mice (Fig. 3C). Numerous studies have implicated neutrophils involvement in human IPF [177-179] and pulmonary fibrosis in murine models [180-183]. We therefore postulate that the effector $CD8^+$ T cells found during MHV68 infection, which express high levels of TNFα and potentially GM-CSF may effect neutrophil activation and survival (as described in [184]).

Finally, with respect to the role of herpesviruses in IFP, an open label study showed that ganciclovir treatment resulted in improvement in 9/14 IPF patients [185]. During this study, treatment was given for 2 weeks and patients were assessed for changes in EBV antibody titers, steroid use, and forced lung vital capacity. Though encouraging, there were several limitations to this study - including absence of a control arm and sample size, necessitating further exploration. Animal models have also shown successful treatment of fibrosis with antiviral cidofovir. Studies conducted by Mora *et al.* revealed that cidofovir treatment was able to reduce fibrotic disease in the MHV68 infected IFNγR-/- C57Bl/6 with treatment given as late as 60 days post infection, well after the onset of fibrotic disease [106]. Certainly gaining a better understanding of how gammaherpesviruses influence the immune response, and what features are critical for disease, may lead to more streamlined treatments. The conflicting data on the role of viral infections, as well as the role of $CD8^+$ T cells, may point toward distinct mechanisms for development of IPF.

Here we identify a role for M1-mediated $V\beta4^+$ $CD8^+$ T cells as mediators in inflammation and fibrotic disease in IFNγR-/- mice. These data support to the role of $CD8^+$ T cells as an important contributor in fibrotic pathology. Furthermore, we highlight

a potential target for therapeutic intervention; in cases were herpesvirus infection is playing a role in disease progression and may be managed pharmacologically or immunologically.

ACKNOWLEDGEMENTS

We thank the members of the Speck lab for helpful comments and suggestions during the preparation of the manuscript. We thank the Emory Children's Pediatric Research Center Flow Cytometry Core for use of the LSRII flow cytometer. Additionally, we would like to thank Dan Rifkin for the generous gift of the MLEC clone 23 cell line, Alexander Misharin for helpful discussion and feedback for the flow cytometry panels, Jake Kohlmeier for helpful discussions and training in lung methods, Mandy Ford and Dave Pinelli for p56 and p79 viral peptides and tetramer antibodies. The work was supported by NIH grants AI073830 and CA095318 to SHS, and HL115618 to BBM.

FIGURES

Figure 1.

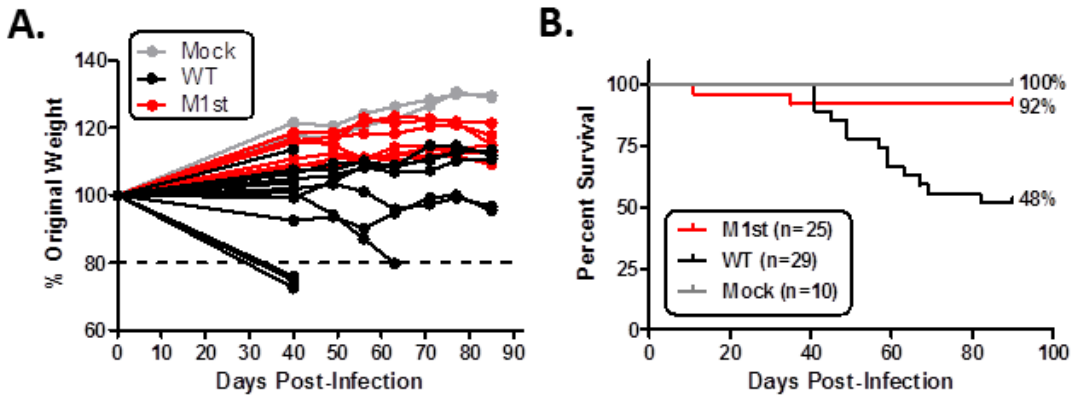

Figure 2.

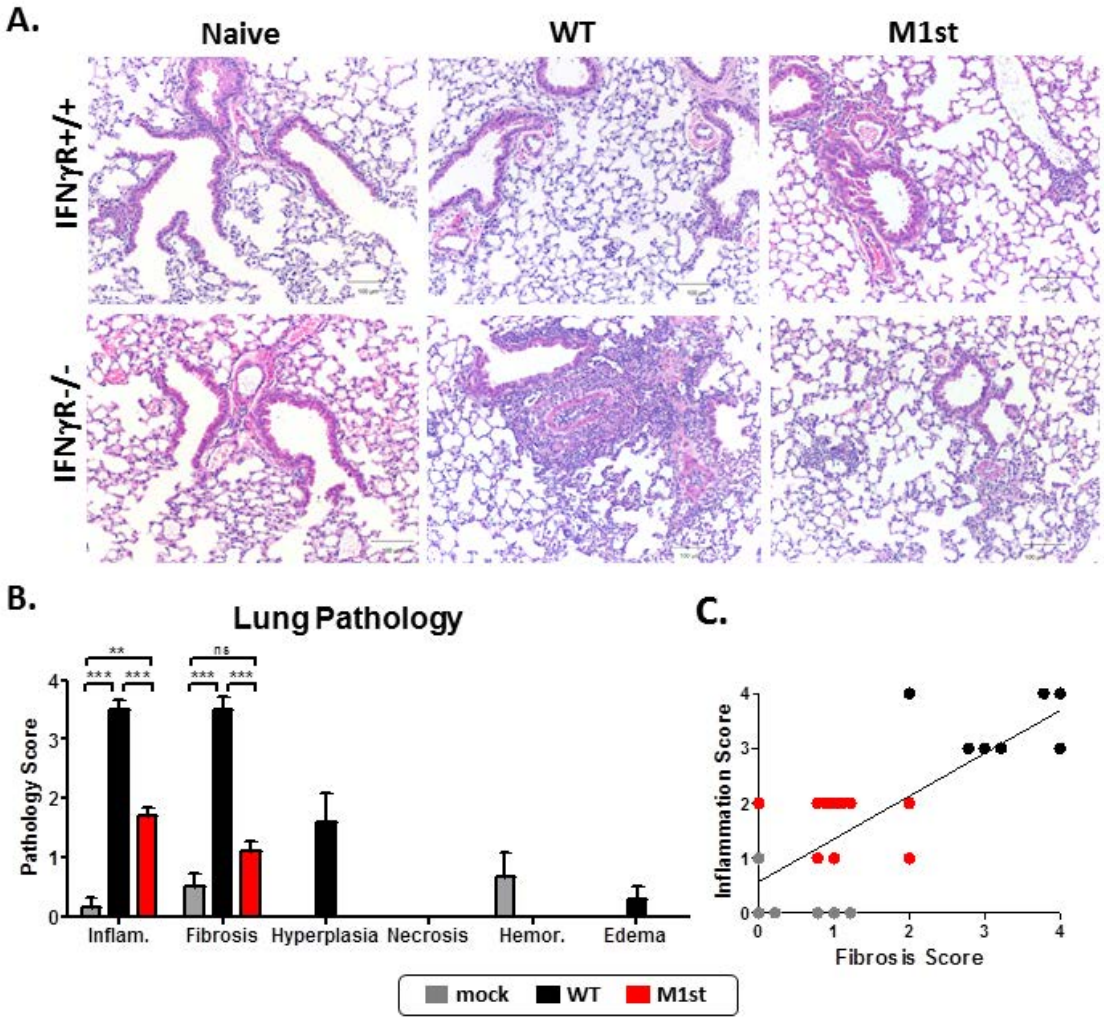
A.
Naive
WT
M1st
IFNγR+/+
IFNγR-/-
B.
Lung Pathology
Pathology Score
Inflam.
Fibrosis
Hyperplasia
Necrosis
Hemor.
Edema
mock
WT
M1st
C.
Inflammation Score
Fibrosis Score

Figure 3.

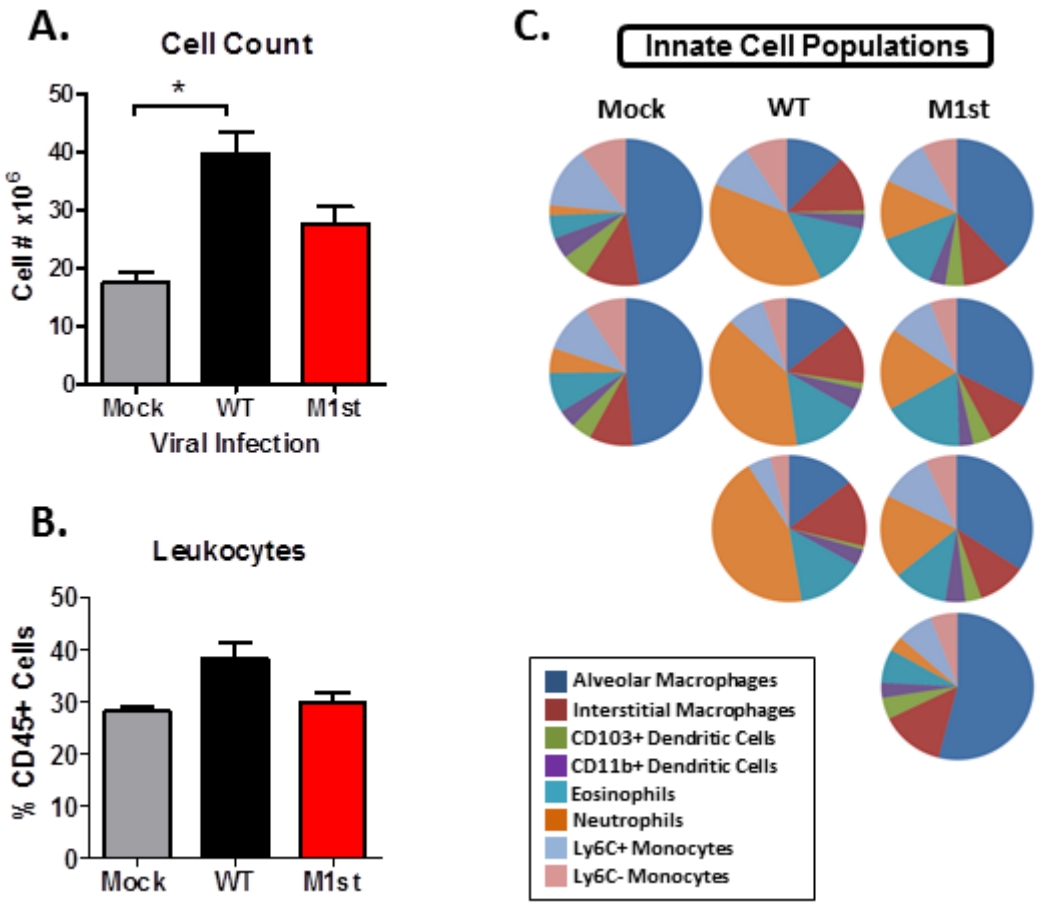
A.
Cell Count
*
50
40
30
20
10
0
Cell # x10^6
Mock
WT
M1st
Viral Infection
B.
Leukocytes
50
40
30
20
10
0
% CD45+ Cells
Mock
WT
M1st
C.
Innate Cell Populations
Mock
WT
M1st
Alveolar Macrophages
Interstitial Macrophages
CD103+ Dendritic Cells
CD11b+ Dendritic Cells
Eosinophils
Neutrophils
Ly6C+ Monocytes
Ly6C- Monocytes

Figure 4.

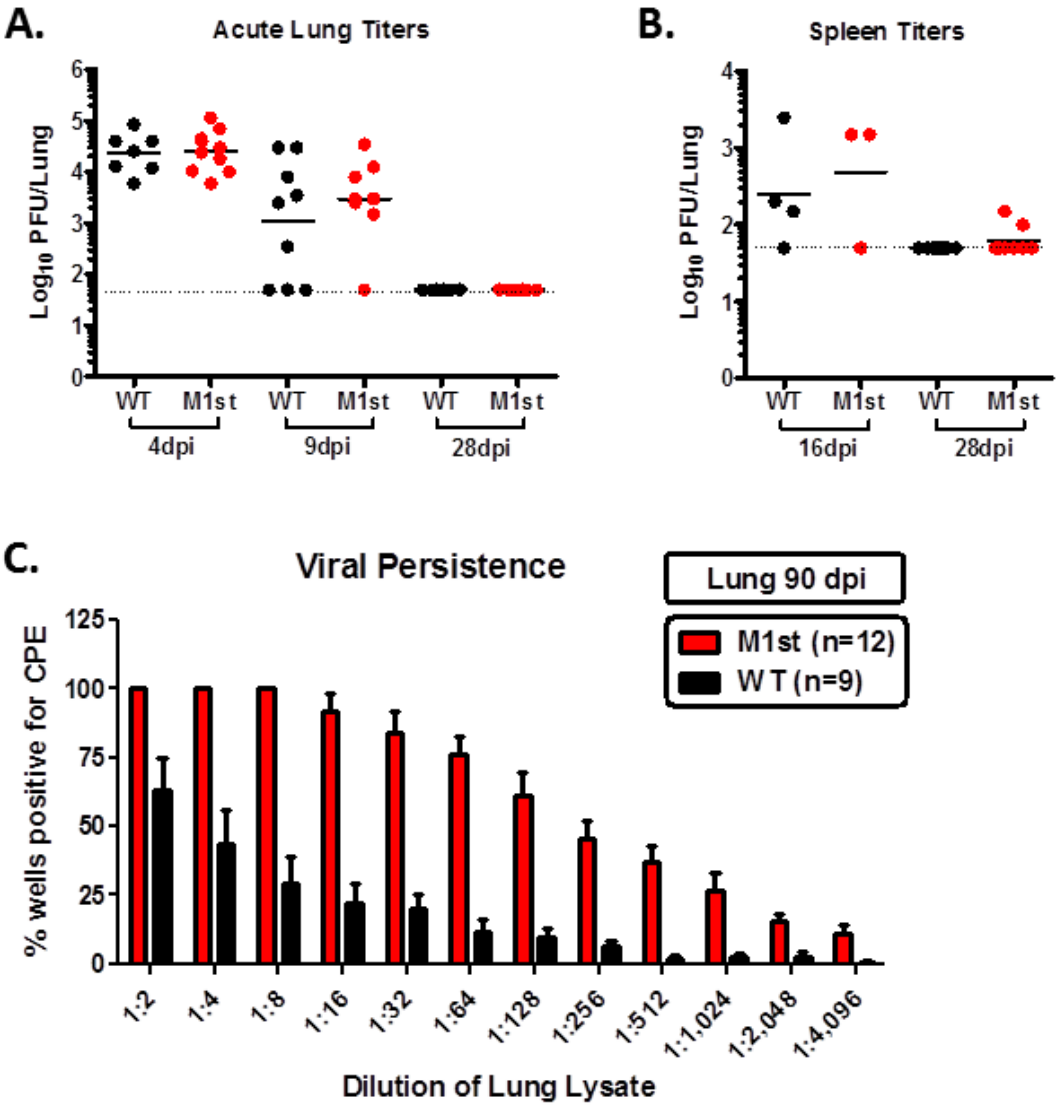
A.
Acute Lung Titers
Log10 PFU/Lung
WT
M1st
4dpi
9dpi
28dpi
B.
Spleen Titers
16dpi
C.
Viral Persistence
Lung 90 dpi
M1st (n=12)
WT (n=9)
% wells positive for CPE
1:2
1:4
1:8
1:16
1:32
1:64
1:128
1:256
1:512
1:1,024
1:2,048
1:4,096
Dilution of Lung Lysate

Figure 5.

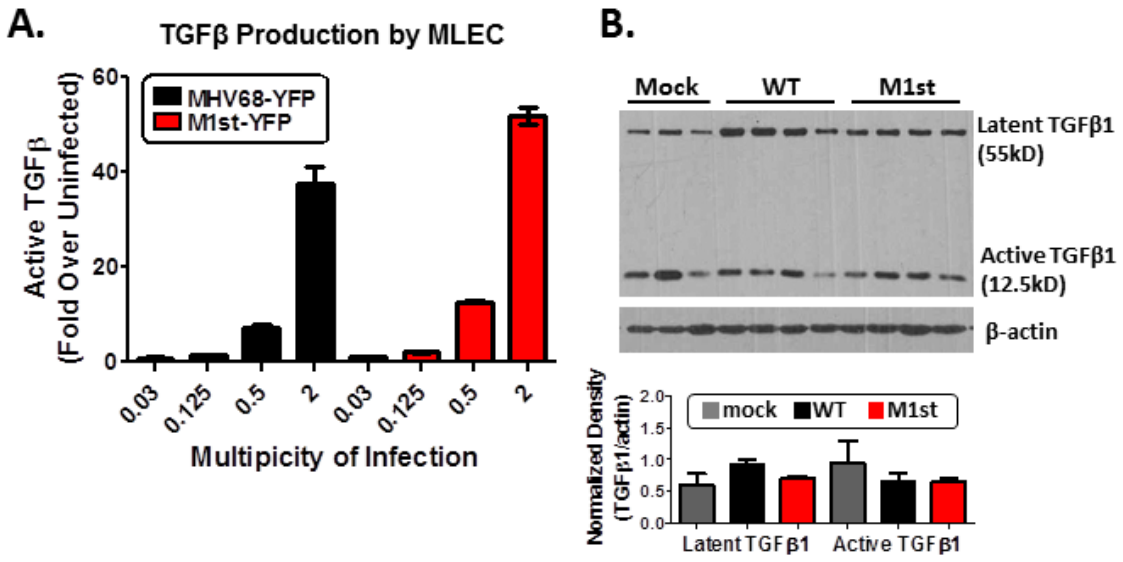
A.
TGFβ Production by MLEC
Active TGFβ
(Fold Over Uninfected)
60
40
20
0
MHV68-YFP
M1st-YFP
0.03
0.125
0.5
2
0.03
0.125
0.5
2
Multipicity of Infection
B.
Mock
WT
M1st
Latent TGFβ1
(55kD)
Active TGFβ1
(12.5kD)
β-actin
Nomalized Density
(TGFβ1/actin)
2.0
1.5
1.0
0.5
0.0
mock
WT
M1st
Latent TGFβ1
Active TGFβ1

Figure 6.

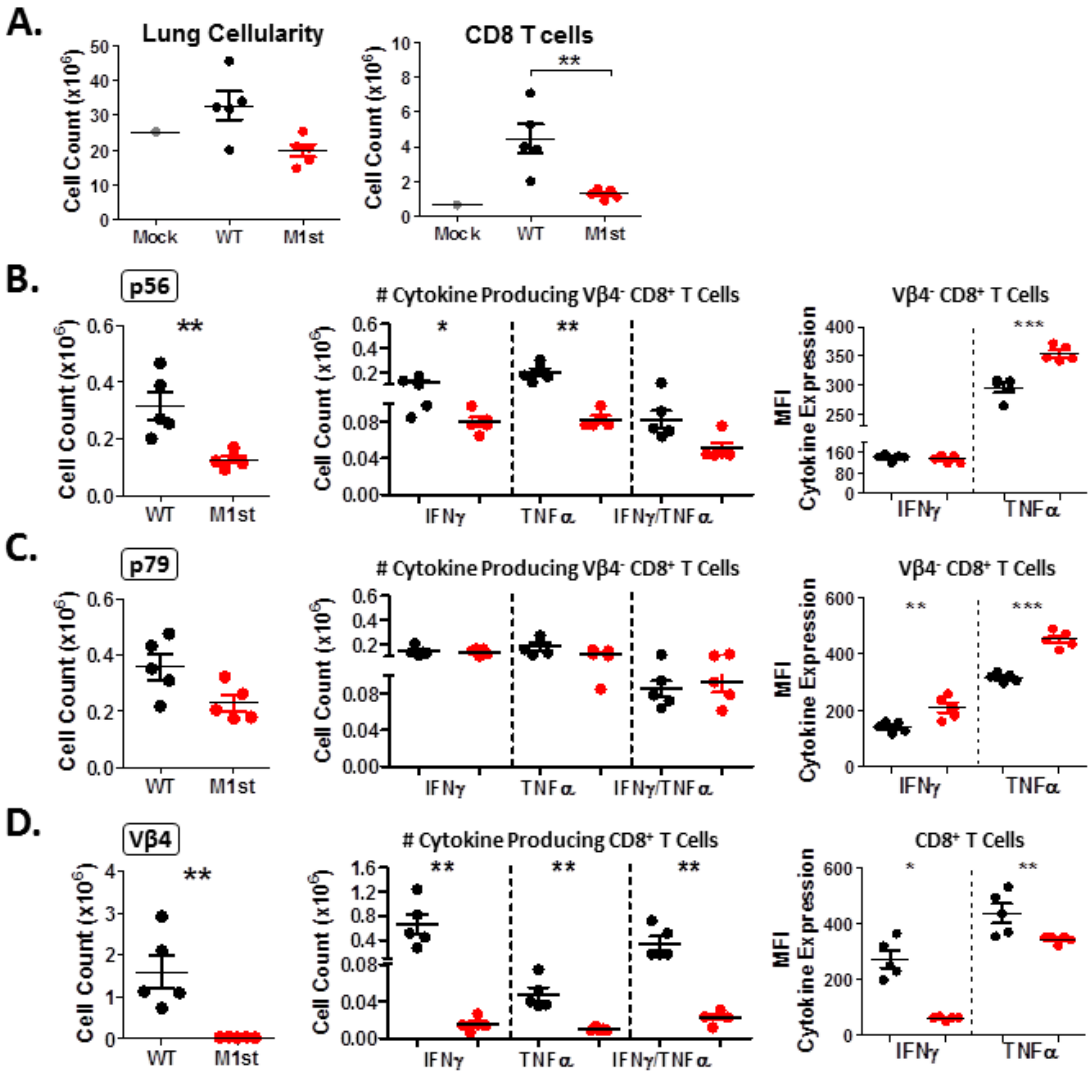
A.
Lung Cellularity
Cell Count (x10^6)
Mock
WT
M1st
CD8 T cells
**
B.
p56
Cytokine Producing Vβ4- CD8+ T Cells
Vβ4- CD8+ T Cells
MFI
Cytokine Expression
IFNγ
TNFα
IFNγ/TNFα
C.
p79
D.
Vβ4
CD8+ T Cells

Figure 7.

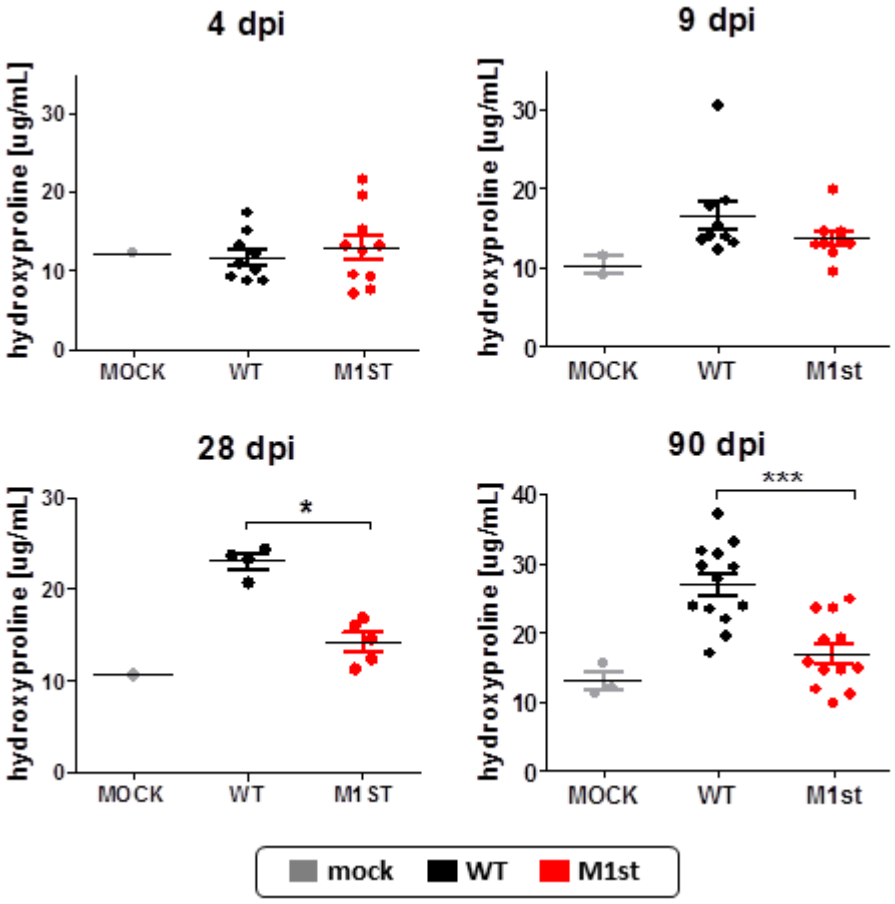
4 dpi
9 dpi
28 dpi
90 dpi
hydroxyproline [ug/mL]
MOCK
WT
M1ST
M1st
*
***
mock
WT
M1st

Figure 8.

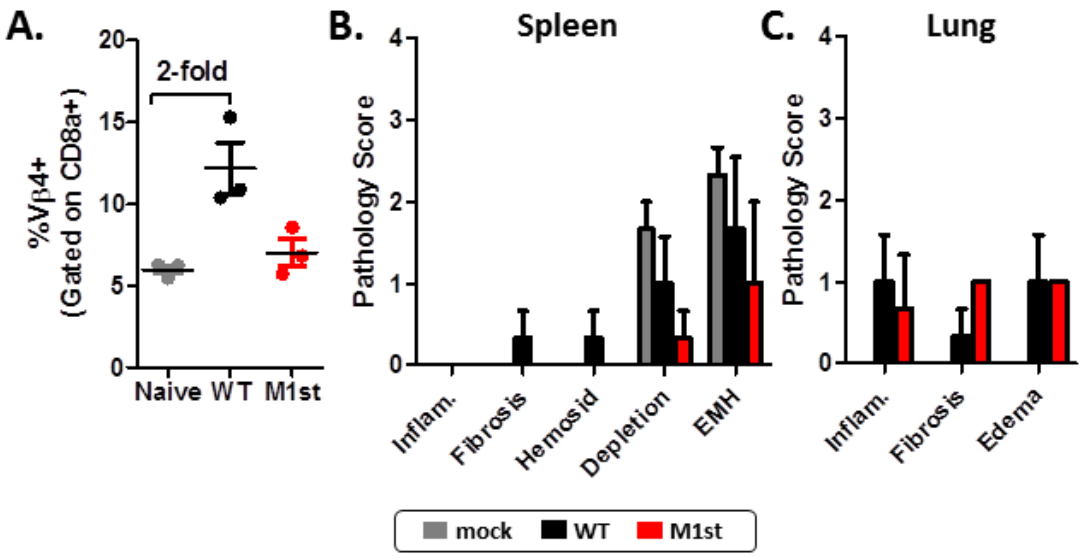
A.
2-fold
%Vβ4+
(Gated on CD8a+)
20
15
10
5
0
Naive
WT
M1st
B.
Spleen
Pathology Score
4
3
2
1
0
Inflam.
Fibrosis
Hemosid
Depletion
EMH
C.
Lung
Pathology Score
4
3
2
1
0
Inflam.
Fibrosis
Edema
mock
WT
M1st

Figure 9.

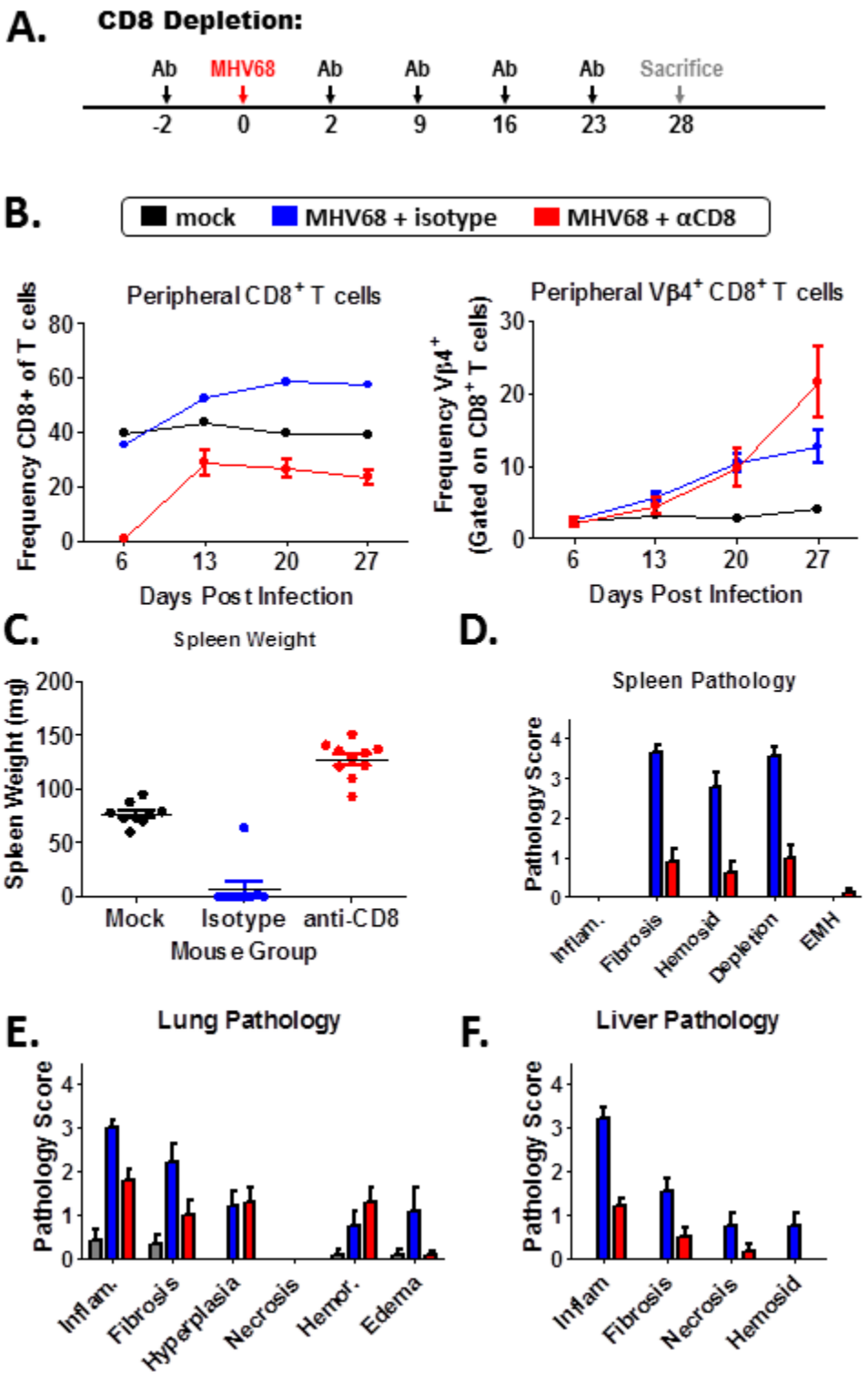
A.
CD8 Depletion:
Ab
MHV68
Ab
Ab
Ab
Ab
Sacrifice
-2
0
2
9
16
23
28
B.
mock
MHV68 + isotype
MHV68 + αCD8
Peripheral CD8+ T cells
Frequency CD8+ of T cells
Days Post Infection
Peripheral Vβ4+ CD8+ T cells
Frequency Vβ4+ (Gated on CD8+ T cells)
Days Post Infection
C.
Spleen Weight
Spleen Weight (mg)
Mock
Isotype
anti-CD8
Mouse Group
D.
Spleen Pathology
Pathology Score
Inflam.
Fibrosis
Hemosid
Depletion
EMH
E.
Lung Pathology
Pathology Score
Inflam.
Fibrosis
Hyperplasia
Necrosis
Hemor.
Edema
F.
Liver Pathology
Pathology Score
Inflam
Fibrosis
Necrosis
Hemosid

Supplemental Figure 1.

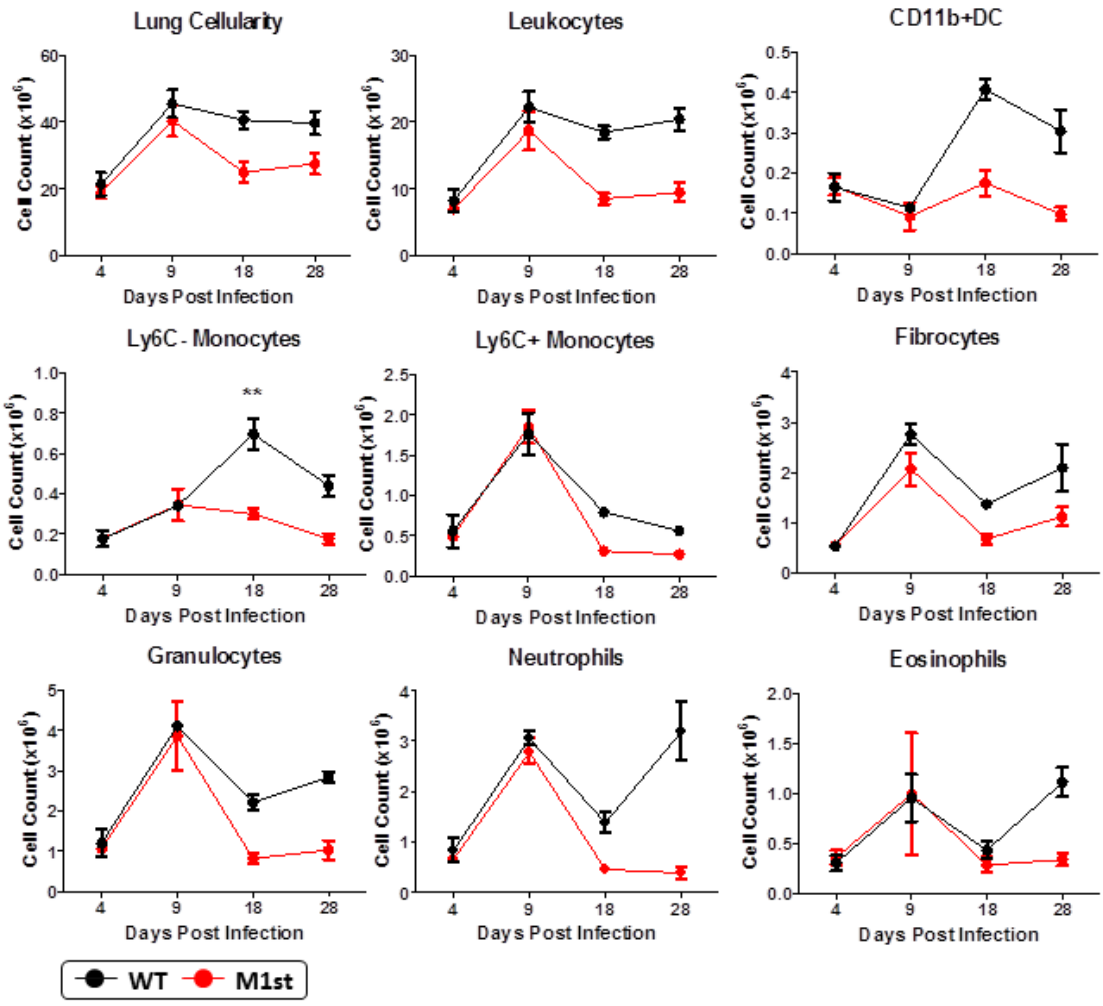

Supplemental Figure 2.

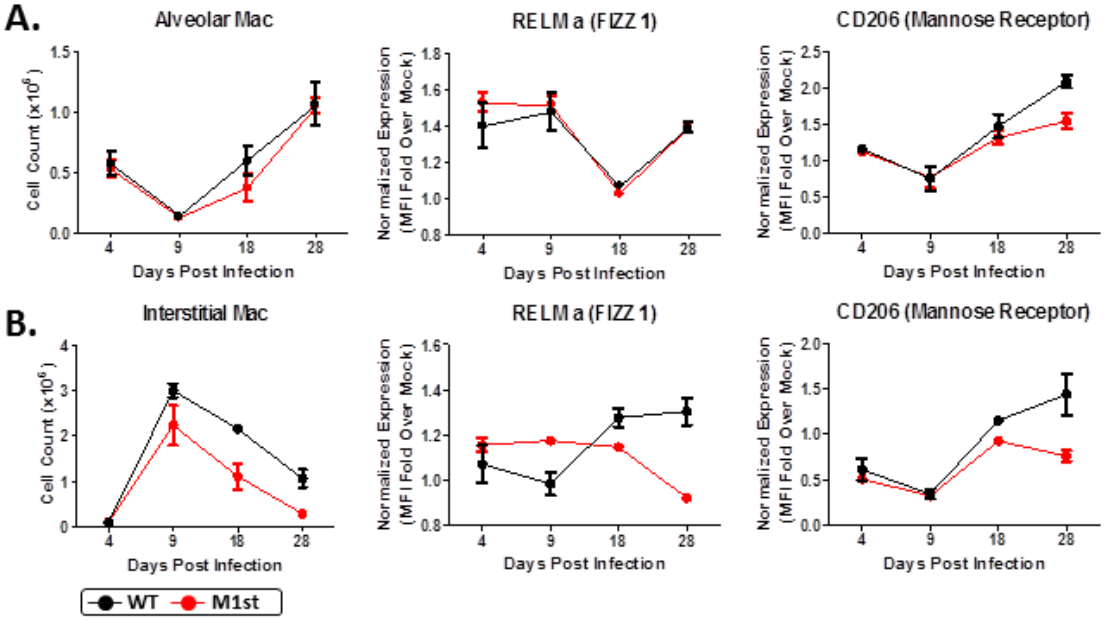

Supplemental Figure 3.

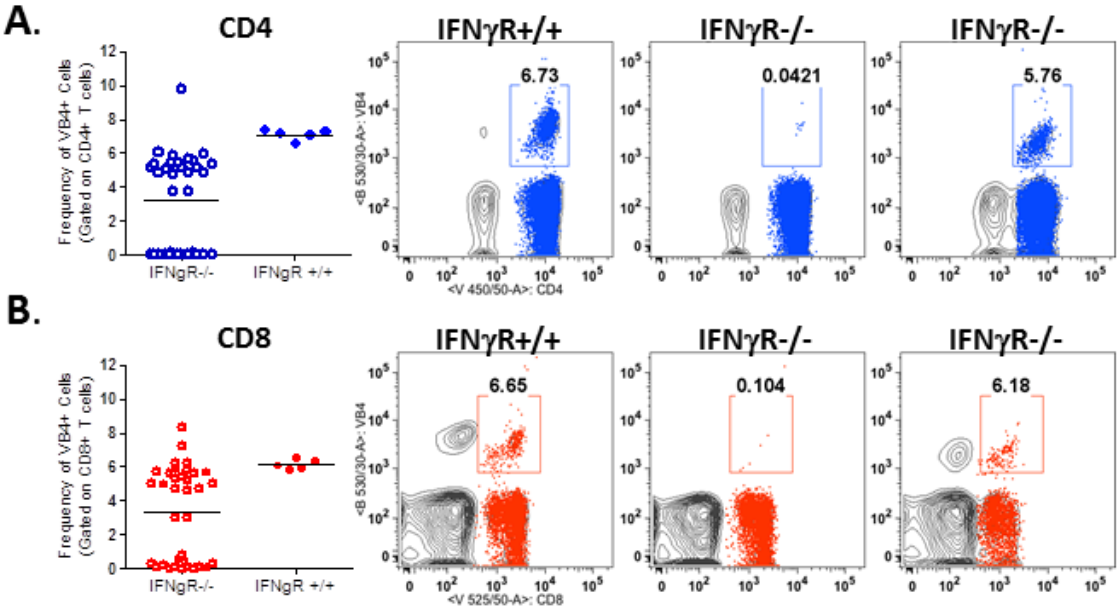

Supplemental Figure 4.

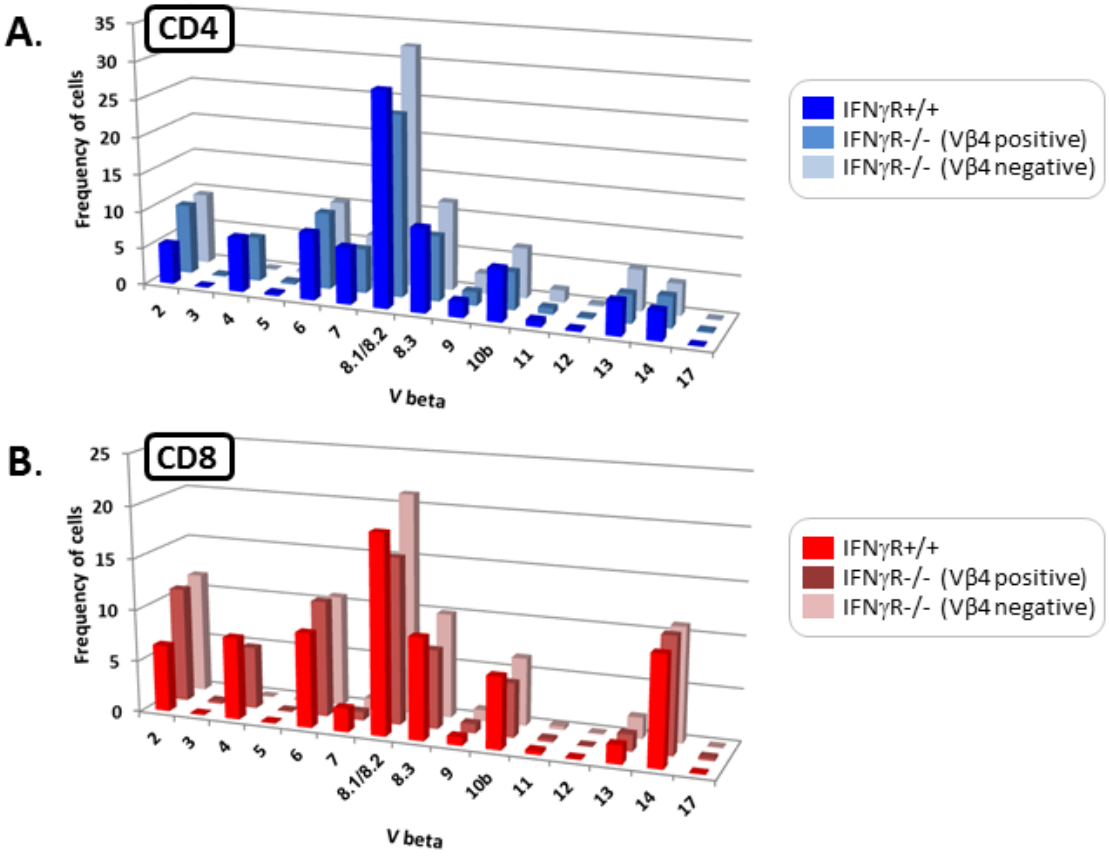

Supplemental Figure 5.

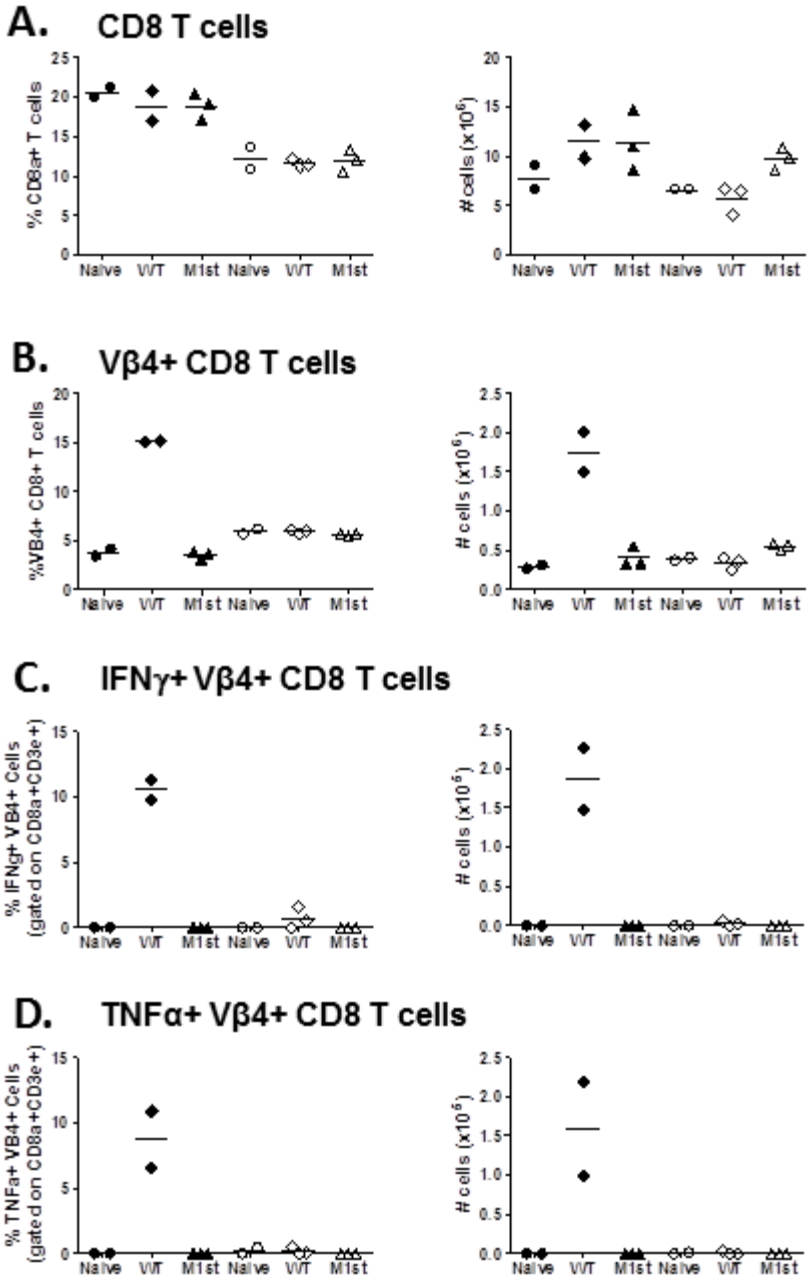

FIGURE LEGENDS

Figure 1. M1 expression is associated with lethality in MHV68 infected IFNγR-/- C57Bl/6 mice. 8-12 week old IFNγR-/- C57Bl/6 mice were intranasally infected with $1x10^5$ pfu MHV68 (WT or M1st) or were mock infected. (A) Mice were observed for weight change from starting weight, a loss of 20 percent or greater resulted in sacrifice. (B) Kaplan-Meier curves indicating mouse survival are shown. Significance was determined using log rank test with GraphPad software. $P = 0.0027$ for WT vs M1st infection.

Figure 2. M1 induced fibrosis in IFNγR-/- C57Bl/6 mice is associated with heightened levels of inflammation in lung tissue. 8-12 week old WT or IFNγR-/- C57Bl/6 mice were intranasally infected with 1000 pfu MHV68 (WT or M1st) or were mock infected and sacrificed at 28 days post infection. Histological analysis was performed on lung tissues stained with hemotoxylin and eosin (H&E) or Masson's Trichrome (MT). (A) Representative H&E stained sections are shown, scale bar = 100μm. Scores were determined for (A) pathology (mean and std. error are shown) from H&E sections and (B) fibrosis scores from MT sections, correlation was assessed using a Pearson's Correlation test, showing R = 0.9929 at $P = 0.0007$, $R^2 = 0.9858$. Mock (n=6), WT (n=10), and M1st (n=10).

Figure 3. Global alterations in cellular composition of lung are observed in fibrotic IFNγR-/- C57Bl/6 mice. 8-12 week old IFNγR-/- C57Bl/6 mice were intranasally infected with $1x10^5$ pfu MHV68 (WT or M1st) or were mock infected and sacrificed at 28 days post infection. Whole lungs were assessed for (A) total number of cells (mean

and std. error shown), (B) frequency of $CD45^+$ cells (mean and std. error), and (C) frequency of innate populations (described in [145]). Statistics were performed using Kruskal-Wallis test with Dunn's post test, $P = 0.0463$. Mock (n=2), WT (n=3), M1st (n=4).

Figure 4. The absence of M1 expression does not impact acute viral replication, and M1 is not required for viral persistence in the lung. 8-12 week old IFNγR-/- C57Bl/6 mice were intranasally infected with $1x10^5$ pfu MHV68 (WT or M1st) and sacrificed at indicated times. (A) Lung titers from mice at days 4, 9, and 28 post infection (n=7-10 mice/group from two independent experiments). (B) Spleen titers from mice at days 16 and 28 days post infection (n=4-9 mice/group one or two independent experiments). (C) Viral persistence was measured by assessing cytopathic effect (CPE) induced by infected lung lysate plated on mouse embryonic fibroblasts (mean and std. error are shown).

Figure 5. The absence of fibrosis in M1st infected IFNγR-/- C57Bl/6 mice is not due to a failure to induce profibrotic mediator TGFβ1. (A) Mink lung epithelial cells (MLEC-clone 32) stably transfected with a plasminogen activator inhibitor-1 fused to a luciferase reporter gene were infected with differing multiplicities of infection and assayed for luciferase activity (a read out of active TGFβ production). 8-12 week old IFNγR-/- C57Bl/6 mice were intranasally infected with $1x10^5$pfu MHV68 (WT or M1st) or mock infected and sacrificed at 28 days post-infection (n=3-4 mice/group). (B) lung lysates (30μg) were assessed for TGFβ1 expression by western blot (mock lane 1-3, WT lane 4-7, M1st lane 8-11), (C) normalized band density is shown.

Figure 6. Reduced $CD8^+$ and effector $CD8^+$ T cells are observed in absence of M1 expression. 8-12 week old IFNγR-/- C57Bl/6 mice were intranasally infected with $1x10^5$ pfu MHV68 (WT or M1st) and sacrificed at 28 days post infection. Whole lungs were harvested and assessed for presence of $CD8^+$ T cell populations and effector function (n=5 mice/group). Mean and std. error are shown for (A) absolute number of lung and $CD8^+$ T cells, (B&C) absolute number of tetramer specific and peptide responsive $CD8^+$ T cells, with MFI of cytokine expression, (D) absolute number of $V\beta4^+$ $CD8^+$ T cells and M1 responsive $CD8^+$ T cells. Statistics were measured using a Mann-Whitney 2 tailed test (* P = 0.0119, ** P = 0.0079, * P = <0.0004).

Figure 7. Development of M1 dependent fibrosis in IFNγR-/- C57Bl/6 mice correlates with timing and kinetics of $V\beta4^+$ $CD8^+$ T cell expansion. 8-12 week old IFNγR-/- C57Bl/6 mice were intranasally infected with $1x10^5$ pfu MHV68 (WT or M1st) or were mock infected and sacrificed at indicated times (n=1-13 mice/group from one or two independent experiments). Right and accessory lobes were harvested and assessed for hydroxyproline content at days 4, 9, 28, and 90 post-infection. Statistics were performed using Mann-Whitney 2 tailed test to compare WT and M1st (* P = 0.0159, *** P = 0.0008).

Figure 8. IFNγR-/- Balb/c mice are protected from MHV68 induced fibrosis. 8-12 week old IFNγR-/- Balbc mice were intranasally infected with 1000 pfu MHV68 (WT or M1st) or mock were infected and sacrificed at 28 days post infection (n=3 mice/group). (A) $V\beta4^+$ $CD8^+$ T cell populations in spleen were assessed by flow cytometry. (B and C)

Pathology scores were determined from H&E stained sections and fibrosis was evaluated with Masson's trichrome stained tissue sections.

Figure 9. Depletion of CD8 T cells ameliorates MHV68 induced fibrotic disease in IFNγR-/- C57Bl/6 mice. 8-12 week old IFNγR-/- C57Bl/6 mice were intranasally infected with $1x10^5$ pfu WT MHV68 and treated with either Rat IgG isotype or Rat αCD8 (clone YTS 169.4) antibodies prior to sacrifice (n=4-5 mice/group). (A) CD8 depletion strategy is shown. (B) Peripheral blood was assessed for $CD8^+$ and $V\beta4^+$ $CD8^+$ T cell frequencies. (C) Mouse spleen weight at sacrifice and (D-F) pathology scores are shown. Scores were determined from H&E stained sections and fibrosis was evaluated with Masson's Trichrome stained tissue sections.

Supplemental Figure 1. Elevated levels of innate cell populations are observed in IFNγR-/- C57Bl/6 mice in the presence of M1 expression. 8-12 week old IFNγR-/- C57Bl/6 mice were intranasally infected with $1x10^5$ pfu MHV68 (WT or M1st) and sacrificed at indicated times post infection (n=3-4 mice/group at each time-point). Whole lungs were harvested and assessed for cellular composition by flow cytometry using a panel to detect innate immune cell populations (described in [145]) and fibrocytes (described in [148]). Statistics were assessed using Mann-Whitney 2 tailed test, ** P = 0.0048.

Supplemental Figure 2. Elevated levels of alternative macrophage activation are observed in lung of fibrotic IFNγR-/- C57Bl/6 mice. 8-12 week old C57Bl/6 IFNγR-/- mice were intranasally infected with $1x10^5$ pfu MHV68 (WT or M1st) and sacrificed at indicated times post infection (n=3-4 mice/group at each timepoint). Whole lungs were harvested and assessed for macrophage population and phenotype. (A-B) Absolute

number of alveolar and interstitial macrophages were quantified and assessed for alternative activation using RELMα and CD206 expression.

Supplemental Figure 3. IFNγR deficiency leads to deletion of Vβ4$^+$ T cells from about half of the IFNγR-/- Balb/c mice. 7-10 week old naïve WT or IFNγR-/- Balb/ mice were assessed for Vβ4$^+$ T cell populations in peripheral blood by flow cytometry. (A-B) Quantitation of CD4 or CD8 T cell populations are shown alongside representative figures of WT or IFNγR-/- Balb/c that have either retained or lost the Vβ4$^+$ T cells. IFNγR-/- Balb/c (n=35) WT Balb/c (n=5).

Supplemental Figure 4. Loss of Vβ4 population does not substantially alter T cell repertoire in IFNγR-/- Balb/c mice. T cell repertoire was evaluated in 15 week old naïve IFNγR-/- Balb/c mice. Spleens were harvested and frequency of Vβ subsets were assessed. (A) CD4 and (B) CD8 T cells is shown. IFNγR-/- Balb/c (n=8) WT Balb/c (n=5).

Supplemental Figure 5 . Lack of M1-induced cytokine response from Vβ4$^+$CD8$^+$ T cells in Balb/c mice. WT C57Bl/6 (filled symbols) and Balb/c mice (opened symbols) were intranasally infected with 1000 pfu MHV68 (WT or M1st) or left naïve and sacrificed at 28 dpi (n=2-3 mice/group). Splenocytes were isolated for *in vitro* stimulation. Cells were left unstimulated, or were stimulated with PMA & Ionomycin, or recombinant protein containing supernatants containing either M1st or M1 prior to intracellular cytokine staining for IFNγ and TNFα. Control treated cells are not show.

TABLES

Table 1. Antibodies used for flow cytometry.

Innate Phenotyping

CD11b	BV421
MHCII	V500
CD45	FITC
CD103	PerCP-Cy5.5
CD64	PE
Siglec F	PE-CF594
CD11c	PE Cy7
CD24	APC
Ly6G	Alexa700
LyGC	APC-Cy7

TCR (Vβ) Repertoire Analysis

VB	FITC
CD19	APC-Cy7
CD4	Pacific Blue
CD3e	PE
CD44	PECy7
CD8a	Pacific Orange

Vβ4 Analysis for CD8 Depletions

CD8	Pacific Orange
CD4	PE
VB4	FITC
CD44	PE-Cy7
CD62L	APC
CD3e	Alexa 700
CD19	APC-Cy7

ICCS of Lung Cells

CD8	Pacific Orange
CD4	PerCP-Cy5.5
CD3e	PE-Cy7
IL2	BV421
IFNγ	APC
TNFα	PE
VB4	FITC
Fixable Via	APC-Cy7

Tetramer Staining

p56	APC
p79	PE
CD62L	Pacific Blue
CD8a	Pacific Orange
CD45	PerCP-Cy5.5
CD44	PE-Cy7
CD3e	Alexa700

Macrophage Activation Phenotyping

CD11b	BV421
MHCII	V500
CD45	FITC
CD64	PE
CD24	PE CF594
CD11c	PE Cy7
one of the following:	
CD40	Alexa647
CD86	APC
CD80	APC
CD71	APC
CD206	Alexa647
RELMa	unconjugated 1°, 2° DαRb Alexa647

Fibrocyte Staining

CD45	PerCP Cy5.5
Col1	unconjugated 1°, 2° DαR PE

Vβ4 Analysis for IFNγR-/- Balb/c

CD8	Pacific Orange
CD4	Pacific Blue
VB4	FITC
VB5	PerCP-Cy5.5
CD62L	APC
CD44	PerCP-Cy5.5
CD19	APC-Cy7
CD3e	PE-Cy7

ICCS of Splenocytes

CD8	BV711
CD3e	PE-Cy5
CD44	PE-Cy7
IL2	BV421
IFNγ	APC
TNFα	PE
VB4	FITC
Fixable Via	APC-Cy7

Chapter IV

SUMMARY, DISCUSSION, AND FUTURE DIRECTIONS

MHV68 provides a unique system to evaluate gammaherpesviral biology and pathogenesis. Exploration of viral mutants in the context of a healthy immunocompetent host reveals gene function and their role in infection; however, significant insights can be gained through evaluation of viral mutants in genetic knock out mice. Clambey *et al.* set the foundation to study the function of M1 with the generation of M1 mutant viruses, MHV68-M1-LacZ and MHV68 M1Δ511. Evaluation of these mutants revealed a hyper-reactivation phenotype for M1 null MHV68 mutants in C57Bl/6 mice, and uncovered a role for M1 in mortality and splenic pathology in IFNγR-/- C57Bl/6 mice [11]. Subsequent studies by Evans *et al.* identified M1 as the viral gene product responsible for $V\beta4^+$ $CD8^+$ T cell expansion [12]. Additionally, these studies made a functional link between $V\beta4^+$ $CD8^+$ T cell expansion and control of viral infection. However, we still have an incomplete understanding of how M1 carries out its function. Studies to evaluate how M1 protein interacts and stimulates $V\beta4^+$ $CD8^+$ T cell activation and expansion have been inconclusive and technically challenging. To gain further insights into M1 function we set out to identify the site, timing, and regulation of M1 expression.

The work presented here aimed to (i) define the site of M1 expression *in vivo* and characterize its transcriptional regulation, and (ii) to further characterize the role of M1 in fibrotic disease in IFNγR-/- mice. In chapter II we identify plasma cells as the primary reservoir of M1 expression *in vivo*, and identify critical transcriptional regulators of M1

gene transcription. We identified a novel interaction between the viral replication and transcription activator (Rta) and host transcription factor interferon regulatory factor 4 (IRF4). Additionally, we identified a novel consensus sequence for Rta binding which is conserved in several other MHV68 genes. These findings highlight one mechanism utilized by MHV68 to regulate lytic gene expression. In the second aim of this dissertation, we follow up on the observation that M1 is required for fibrotic disease [11,12], exploring the role of M1-driven $V\beta4^+$ $CD8^+$ T cell expansion in pulmonary fibrosis in Chapter III. Here we showed that M1 is required for inflammation in the lung, which is strongly correlated with fibrosis. A notable change in cellular composition of the lung is observed during the course of infection. Infiltrating cells are comprised of many populations, with the most striking differences observed in the neutrophil and $CD8^+$ T cells population at 28 days-post infection. We show a reduced $CD8^+$ T cell response in the M1st infections, with reduced levels of viral epitope specific cells and cytokine producing cells in the lung. Additionally, we observe protection from pulmonary fibrosis in IFNγR-/- Balb/c mice which lack $V\beta4^+$ $CD8^+$ T cell expansions. Taken together these data suggest a role for $V\beta4^+$ $CD8^+$ T cells in providing an inflammatory environment that increases cellular trafficking to the lung – ultimately resulting in immunopathology and fibrosis. We confirmed the role of $CD8^+$ T cells through $CD8^+$ T cell depletion analyses, where we show that depletion of this population of cells protects mice from fibrosis and lethality. The implications for these findings and future experiments are discussed below.

Characterizing M1 expression *in vivo and its* transcriptional regulation

M1 expression *in vitro* and *in vivo* has been poorly characterized, and what little

was known came from large scale, global analyses of MHV68 gene expression [10,19-24]. Furthermore, nothing was known about its transcriptional regulation. The studies presented in Chapter II set out to (i) identify the major reservoir(s) of M1 expression *in vivo*, and (ii) examine the transcriptional regulation of M1. Here we identified plasma cells as the primary reservoir of M1 expression. Notably, plasma cell differentiation has been linked with gammaherpesviral reactivation for EBV and KSHV [29-32,34]; and plasma cells have been shown to be the predominant source of MHV68 reactivation from the spleen upon explant into tissue culture [9]. Given this link, the observation that M1 was expressed from this cellular reservoir supported a hypothesis where M1 expression would be influenced by Rta expression, the major viral transcriptional activator that triggers virus reactivation from latency. Our findings revealed basal M1 promoter expression in a plasma cell line that is dependent on IRF4 interaction with M1 promoter. Further, over-expression of MHV68 Rta resulted in greatly increased levels of M1 promoter activity. To extend these observations, we evaluated the response of the M1 promoter in 293T cells, where neither Rta or IRF4 are expressed, and observed a robust synergy between Rta and IRF4. A likely feature of evolutionary development, Rta has been shown to modulate viral gene expression through direct DNA protein interaction, as well as through more complex protein-protein mediated interactions (Reviewed in [131]) – allowing viral gene expression to be regulated in a context and cell type specific manner. Many interacting partners of Rta have been identified in the gammaherpesvirus subfamily. KSHV Rta (kRta) has been shown to interact with a hypothetical human protein MGC2663, later annotated as KSHV RNA binding protein K-RBP [186] and human proteins Oct1 and RBPJκ [128,129,187,188]; as well as viral proteins kBZIP,

ORF59 (a DNA polymerase processing factor), and vIRF4 [130,189,190] to modulate ORF59, OriLyt, and KSHV bZIP expression [129,188,190]. In EBV interactions have been noted between Rta (R, BRLF1) and viral ZTA (Z, BZLF1) and RanBPM, as well as with host retinoblastoma protein, CBP, MCAF, and Oct1 [191-196]. In herpesvirus saimiri, Rta has been shown to interact with host TATA binding protein [197]. Little is known about the interacting proteins of MHV68 Rta. Xuan *et al.* reported the ability of Rta to antagonize host antiviral protein, ZAP; however the authors noted that coimmunoprecipitation of Rta and ZAP failed, suggesting that the interaction may be too weak to observe by this method [198]. Thus, it was of significant interest that we were able to demonstrate that the synergistic effects of Rta and IRF4 on M1 promoter were mediated through protein-protein interactions. This provided the first description of an MHV68 Rta interacting partner. This partnered interaction reflects a mechanism utilized by the virus to fine tune gene expression in a cellular and context specific manner. It will be of interest to identify the interacting motifs in Rta and IRF4, in order to discern whether they interact directly, or through a larger multi-protein complex. Additionally, it will be of interest to identify other host and viral genes regulated by Rta and IRF4.

In the human herpesviruses, Rta binding sequences have been identified in KSHV PAN, K12, and vIL6 genes (Reviewed in [131]). Two Rta response elements (RRE) have been identified in MHV68 Rta responsive ORF57 promoter, one of which contains 2 RBPJk/CBF1 sites [126,127]. Additional RRE sites have been noted in MHV68 ORF18 and K3, which share a conserved 15 base pair sequence [199]. In Chapter II we describe a novel RRE in the M1 promoter. Notably, this seven base pair core sequence was identified in other MHV68 promoter regions. We found Rta responsiveness in ORF8, 22,

and 63 promoters, ORF50 N4/N5 promoter, and ORF50 proximal promoter. This novel RRE adds to the short list of known RRE in MHV68. It is noteworthy that this sequence is both shared and functional in several other MHV68 promoters. Despite the fact that these promoters were responsive to Rta alone, where co-expression with IRF4 showed no further effect, it is likely that other host or viral proteins might mediate specificity of expression. Whether additional host proteins interact with Rta to mediate its effect on the M1pRRE containing promoters remains to be determined. Another important question to be addressed is what impact mutagenesis of this sequence will have on M1 expression and function *in vivo*. To evaluate this, we can engineer mutations into the M1pRRE sequence of the M1pYFP virus, and evaluate phenotypic changes in YFP expressing populations.

In addition to the synergistic regulation of M1 promoter between Rta and IRF4, we have observed synergy between IRF8 and Rta (data not shown). These proteins share a core IRF binding sequence (described in [125]). As M1 promoter activity was observed in both germinal center B cells and plasma cells, it is possible that Rta partners with both host proteins. Higher levels of IRF8 are observed in germinal center B cells, but they rapidly decline in favor of IRF4 during plasma cell differentiation. Perhaps these interacting partners provide a way to restrict M1 promoter expression to B cells during MHV68 infection. Future studies with the mutant M1pRRE M1pYFP virus would allow evaluation of the significance of these Rta partnerships *in vivo*.

Evaluating the role of M1 in MHV68 induced fibrosis

Significant progress has been made in the field of pulmonary fibrosis; however,

the role and contribution of viral infections remains elusive. There is mounting evidence suggesting a role for occult viral infections as a contributing factor in disease pathogenesis (reviewed in [155] and [51]). Although it is well accepted that viral infections trigger acute exacerbations in COPD patients [200], ongoing research continues to explore the role of infection in acute exacerbations of IPF (AE-IPF). Numerous studies have shown a correlation between infection and IPF (discussed at length in Chapter I). Additionally, there is an increasing appreciation for the impact of viral infections on lung homeostasis; respiratory infections may result in tissue damage and subsequent repair, and in concert with other predispositions, a chronic or reactivating virus may influence the development of pulmonary fibrosis [155]. EBV has been shown to infect alveolar epithelial cells, leading to elevated expression of the profibrotic mediator TGFβ, and induction of epithelial to mesenchymal transition [74-76]. These, and many other features, are mirrored in our model system of gammaherpesvirus induced pulmonary fibrosis [104,148].

Previous work revealed a critical role for $CD8^+$ T cells in development of fibrosis [99]. Taken with the observation that M1 is required for multi-organ fibrosis in IFNγR-/- mice [11,12], we hypothesized that M1 contributes to fibrosis through its induction of $V\beta4^+$ $CD8^+$ T cell expansion. The studies presented in chapter III set out to (i) characterize the immunological differences in M1st and WT infection of IFNγR-/- mice, and (ii) to evaluate how $V\beta4^+$ $CD8^+$ and $CD8^+$ T cells influence pulmonary fibrosis.

We found a strong correlation between inflammation of the lung and fibrosis, noting close proximity of inflammatory cells and areas of collagen deposition. Flow cytometric analysis of the cellular composition of the lung revealed a striking M1-

dependent cellular infiltrate between days four and nine post infection, which remained elevated throughout latency. The most striking changes in cellular composition in the lung were increased levels of neutrophil and $CD8^+$ T cells at 28 days-post infection. Elevated neutrophil levels have been observed in BALF and lung parenchyma of IPF patients [177,178] and in murine models of pulmonary fibrosis [180,181]. Elevated neutrophil elastase-a1inhibitor complex levels in BALF and serum of IPF patients have been shown to correlate with severity of clinical symptoms [178,179]. Experimental inhibition of neutrophil elastase with sivelestat in a bleomycin induced fibrosis model revealed critical functions in TGFβ activation and inflammatory cell recruitment [181]. Additionally, inhibition of neutrophil chemotaxis by blocking CXCL6, resulted in reduced neutrophil infiltration, collagen deposition, inflammation, and expression of IL1β, CXCL6, and TIMP1 [182]. Further, *in vitro* treatment of lung fibroblasts with neutrophil elastase has been shown to cause proliferation and myofibroblast differentiation, offering a potential mechanism for pathogenesis [183]. The striking levels of neutrophils present in the fibrotic lung, suggest that this cell population may play a critical role in our fibrosis model. To better understand the role of neutrophils in our model, mice can be treatment with anti-CXCL6 or sivelestat to evaluate changes in fibrosis.

Interestingly, Pelletier *et al.* reported that activated T cells can modulate survival and activation of human neutrophils through cytokine production [201]. TNFα, IFNγ, and GM-CSF were shown to stimulate the survival and expression of activation markers on neutrophils. Here we have shown that in the absence of M1 expression in IFNγR-/- mice, there are reduced levels $CD8^+$ T cells, as well as a dramatic reduction in viral antigen

specific $CD8^+$ T cells. Importantly, this reduction in antigen specific $CD8^+$ T cells leads to a significant decrease in the number of IFNγ and TNFα secreting cells. Taken together, this data may explain the reduced levels of neutrophil in M1st infected mice. Future studies will be necessary to determine if the effector $CD8^+$ and $V\beta4^+$ $CD8^+$ T cell populations make GM-CSF, in addition to the IFNγ and TNFα shown here. It will also be important to evaluate what impact these populations have on neutrophil survival, activation, and development of fibrosis. Additionally, we hope to determine what role the M1-dependent $V\beta4^+$ $CD8^+$ T cell expansion has on recruitment or propagation of the epitope specific T cell response in this background. Evaluating the cellular composition in the lung following $CD8^+$ T cell depletion or inhibition may provide important clues into which cells are most critical in disease development.

Persistent viral infection of the lung has been suggested to play a critical role in fibrotic disease in IFNγR-/- mice [107,108]. We find that M1 expression is not required to maintain high levels of viral persistence in the lung, suggesting that viral persistence alone is not a requirement for pulmonary fibrosis. As we failed to find a difference in viral persistence in the lung, we postulated that the difference in fibrosis might be related to the ability of the M1st virus to produce profibrotic mediator, TGFβ. However, we show that WT and M1st infected mice have similar levels of active and latent TGFβ in the lung at 28 days post infection, and *in vitro* infection of alveolar epithelial cells results in similar levels of active TGFβ. These data suggest that rather than being a viral intrinsic defect, M1st virus fails to induce the inflammatory environment that promotes fibrosis.

Because of M1's role in $V\beta4^+$ $CD8^+$ T cell expansion during MHV68 infection, we hypothesized that this cellular population might directly contribute to fibrosis. We

find no defect in number or function of $CD8^+$ T cell in the spleen of M1st infected C57Bl/6 mice. In Chapter III we show a significant difference in the $CD8^+$ T cell response in the lungs of M1st infected IFNγR-/- mice vs WT MHV68 infected IFNγR-/- mice, which included: (i) a lack of expansion and activation of $V\beta4^+$ $CD8^+$ T cells (ii) overall reduced levels of $CD8^+$ T cells, including MHV68 epitope specific T cells; (iii) reduced levels of cytokine producing $CD8^+$ T cells. Another noteworthy finding was the observation that IFNγR-/- Balb/c mice, which fail to develop a significant $V\beta4^+$ $CD8^+$ T cell expansion, were protected from fibrosis. Our interpretation of these findings suggests a role for $V\beta4^+$ $CD8^+$ T cell-mediated inflammation in cellular recruitment to the lung. In the M1st infection of mice on the C57Bl/6 background, lower levels of inflammation resulted in reduced cellular recruitment and therefore reduced immunopathology and subsequent fibrosis. To extend these findings we carried out global $CD8^+$ T cell depletion. Consistent with the observations of Dutia and colleagues, we observed a dramatic reduction in fibrosis following $CD8^+$ T cell depletion. Though this method failed to reduce $V\beta4^+$ $CD8^+$ T cell levels, we observed an ca. 50% reduction in overall $CD8^+$ T cell levels. An apparent resistance to depletion of $CD8^+$ T cells with an activated phenotype ($CD44^{hi}$ $CD62^{lo}$) was observed, perhaps explaining the incomplete depletion of $CD8^+$ T cells and failure to deplete $V\beta4^+$ $CD8^+$ T cells – which have previously been shown to have an effector memory phenotype [12]. Despite these shortcomings we were able to observe significant changes in pathology and mouse survival.

Collectively these data suggest a critical role for $CD8^+$ T cells in development of fibrotic disease in IFNγR-/- mice. Future studies will be necessary to understand the contributions of $CD8^+$ T cells in this model. Are the $CD8^+$ T cells directly inducing

immunopathology or do they stimulate other immune cell populations that are detrimental to the host? It will be interesting to evaluate how $CD8^+$ T cell depletion alters cellular trafficking in the lung, and what if any effect his may have on viral replication and persistence.

A critical aspect of these studies is our understanding of what role $CD8^+$ T cells play in pulmonary fibrosis. Certainly conflicting opinions on the role of T cells in IPF are present in the field. T cells are a well-documented finding in the lung of IPF patients, associated most strongly with areas of interstitial fibrosis [161-164]. Researchers have shown an association between T cell presence in the lung and disease progression. Some researchers have shown an association between $CD8^+$ T cells and a more deleterious disease course [165-167], while others have suggest elevated $CD4^+$ levels with an abnormal phenotype influence disease progression [168]. Feghali-Bostwick *et al.* show clonally expanded $CD4^+$ T cells with augmented effector function are able to mediate pathogenic response [168]. Notably, the T cells associated with fibrosis have been shown to have an activated or memory T cell phenotype [202,203]. $CD4^+$ T cell activation has been associated with poor clinical outcome [169]. The multi-center "correlating outcomes with biochemical markers to estimate time-progression in IPF (COMET)" study recently reported correlations between $CD25^+$ $CD4^+$ cells and $CXCR3^+$ T cells found in peripheral blood with disease progression [204]. Interestingly, down regulation of CD28 was observed in $CD8^+$ T cells and not $CD4^+$ T cells [204]. Conversely, other investigators have shown a positive association between T cell activation and disease progression. In a study to identify biomarkers to predict IPF outcome, Herazo-Maya and colleagues found that decreased expression of genes associated with T cell signaling and activation was

associated with a shorter transplant free survival time [170]. Further complicating the role of T cells in fibrosis, small animal models reveal disparate evidence (reviewed [171]). It has been suggested that T cells may play either profibrotic or antifibrotic roles depending on the inflammatory milieu in the host [171]. Here we show that $CD8^+$ T cells are critical mediators of fibrotic disease in IFNγR-/- mice. Future work to dissect the interactions and effects that these cells are having during acute infection and latency will provide insights into how they contribute to pathogenesis and immune dysfunction.

Concluding Remarks

The work in this thesis has provided insights into M1 function in immunocompetant and immunocompromised mice. Building on previous work which described a role for M1 in control of viral reactivation from peritoneal exudate cells through a $V\beta4^+$ $CD8^+$ T cell expansion, we evaluate M1 expression *in vivo* and characterize its transcriptional regulation. The major findings from the first section of this thesis show that (i) M1 is primarily expressed from plasma cells contributing to the existing model of M1 function (Fig. 1), (ii) viral Rta and host IRF4 regulate M1 transcription, and (iii) this transcriptional regulation which fine tunes viral gene expression in response to host environment, may be conserved among other viral genes. In the second section of this thesis, we evaluate the role of M1 and the $V\beta4^+$ $CD8^+$ T cell expansion in fibrotic disease of the lung. Using IFNγR-/- mice we show that (i) M1 dependent fibrosis is strongly correlated with lung inflammation, (ii) this inflammation results from a global influx of cells into the lung for which M1 is required; we further show that (iii) M1 is required for an efficient $CD8^+$ T cell response in the lung during

infection, and (iv) that depletion of $CD8^+$ T cells results in decreased inflammation and significant reduction in fibrosis and pathology.

FIGURES

Figure 1.

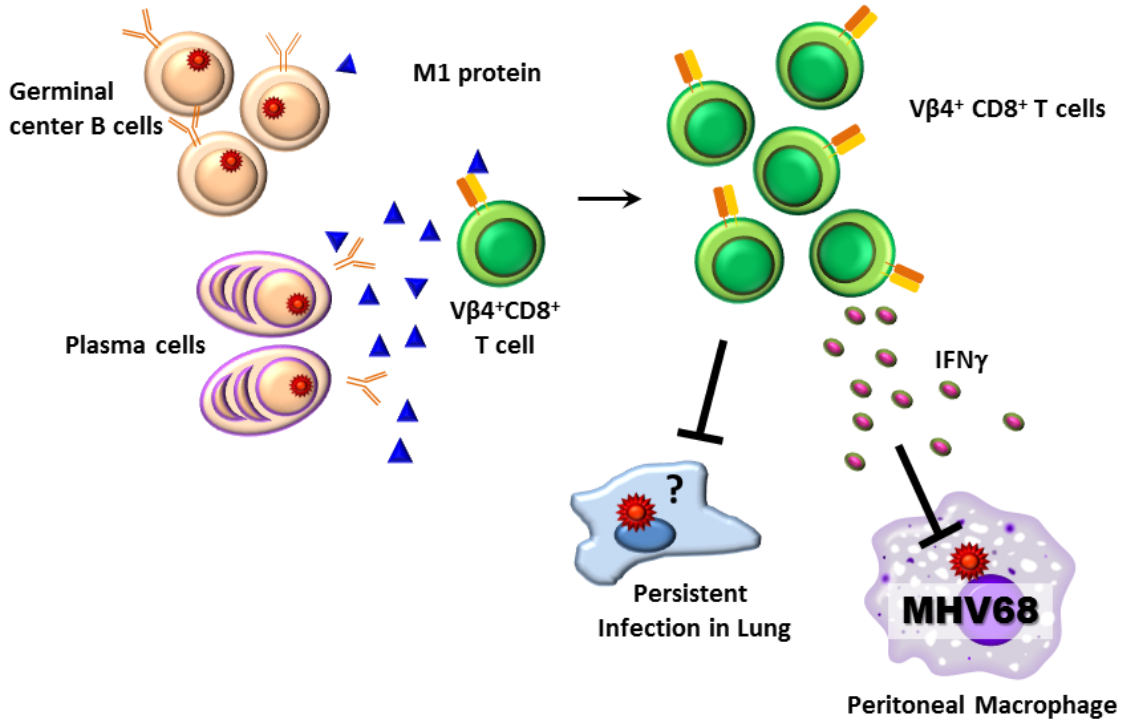

FIGURE LEGEND

Figure 1. Expression and function of M1 protein in MHV68 infection. During MHV68 infection, the stimulatory ligand for $V\beta4^+$ $CD8^+$ T cell activation is expressed from germinal center B cells and plasma cells in the spleen (Chapter II). We have shown that plasma cells are the predominant source for secreted M1 protein. Evans and colleagues identified this stimulatory ligand as MHV68 M1 [12]. During infection, M1 is expressed as a secreted protein capable of inducing $V\beta4^+$ $CD8^+$ T cell activation and expansion independent of antigen processing and presentation. This population of cells traffics to different sites in the mouse including peripheral blood, lung, spleen, and peritoneum. These activated T cells produce high levels of interferon gamma (IFNγ), as a result of M1 stimulation, which is capable of suppressing the MHV68 ORF50 (Rta) promoter in a Stat 6 dependent manner in the peritoneal macrophage population. Blocking the ORF50 promoter prevents Rta mediated transactivation, thus allowing the virus to maintain latency. Additionally, a novel role for $V\beta4^+$ $CD8^+$ T cells in control of viral persistence in the lung has recently been suggested [18] which awaits further investigation.

Figure modified from Evans et al. [12]

REFERENCES

1. Roizman B, Baines J (1991) The diversity and unity of Herpesviridae. Comp Immunol Microbiol Infect Dis 14: 63-79.
2. Albrecht T. ea (1996) Medical Microbiology 4th Edition: The University of Texas Medical Branch at Galveston.
3. Davison AJ, Eberle R, Ehlers B, Hayward GS, McGeoch DJ, et al. (2009) The order Herpesvirales. Arch Virol 154: 171-177.
4. McGeoch DJ, Gatherer D, Dolan A (2005) On phylogenetic relationships among major lineages of the Gammaherpesvirinae. J Gen Virol 86: 307-316.
5. Kutok JL, Wang F (2006) Spectrum of Epstein-Barr virus-associated diseases. Annu Rev Pathol 1: 375-404.
6. Martin JN (2007) The epidemiology of KSHV and its association with malignant disease. In: Arvin A, Campadelli-Fiume G, Mocarski E, Moore PS, Roizman B et al., editors. Human Herpesviruses: Biology, Therapy, and Immunoprophylaxis. Cambridge: Cambridge University Pres.
7. Blaskovic D, Stancekova M, Svobodova J, Mistrikova J (1980) Isolation of five strains of herpesviruses from two species of free living small rodents. Acta Virol 24: 468.
8. Collins CM, Boss JM, Speck SH (2009) Identification of infected B-cell populations by using a recombinant murine gammaherpesvirus 68 expressing a fluorescent protein. J Virol 83: 6484-6493.
9. Liang X, Collins CM, Mendel JB, Iwakoshi NN, Speck SH (2009) Gammaherpesvirus-driven plasma cell differentiation regulates virus reactivation from latently infected B lymphocytes. PLoS Pathog 5: e1000677.
10. Virgin HWt, Presti RM, Li XY, Liu C, Speck SH (1999) Three distinct regions of the murine gammaherpesvirus 68 genome are transcriptionally active in latently infected mice. J Virol 73: 2321-2332.
11. Clambey ET, Virgin HWt, Speck SH (2000) Disruption of the murine gammaherpesvirus 68 M1 open reading frame leads to enhanced reactivation from latency. J Virol 74: 1973-1984.
12. Evans AG, Moser JM, Krug LT, Pozharskaya V, Mora AL, et al. (2008) A gammaherpesvirus-secreted activator of Vbeta4+ CD8+ T cells regulates chronic infection and immunopathology. J Exp Med 205: 669-684.
13. Tripp RA, Hamilton-Easton AM, Cardin RD, Nguyen P, Behm FG, et al. (1997) Pathogenesis of an infectious mononucleosis-like disease induced by a murine gamma-herpesvirus: role for a viral superantigen? J Exp Med 185: 1641-1650.
14. Weck KE, Barkon ML, Yoo LI, Speck SH, Virgin HI (1996) Mature B cells are required for acute splenic infection, but not for establishment of latency, by murine gammaherpesvirus 68. J Virol 70: 6775-6780.
15. Steed A, Buch T, Waisman A, Virgin HWt (2007) Gamma interferon blocks gammaherpesvirus reactivation from latency in a cell type-specific manner. J Virol 81: 6134-6140.
16. Goodwin MM, Canny S, Steed A, Virgin HW (2010) Murine gammaherpesvirus 68 has evolved gamma interferon and stat1-repressible promoters for the lytic switch gene 50. J Virol 84: 3711-3717.
17. Steed AL, Barton ES, Tibbetts SA, Popkin DL, Lutzke ML, et al. (2006) Gamma interferon blocks gammaherpesvirus reactivation from latency. J Virol 80: 192-200.

18. Krug LT, Evans AG, Gargano LM, Paden CR, Speck SH (2013) The absence of M1 leads to increased establishment of murine gammaherpesvirus 68 latency in IgD-negative B cells. J Virol 87: 3597-3604.
19. Ahn JW, Powell KL, Kellam P, Alber DG (2002) Gammaherpesvirus lytic gene expression as characterized by DNA array. J Virol 76: 6244-6256.
20. Ebrahimi B, Dutia BM, Roberts KL, Garcia-Ramirez JJ, Dickinson P, et al. (2003) Transcriptome profile of murine gammaherpesvirus-68 lytic infection. J Gen Virol 84: 99-109.
21. Martinez-Guzman D, Rickabaugh T, Wu TT, Brown H, Cole S, et al. (2003) Transcription program of murine gammaherpesvirus 68. J Virol 77: 10488-10503.
22. Johnson LS, Willert EK, Virgin HW (2010) Redefining the genetics of murine gammaherpesvirus 68 via transcriptome-based annotation. Cell Host Microbe 7: 516-526.
23. Marques S, Efstathiou S, Smith KG, Haury M, Simas JP (2003) Selective gene expression of latent murine gammaherpesvirus 68 in B lymphocytes. J Virol 77: 7308-7318.
24. Simas JP, Swann D, Bowden R, Efstathiou S (1999) Analysis of murine gammaherpesvirus-68 transcription during lytic and latent infection. J Gen Virol 80 (Pt 1): 75-82.
25. Cordier-Bussat M, Billaud M, Calender A, Lenoir GM (1993) Epstein-Barr virus (EBV) nuclear-antigen-2-induced up-regulation of CD21 and CD23 molecules is dependent on a permissive cellular context. Int J Cancer 53: 153-160.
26. Kempkes B, Pawlita M, Zimber-Strobl U, Eissner G, Laux G, et al. (1995) Epstein-Barr virus nuclear antigen 2-estrogen receptor fusion proteins transactivate viral and cellular genes and interact with RBP-J kappa in a conditional fashion. Virology 214: 675-679.
27. Larcher C, Kempkes B, Kremmer E, Prodinger WM, Pawlita M, et al. (1995) Expression of Epstein-Barr virus nuclear antigen-2 (EBNA2) induces CD21/CR2 on B and T cell lines and shedding of soluble CD21. Eur J Immunol 25: 1713-1719.
28. Chang H, Gwack Y, Kingston D, Souvlis J, Liang X, et al. (2005) Activation of CD21 and CD23 gene expression by Kaposi's sarcoma-associated herpesvirus RTA. J Virol 79: 4651-4663.
29. Laichalk LL, Thorley-Lawson DA (2005) Terminal differentiation into plasma cells initiates the replicative cycle of Epstein-Barr virus in vivo. J Virol 79: 1296-1307.
30. Crawford DH, Ando I (1986) EB virus induction is associated with B-cell maturation. Immunology 59: 405-409.
31. Wilson SJ, Tsao EH, Webb BL, Ye H, Dalton-Griffin L, et al. (2007) X box binding protein XBP-1s transactivates the Kaposi's sarcoma-associated herpesvirus (KSHV) ORF50 promoter, linking plasma cell differentiation to KSHV reactivation from latency. J Virol 81: 13578-13586.
32. Bhende PM, Dickerson SJ, Sun X, Feng WH, Kenney SC (2007) X-box-binding protein 1 activates lytic Epstein-Barr virus gene expression in combination with protein kinase D. J Virol 81: 7363-7370.
33. Sun CC, Thorley-Lawson DA (2007) Plasma cell-specific transcription factor XBP-1s binds to and transactivates the Epstein-Barr virus BZLF1 promoter. J Virol 81: 13566-13577.
34. Yu F, Feng J, Harada JN, Chanda SK, Kenney SC, et al. (2007) B cell terminal differentiation factor XBP-1 induces reactivation of Kaposi's sarcoma-associated herpesvirus. FEBS Lett 581: 3485-3488.
35. Brooks JW, Hamilton-Easton AM, Christensen JP, Cardin RD, Hardy CL, et al. (1999) Requirement for CD40 ligand, CD4(+) T cells, and B cells in an infectious mononucleosis-like syndrome. J Virol 73: 9650-9654.

36. McClellan KB, Gangappa S, Speck SH, Virgin HWt (2006) Antibody-independent control of gamma-herpesvirus latency via B cell induction of anti-viral T cell responses. PLoS Pathog 2: e58.
37. Flano E, Woodland DL, Blackman MA (1999) Requirement for CD4+ T cells in V beta 4+CD8+ T cell activation associated with latent murine gammaherpesvirus infection. J Immunol 163: 3403-3408.
38. Sutkowski N, Chen G, Calderon G, Huber BT (2004) Epstein-Barr virus latent membrane protein LMP-2A is sufficient for transactivation of the human endogenous retrovirus HERV-K18 superantigen. J Virol 78: 7852-7860.
39. Sutkowski N, Conrad B, Thorley-Lawson DA, Huber BT (2001) Epstein-Barr virus transactivates the human endogenous retrovirus HERV-K18 that encodes a superantigen. Immunity 15: 579-589.
40. Sutkowski N, Palkama T, Ciurli C, Sekaly RP, Thorley-Lawson DA, et al. (1996) An Epstein-Barr virus-associated superantigen. J Exp Med 184: 971-980.
41. Knappe A, Hiller C, Thurau M, Wittmann S, Hofmann H, et al. (1997) The superantigen-homologous viral immediate-early gene ie14/vsag in herpesvirus saimiri-transformed human T cells. J Virol 71: 9124-9133.
42. Rosenbloom J, Castro SV, Jimenez SA (2010) Narrative review: fibrotic diseases: cellular and molecular mechanisms and novel therapies. Ann Intern Med 152: 159-166.
43. King C, Nathan SD (2013) Identification and treatment of comorbidities in idiopathic pulmonary fibrosis and other fibrotic lung diseases. Curr Opin Pulm Med 19: 466-473.
44. Raghu G, Collard HR, Egan JJ, Martinez FJ, Behr J, et al. (2011) An official ATS/ERS/JRS/ALAT statement: idiopathic pulmonary fibrosis: evidence-based guidelines for diagnosis and management. Am J Respir Crit Care Med 183: 788-824.
45. Collard HR, Moore BB, Flaherty KR, Brown KK, Kaner RJ, et al. (2007) Acute exacerbations of idiopathic pulmonary fibrosis. Am J Respir Crit Care Med 176: 636-643.
46. Meltzer EB, Noble PW (2008) Idiopathic pulmonary fibrosis. Orphanet J Rare Dis 3: 8.
47. King TE, Jr., Bradford WZ, Castro-Bernardini S, Fagan EA, Glaspole I, et al. (2014) A phase 3 trial of pirfenidone in patients with idiopathic pulmonary fibrosis. N Engl J Med 370: 2083-2092.
48. Richeldi L, du Bois RM, Raghu G, Azuma A, Brown KK, et al. (2014) Efficacy and safety of nintedanib in idiopathic pulmonary fibrosis. N Engl J Med 370: 2071-2082.
49. Wolters PJ, Collard HR, Jones KD (2014) Pathogenesis of idiopathic pulmonary fibrosis. Annu Rev Pathol 9: 157-179.
50. Selman M, King TE, Pardo A (2001) Idiopathic pulmonary fibrosis: prevailing and evolving hypotheses about its pathogenesis and implications for therapy. Ann Intern Med 134: 136-151.
51. Vannella KM, Moore BB (2008) Viruses as co-factors for the initiation or exacerbation of lung fibrosis. Fibrogenesis Tissue Repair 1: 2.
52. Bandyopadhyay S, Kolliputi N (2012) Viruses: Cofactors in Idiopathic Pulmonary Fibrosis. Virology & Mycology 1:e104.
53. Naik PK, Moore BB (2010) Viral infection and aging as cofactors for the development of pulmonary fibrosis. Expert Rev Respir Med 4: 759-771.
54. Ueda T, Ohta K, Suzuki N, Yamaguchi M, Hirai K, et al. (1992) Idiopathic pulmonary fibrosis and high prevalence of serum antibodies to hepatitis C virus. Am Rev Respir Dis 146: 266-268.
55. Meliconi R, Andreone P, Fasano L, Galli S, Pacilli A, et al. (1996) Incidence of hepatitis C virus infection in Italian patients with idiopathic pulmonary fibrosis. Thorax 51: 315-317.

56. Irving WL, Day S, Johnston ID (1993) Idiopathic pulmonary fibrosis and hepatitis C virus infection. Am Rev Respir Dis 148: 1683-1684.
57. Arase Y, Suzuki F, Suzuki Y, Akuta N, Kobayashi M, et al. (2008) Hepatitis C virus enhances incidence of idiopathic pulmonary fibrosis. World J Gastroenterol 14: 5880-5886.
58. Bando M, Ohno S, Oshikawa K, Takahashi M, Okamoto H, et al. (2001) Infection of TT virus in patients with idiopathic pulmonary fibrosis. Respir Med 95: 935-942.
59. Bando M, Takahashi M, Ohno S, Hosono T, Hironaka M, et al. (2008) Torque teno virus DNA titre elevated in idiopathic pulmonary fibrosis with primary lung cancer. Respirology 13: 263-269.
60. Wootton SC, Kim DS, Kondoh Y, Chen E, Lee JS, et al. (2011) Viral infection in acute exacerbation of idiopathic pulmonary fibrosis. Am J Respir Crit Care Med 183: 1698-1702.
61. Hayashi S, Hogg JC (2007) Adenovirus infections and lung disease. Curr Opin Pharmacol 7: 237-243.
62. Kuwano K, Nomoto Y, Kunitake R, Hagimoto N, Matsuba T, et al. (1997) Detection of adenovirus E1A DNA in pulmonary fibrosis using nested polymerase chain reaction. Eur Respir J 10: 1445-1449.
63. Yonemaru M, Kasuga I, Kusumoto H, Kunisawa A, Kiyokawa H, et al. (1997) Elevation of antibodies to cytomegalovirus and other herpes viruses in pulmonary fibrosis. Eur Respir J 10: 2040-2045.
64. Umeda Y, Morikawa M, Anzai M, Sumida Y, Kadowaki M, et al. (2010) Acute exacerbation of idiopathic pulmonary fibrosis after pandemic influenza A (H1N1) vaccination. Intern Med 49: 2333-2336.
65. Fujino N, Kubo H, Ota C, Suzuki T, Takahashi T, et al. (2013) Increased severity of 2009 pandemic influenza A virus subtype H1N1 infection in alveolar type II cells from patients with pulmonary fibrosis. J Infect Dis 207: 692-693.
66. Tang YW, Johnson JE, Browning PJ, Cruz-Gervis RA, Davis A, et al. (2003) Herpesvirus DNA is consistently detected in lungs of patients with idiopathic pulmonary fibrosis. J Clin Microbiol 41: 2633-2640.
67. Magro CM, Allen J, Pope-Harman A, Waldman WJ, Moh P, et al. (2003) The role of microvascular injury in the evolution of idiopathic pulmonary fibrosis. Am J Clin Pathol 119: 556-567.
68. Santos GC, Parra ER, Stegun FW, Cirqueira CS, Capelozzi VL (2013) Immunohistochemical detection of virus through its nuclear cytopathic effect in idiopathic interstitial pneumonia other than acute exacerbation. Braz J Med Biol Res 46: 985-992.
69. Dworniczak S, Ziora D, Kapral M, Mazurek U, Niepsuj G, et al. (2004) Human cytomegalovirus DNA level in patients with idiopathic pulmonary fibrosis. J Physiol Pharmacol 55 Suppl 3: 67-75.
70. Vergnon JM, Vincent M, de The G, Mornex JF, Weynants P, et al. (1984) Cryptogenic fibrosing alveolitis and Epstein-Barr virus: an association? Lancet 2: 768-771.
71. Stewart JP, Egan JJ, Ross AJ, Kelly BG, Lok SS, et al. (1999) The detection of Epstein-Barr virus DNA in lung tissue from patients with idiopathic pulmonary fibrosis. Am J Respir Crit Care Med 159: 1336-1341.
72. Kelly BG, Lok SS, Hasleton PS, Egan JJ, Stewart JP (2002) A rearranged form of Epstein-Barr virus DNA is associated with idiopathic pulmonary fibrosis. Am J Respir Crit Care Med 166: 510-513.

73. Manika K, Alexiou-Daniel S, Papakosta D, Papa A, Kontakiotis T, et al. (2007) Epstein-Barr virus DNA in bronchoalveolar lavage fluid from patients with idiopathic pulmonary fibrosis. Sarcoidosis Vasc Diffuse Lung Dis 24: 134-140.
74. Egan JJ, Stewart JP, Hasleton PS, Arrand JR, Carroll KB, et al. (1995) Epstein-Barr virus replication within pulmonary epithelial cells in cryptogenic fibrosing alveolitis. Thorax 50: 1234-1239.
75. Malizia AP, Keating DT, Smith SM, Walls D, Doran PP, et al. (2008) Alveolar epithelial cell injury with Epstein-Barr virus upregulates TGFbeta1 expression. Am J Physiol Lung Cell Mol Physiol 295: L451-460.
76. Sides MD, Klingsberg RC, Shan B, Gordon KA, Nguyen HT, et al. (2011) The Epstein-Barr virus latent membrane protein 1 and transforming growth factor--beta1 synergistically induce epithelial--mesenchymal transition in lung epithelial cells. Am J Respir Cell Mol Biol 44: 852-862.
77. Malizia AP, Egan JJ, Doran PP (2009) IL-4 increases CD21-dependent infection of pulmonary alveolar epithelial type II cells by EBV. Mol Immunol 46: 1905-1910.
78. Lawson WE, Crossno PF, Polosukhin VV, Roldan J, Cheng DS, et al. (2008) Endoplasmic reticulum stress in alveolar epithelial cells is prominent in IPF: association with altered surfactant protein processing and herpesvirus infection. Am J Physiol Lung Cell Mol Physiol 294: L1119-1126.
79. Wangoo A, Shaw RJ, Diss TC, Farrell PJ, du Bois RM, et al. (1997) Cryptogenic fibrosing alveolitis: lack of association with Epstein-Barr virus infection. Thorax 52: 888-891.
80. Zamo A, Poletti V, Reghellin D, Montagna L, Pedron S, et al. (2005) HHV-8 and EBV are not commonly found in idiopathic pulmonary fibrosis. Sarcoidosis Vasc Diffuse Lung Dis 22: 123-128.
81. Corcoran BM, Dukes-McEwan J, Rhind S, French A (1999) Idiopathic pulmonary fibrosis in a Staffordshire bull terrier with hypothyroidism. J Small Anim Pract 40: 185-188.
82. Corcoran BM, Cobb M, Martin MW, Dukes-McEwan J, French A, et al. (1999) Chronic pulmonary disease in West Highland white terriers. Vet Rec 144: 611-616.
83. Lobetti RG, Milner R, Lane E (2001) Chronic idiopathic pulmonary fibrosis in five dogs. J Am Anim Hosp Assoc 37: 119-127.
84. Webb JA, Armstrong J (2002) Chronic idiopathic pulmonary fibrosis in a West Highland white terrier. Can Vet J 43: 703-705.
85. Cohn LA, Norris CR, Hawkins EC, Dye JA, Johnson CA, et al. (2004) Identification and characterization of an idiopathic pulmonary fibrosis-like condition in cats. J Vet Intern Med 18: 632-641.
86. Williams K, Malarkey D, Cohn L, Patrick D, Dye J, et al. (2004) Identification of spontaneous feline idiopathic pulmonary fibrosis: morphology and ultrastructural evidence for a type II pneumocyte defect. Chest 125: 2278-2288.
87. Evola MG, Edmondson EF, Reichle JK, Biller DS, Mitchell CW, et al. (2014) Radiographic and histopathologic characteristics of pulmonary fibrosis in nine cats. Vet Radiol Ultrasound 55: 133-140.
88. Le Boedec K, Roady PJ, O'Brien RT (2014) A case of atypical diffuse feline fibrotic lung disease. J Feline Med Surg 16: 858-863.
89. Williams KJ (2014) Gammaherpesviruses and pulmonary fibrosis: evidence from humans, horses, and rodents. Vet Pathol 51: 372-384.
90. Williams KJ, Maes R, Del Piero F, Lim A, Wise A, et al. (2007) Equine multinodular pulmonary fibrosis: a newly recognized herpesvirus-associated fibrotic lung disease. Vet Pathol 44: 849-862.

91. Wong DM, Belgrave RL, Williams KJ, Del Piero F, Alcott CJ, et al. (2008) Multinodular pulmonary fibrosis in five horses. J Am Vet Med Assoc 232: 898-905.
92. Marenzoni ML, Passamonti F, Lepri E, Cercone M, Capomaccio S, et al. (2011) Quantification of Equid herpesvirus 5 DNA in clinical and necropsy specimens collected from a horse with equine multinodular pulmonary fibrosis. J Vet Diagn Invest 23: 802-806.
93. Back H, Kendall A, Grandon R, Ullman K, Treiberg-Berndtsson L, et al. (2012) Equine multinodular pulmonary fibrosis in association with asinine herpesvirus type 5 and equine herpesvirus type 5: a case report. Acta Vet Scand 54: 57.
94. Schwarz B, Klang A, Bezdekova B, Sardi S, Kutasi O, et al. (2013) Equine multinodular pulmonary fibrosis (EMPF): Five case reports. Acta Vet Hung 61: 319-332.
95. Spelta CW, Axon JE, Begg A, Diallo IS, Carrick JB, et al. (2013) Equine multinodular pulmonary fibrosis in three horses in Australia. Aust Vet J 91: 274-280.
96. Moore BB, Lawson WE, Oury TD, Sisson TH, Raghaendran K, et al. (2013) Animal Models of Fibrotic Lung Disease. American Journal of Respiratory Cell and Molecular Biology 49: 167-179.
97. Moore BB, Hogaboam CM (2008) Murine models of pulmonary fibrosis. Am J Physiol Lung Cell Mol Physiol 294: L152-160.
98. Meneghin A, Hogaboam CM (2007) Infectious disease, the innate immune response, and fibrosis. J Clin Invest 117: 530-538.
99. Dutia BM, Clarke CJ, Allen DJ, Nash AA (1997) Pathological changes in the spleens of gamma interferon receptor-deficient mice infected with murine gammaherpesvirus: a role for CD8 T cells. J Virol 71: 4278-4283.
100. Dal Canto AJ, Virgin HWt, Speck SH (2000) Ongoing viral replication is required for gammaherpesvirus 68-induced vascular damage. J Virol 74: 11304-11310.
101. Ebrahimi B, Dutia BM, Brownstein DG, Nash AA (2001) Murine gammaherpesvirus-68 infection causes multi-organ fibrosis and alters leukocyte trafficking in interferon-gamma receptor knockout mice. Am J Pathol 158: 2117-2125.
102. Gangadharan B, Hoeve MA, Allen JE, Ebrahimi B, Rhind SM, et al. (2008) Murine gammaherpesvirus-induced fibrosis is associated with the development of alternatively activated macrophages. J Leukoc Biol 84: 50-58.
103. Gangadharan B, Dutia BM, Rhind SM, Nash AA (2009) Murid herpesvirus-4 induces chronic inflammation of intrahepatic bile ducts in mice deficient in gamma-interferon signalling. Hepatol Res 39: 187-194.
104. Mora AL, Woods CR, Garcia A, Xu J, Rojas M, et al. (2005) Lung infection with gamma-herpesvirus induces progressive pulmonary fibrosis in Th2-biased mice. Am J Physiol Lung Cell Mol Physiol 289: L711-721.
105. Mora AL, Torres-Gonzalez E, Rojas M, Corredor C, Ritzenthaler J, et al. (2006) Activation of alveolar macrophages via the alternative pathway in herpesvirus-induced lung fibrosis. Am J Respir Cell Mol Biol 35: 466-473.
106. Mora AL, Torres-Gonzalez E, Rojas M, Xu J, Ritzenthaler J, et al. (2007) Control of virus reactivation arrests pulmonary herpesvirus-induced fibrosis in IFN-gamma receptor-deficient mice. Am J Respir Crit Care Med 175: 1139-1150.
107. Lee KS, Groshong SD, Cool CD, Kleinschmidt-DeMasters BK, van Dyk LF (2009) Murine gammaherpesvirus 68 infection of IFNgamma unresponsive mice: a small animal model for gammaherpesvirus-associated B-cell lymphoproliferative disease. Cancer Res 69: 5481-5489.

108. Krug LT, Torres-Gonzalez E, Qin Q, Sorescu D, Rojas M, et al. (2010) Inhibition of NF-kappaB signaling reduces virus load and gammaherpesvirus-induced pulmonary fibrosis. Am J Pathol 177: 608-621.
109. Coppola MA, Flano E, Nguyen P, Hardy CL, Cardin RD, et al. (1999) Apparent MHC-independent stimulation of CD8+ T cells in vivo during latent murine gammaherpesvirus infection. J Immunol 163: 1481-1489.
110. Wakeman BS, Johnson LS, Paden CR, Gray KS, Virgin HW, et al. (2014) Identification of Alternative Transcripts Encoding the Essential Murine Gammaherpesvirus Lytic Transactivator RTA. J Virol 88: 5474-5490.
111. Hardy CL, Flano E, Cardin RD, Kim IJ, Nguyen P, et al. (2001) Factors controlling levels of CD8+ T-cell lymphocytosis associated with murine gamma-herpesvirus infection. Viral Immunol 14: 391-402.
112. Tibbetts SA, van Dyk LF, Speck SH, Virgin HWt (2002) Immune control of the number and reactivation phenotype of cells latently infected with a gammaherpesvirus. J Virol 76: 7125-7132.
113. Flano E, Hardy CL, Kim IJ, Frankling C, Coppola MA, et al. (2004) T cell reactivity during infectious mononucleosis and persistent gammaherpesvirus infection in mice. J Immunol 172: 3078-3085.
114. Flano E, Kim IJ, Woodland DL, Blackman MA (2002) Gamma-herpesvirus latency is preferentially maintained in splenic germinal center and memory B cells. J Exp Med 196: 1363-1372.
115. Krug LT, Moser JM, Dickerson SM, Speck SH (2007) Inhibition of NF-kappaB activation in vivo impairs establishment of gammaherpesvirus latency. PLoS Pathog 3: e11.
116. Kwon H, Thierry-Mieg D, Thierry-Mieg J, Kim HP, Oh J, et al. (2009) Analysis of interleukin-21-induced Prdm1 gene regulation reveals functional cooperation of STAT3 and IRF4 transcription factors. Immunity 31: 941-952.
117. Simas JP, Bowden RJ, Paige V, Efstathiou S (1998) Four tRNA-like sequences and a serpin homologue encoded by murine gammaherpesvirus 68 are dispensable for lytic replication in vitro and latency in vivo. J Gen Virol 79 (Pt 1): 149-153.
118. Collins CM, Speck SH (2012) Tracking murine gammaherpesvirus 68 infection of germinal center B cells in vivo. PLoS One 7: e33230.
119. Collins CM, Speck SH (2014) Expansion of murine gammaherpesvirus latently infected B cells requires T follicular help. PLoS Pathog 10: e1004106.
120. Forrest JC, Speck SH (2008) Establishment of B-cell lines latently infected with reactivation-competent murine gammaherpesvirus 68 provides evidence for viral alteration of a DNA damage-signaling cascade. J Virol 82: 7688-7699.
121. Klein U, Casola S, Cattoretti G, Shen Q, Lia M, et al. (2006) Transcription factor IRF4 controls plasma cell differentiation and class-switch recombination. Nat Immunol 7: 773-782.
122. Ochiai K, Maienschein-Cline M, Simonetti G, Chen J, Rosenthal R, et al. (2013) Transcriptional regulation of germinal center B and plasma cell fates by dynamical control of IRF4. Immunity 38: 918-929.
123. Sciammas R, Shaffer AL, Schatz JH, Zhao H, Staudt LM, et al. (2006) Graded expression of interferon regulatory factor-4 coordinates isotype switching with plasma cell differentiation. Immunity 25: 225-236.
124. De Silva NS, Simonetti G, Heise N, Klein U (2012) The diverse roles of IRF4 in late germinal center B-cell differentiation. Immunol Rev 247: 73-92.

125. Driggers PH, Ennist DL, Gleason SL, Mak WH, Marks MS, et al. (1990) An interferon gamma-regulated protein that binds the interferon-inducible enhancer element of major histocompatibility complex class I genes. Proc Natl Acad Sci U S A 87: 3743-3747.
126. Liu S, Pavlova IV, Virgin HWt, Speck SH (2000) Characterization of gammaherpesvirus 68 gene 50 transcription. J Virol 74: 2029-2037.
127. Pavlova I, Lin CY, Speck SH (2005) Murine gammaherpesvirus 68 Rta-dependent activation of the gene 57 promoter. Virology 333: 169-179.
128. Palmeri D, Carroll KD, Gonzalez-Lopez O, Lukac DM (2011) Kaposi's sarcoma-associated herpesvirus Rta tetramers make high-affinity interactions with repetitive DNA elements in the Mta promoter to stimulate DNA binding of RBP-Jk/CSL. J Virol 85: 11901-11915.
129. Carroll KD, Khadim F, Spadavecchia S, Palmeri D, Lukac DM (2007) Direct interactions of Kaposi's sarcoma-associated herpesvirus/human herpesvirus 8 ORF50/Rta protein with the cellular protein octamer-1 and DNA are critical for specifying transactivation of a delayed-early promoter and stimulating viral reactivation. J Virol 81: 8451-8467.
130. Xi X, Persson LM, O'Brien MW, Mohr I, Wilson AC (2012) Cooperation between viral interferon regulatory factor 4 and RTA to activate a subset of Kaposi's sarcoma-associated herpesvirus lytic promoters. J Virol 86: 1021-1033.
131. Guito J, Lukac DM (2012) KSHV Rta Promoter Specification and Viral Reactivation. Front Microbiol 3: 30.
132. Braaten DC, McClellan JS, Messaoudi I, Tibbetts SA, McClellan KB, et al. (2006) Effective control of chronic gamma-herpesvirus infection by unconventional MHC Class Ia-independent CD8 T cells. PLoS Pathog 2: e37.
133. Rangaswamy US, Speck SH (2014) Murine Gammaherpesvirus M2 Protein Induction of IRF4 via the NFAT Pathway Leads to IL-10 Expression in B Cells. PLoS Pathog 10: e1003858.
134. Jacoby MA, Virgin HWt, Speck SH (2002) Disruption of the M2 gene of murine gammaherpesvirus 68 alters splenic latency following intranasal, but not intraperitoneal, inoculation. J Virol 76: 1790-1801.
135. Herskowitz JH, Jacoby MA, Speck SH (2005) The murine gammaherpesvirus 68 M2 gene is required for efficient reactivation from latently infected B cells. J Virol 79: 2261-2273.
136. Siegel AM, Herskowitz JH, Speck SH (2008) The MHV68 M2 protein drives IL-10 dependent B cell proliferation and differentiation. PLoS Pathog 4: e1000039.
137. Verma SC, Robertson ES (2003) Molecular biology and pathogenesis of Kaposi sarcoma-associated herpesvirus. FEMS Microbiol Lett 222: 155-163.
138. de Oliveira VL, Almeida SC, Soares HR, Parkhouse RM (2013) Selective B-cell expression of the MHV-68 latency-associated M2 protein regulates T-dependent antibody response and inhibits apoptosis upon viral infection. J Gen Virol 94: 1613-1623.
139. Wynn TA (2004) Fibrotic disease and the T(H)1/T(H)2 paradigm. Nat Rev Immunol 4: 583-594.
140. Molyneaux PL, Maher TM (2013) The role of infection in the pathogenesis of idiopathic pulmonary fibrosis. Eur Respir Rev 22: 376-381.
141. Kropski JA, Lawson WE, Young LR, Blackwell TS (2013) Genetic studies provide clues on the pathogenesis of idiopathic pulmonary fibrosis. Dis Model Mech 6: 9-17.
142. Pozharskaya V, Torres-Gonzalez E, Rojas M, Gal A, Amin M, et al. (2009) Twist: a regulator of epithelial-mesenchymal transition in lung fibrosis. PLoS One 4: e7559.
143. Paden CR, Forrest JC, Moorman NJ, Speck SH (2010) Murine gammaherpesvirus 68 LANA is essential for virus reactivation from splenocytes but not long-term carriage of viral genome. J Virol 84: 7214-7224.

144. Moore BB, Paine R, 3rd, Christensen PJ, Moore TA, Sitterding S, et al. (2001) Protection from pulmonary fibrosis in the absence of CCR2 signaling. J Immunol 167: 4368-4377.
145. Misharin AV, Morales-Nebreda L, Mutlu GM, Budinger GR, Perlman H (2013) Flow cytometric analysis of macrophages and dendritic cell subsets in the mouse lung. Am J Respir Cell Mol Biol 49: 503-510.
146. Pohlers D, Brenmoehl J, Loffler I, Muller CK, Leipner C, et al. (2009) TGF-beta and fibrosis in different organs - molecular pathway imprints. Biochim Biophys Acta 1792: 746-756.
147. Stoolman JS, Vannella KM, Coomes SM, Wilke CA, Sisson TH, et al. (2011) Latent infection by gammaherpesvirus stimulates profibrotic mediator release from multiple cell types. Am J Physiol Lung Cell Mol Physiol 300: L274-285.
148. Vannella KM, Luckhardt TR, Wilke CA, van Dyk LF, Toews GB, et al. (2010) Latent herpesvirus infection augments experimental pulmonary fibrosis. Am J Respir Crit Care Med 181: 465-477.
149. Abe M, Harpel JG, Metz CN, Nunes I, Loskutoff DJ, et al. (1994) An assay for transforming growth factor-beta using cells transfected with a plasminogen activator inhibitor-1 promoter-luciferase construct. Anal Biochem 216: 276-284.
150. Stevenson PG, Belz GT, Castrucci MR, Altman JD, Doherty PC (1999) A gamma-herpesvirus sneaks through a CD8(+) T cell response primed to a lytic-phase epitope. Proc Natl Acad Sci U S A 96: 9281-9286.
151. Liu L, Usherwood EJ, Blackman MA, Woodland DL (1999) T-cell vaccination alters the course of murine herpesvirus 68 infection and the establishment of viral latency in mice. J Virol 73: 9849-9857.
152. Freeman ML, Burkum CE, Jensen MK, Woodland DL, Blackman MA (2012) gamma-Herpesvirus reactivation differentially stimulates epitope-specific CD8 T cell responses. J Immunol 188: 3812-3819.
153. Gredmark-Russ S, Cheung EJ, Isaacson MK, Ploegh HL, Grotenbreg GM (2008) The CD8 T-cell response against murine gammaherpesvirus 68 is directed toward a broad repertoire of epitopes from both early and late antigens. J Virol 82: 12205-12212.
154. Freeman ML, Lanzer KG, Cookenham T, Peters B, Sidney J, et al. (2010) Two kinetic patterns of epitope-specific CD8 T-cell responses following murine gammaherpesvirus 68 infection. J Virol 84: 2881-2892.
155. Kropski JA, Lawson WE, Blackwell TS (2012) Right place, right time: the evolving role of herpesvirus infection as a "second hit" in idiopathic pulmonary fibrosis. Am J Physiol Lung Cell Mol Physiol 302: L441-444.
156. Pozharskaya VP., Amin MM., Dollard S, Roman J, Perez R, et al. (2011) Prospective Longitudinal Evaluation Of EBV Load In Idiopathic Pulmonary Fibrosis: American Thoracic Society. A3807 p.
157. Bringardner BD, Baran CP, Eubank TD, Marsh CB (2008) The role of inflammation in the pathogenesis of idiopathic pulmonary fibrosis. Antioxid Redox Signal 10: 287-301.
158. Flaherty KR, Toews GB, Lynch JP, 3rd, Kazerooni EA, Gross BH, et al. (2001) Steroids in idiopathic pulmonary fibrosis: a prospective assessment of adverse reactions, response to therapy, and survival. Am J Med 110: 278-282.
159. Nagai S, Kitaichi M, Hamada K, Nagao T, Hoshino Y, et al. (1999) Hospital-based historical cohort study of 234 histologically proven Japanese patients with IPF. Sarcoidosis Vasc Diffuse Lung Dis 16: 209-214.
160. Raghu G, Anstrom KJ, King TE, Jr., Lasky JA, Martinez FJ (2012) Prednisone, azathioprine, and N-acetylcysteine for pulmonary fibrosis. N Engl J Med 366: 1968-1977.

161. Kradin RL, Divertie MB, Colvin RB, Ramirez J, Ryu J, et al. (1986) Usual interstitial pneumonitis is a T-cell alveolitis. Clin Immunol Immunopathol 40: 224-235.
162. Papiris SA, Kollintza A, Kitsanta P, Kapotsis G, Karatza M, et al. (2005) Relationship of BAL and lung tissue CD4+ and CD8+ T lymphocytes, and their ratio in idiopathic pulmonary fibrosis. Chest 128: 2971-2977.
163. Parra ER, Kairalla RA, Ribeiro de Carvalho CR, Eher E, Capelozzi VL (2007) Inflammatory cell phenotyping of the pulmonary interstitium in idiopathic interstitial pneumonia. Respiration 74: 159-169.
164. Nuovo GJ, Hagood JS, Magro CM, Chin N, Kapil R, et al. (2012) The distribution of immunomodulatory cells in the lungs of patients with idiopathic pulmonary fibrosis. Mod Pathol 25: 416-433.
165. Fireman E, Vardinon N, Burke M, Spizer S, Levin S, et al. (1998) Predictive value of response to treatment of T-lymphocyte subpopulations in idiopathic pulmonary fibrosis. Eur Respir J 11: 706-711.
166. Daniil Z, Kitsanta P, Kapotsis G, Mathioudaki M, Kollintza A, et al. (2005) CD8+ T lymphocytes in lung tissue from patients with idiopathic pulmonary fibrosis. Respir Res 6: 81.
167. Papiris SA, Kollintza A, Karatza M, Manali ED, Sotiropoulou C, et al. (2007) CD8+ T lymphocytes in bronchoalveolar lavage in idiopathic pulmonary fibrosis. J Inflamm (Lond) 4: 14.
168. Feghali-Bostwick CA, Tsai CG, Valentine VG, Kantrow S, Stoner MW, et al. (2007) Cellular and humoral autoreactivity in idiopathic pulmonary fibrosis. J Immunol 179: 2592-2599.
169. Gilani SR, Vuga LJ, Lindell KO, Gibson KF, Xue J, et al. (2010) CD28 down-regulation on circulating CD4 T-cells is associated with poor prognoses of patients with idiopathic pulmonary fibrosis. PLoS One 5: e8959.
170. Herazo-Maya JD, Noth I, Duncan SR, Kim S, Ma SF, et al. (2013) Peripheral blood mononuclear cell gene expression profiles predict poor outcome in idiopathic pulmonary fibrosis. Sci Transl Med 5: 205ra136.
171. Luzina IG, Todd NW, Iacono AT, Atamas SP (2008) Roles of T lymphocytes in pulmonary fibrosis. J Leukoc Biol 83: 237-244.
172. Helene M, Lake-Bullock V, Zhu J, Hao H, Cohen DA, et al. (1999) T cell independence of bleomycin-induced pulmonary fibrosis. J Leukoc Biol 65: 187-195.
173. Christensen PJ, Goodman RE, Pastoriza L, Moore B, Toews GB (1999) Induction of lung fibrosis in the mouse by intratracheal instillation of fluorescein isothiocyanate is not T-cell-dependent. Am J Pathol 155: 1773-1779.
174. Corsini E, Luster MI, Mahler J, Craig WA, Blazka ME, et al. (1994) A protective role for T lymphocytes in asbestos-induced pulmonary inflammation and collagen deposition. Am J Respir Cell Mol Biol 11: 531-539.
175. Okazaki T, Nakao A, Nakano H, Takahashi F, Takahashi K, et al. (2001) Impairment of bleomycin-induced lung fibrosis in CD28-deficient mice. J Immunol 167: 1977-1981.
176. Luzina IG, Papadimitriou JC, Anderson R, Pochetuhen K, Atamas SP (2006) Induction of prolonged infiltration of T lymphocytes and transient T lymphocyte-dependent collagen deposition in mouse lungs following adenoviral gene transfer of CCL18. Arthritis Rheum 54: 2643-2655.
177. Hunninghake GW, Gadek JE, Lawley TJ, Crystal RG (1981) Mechanisms of neutrophil accumulation in the lungs of patients with idiopathic pulmonary fibrosis. J Clin Invest 68: 259-269.

178. Obayashi Y, Yamadori I, Fujita J, Yoshinouchi T, Ueda N, et al. (1997) The role of neutrophils in the pathogenesis of idiopathic pulmonary fibrosis. Chest 112: 1338-1343.
179. Yamanouchi H, Fujita J, Hojo S, Yoshinouchi T, Kamei T, et al. (1998) Neutrophil elastase: alpha-1-proteinase inhibitor complex in serum and bronchoalveolar lavage fluid in patients with pulmonary fibrosis. Eur Respir J 11: 120-125.
180. Song JS, Kang CM, Rhee CK, Yoon HK, Kim YK, et al. (2009) Effects of elastase inhibitor on the epithelial cell apoptosis in bleomycin-induced pulmonary fibrosis. Exp Lung Res 35: 817-829.
181. Takemasa A, Ishii Y, Fukuda T (2012) A neutrophil elastase inhibitor prevents bleomycin-induced pulmonary fibrosis in mice. Eur Respir J 40: 1475-1482.
182. Besnard AG, Struyf S, Guabiraba R, Fauconnier L, Rouxel N, et al. (2013) CXCL6 antibody neutralization prevents lung inflammation and fibrosis in mice in the bleomycin model. J Leukoc Biol 94: 1317-1323.
183. Gregory AD, Kliment CR, Metz HE, Kim KH, Kargl J, et al. (2015) Neutrophil elastase promotes myofibroblast differentiation in lung fibrosis. J Leukoc Biol.
184. Mantovani A, Cassatella MA, Costantini C, Jaillon S (2011) Neutrophils in the activation and regulation of innate and adaptive immunity. Nat Rev Immunol 11: 519-531.
185. Egan JJ, Adamali HI, Lok SS, Stewart JP, Woodcock AA (2011) Ganciclovir antiviral therapy in advanced idiopathic pulmonary fibrosis: an open pilot study. Pulm Med 2011: 240805.
186. Wang S, Liu S, Wu MH, Geng Y, Wood C (2001) Identification of a cellular protein that interacts and synergizes with the RTA (ORF50) protein of Kaposi's sarcoma-associated herpesvirus in transcriptional activation. J Virol 75: 11961-11973.
187. Liu Y, Cao Y, Liang D, Gao Y, Xia T, et al. (2008) Kaposi's sarcoma-associated herpesvirus RTA activates the processivity factor ORF59 through interaction with RBP-Jkappa and a cis-acting RTA responsive element. Virology 380: 264-275.
188. Rossetto C, Yamboliev I, Pari GS (2009) Kaposi's sarcoma-associated herpesvirus/human herpesvirus 8 K-bZIP modulates latency-associated nuclear protein-mediated suppression of lytic origin-dependent DNA synthesis. J Virol 83: 8492-8501.
189. AuCoin DP, Colletti KS, Cei SA, Papouskova I, Tarrant M, et al. (2004) Amplification of the Kaposi's sarcoma-associated herpesvirus/human herpesvirus 8 lytic origin of DNA replication is dependent upon a cis-acting AT-rich region and an ORF50 response element and the trans-acting factors ORF50 (K-Rta) and K8 (K-bZIP). Virology 318: 542-555.
190. Rossetto CC, Susilarini NK, Pari GS (2011) Interaction of Kaposi's sarcoma-associated herpesvirus ORF59 with oriLyt is dependent on binding with K-Rta. J Virol 85: 3833-3841.
191. Quinlivan EB, Holley-Guthrie EA, Norris M, Gutsch D, Bachenheimer SL, et al. (1993) Direct BRLF1 binding is required for cooperative BZLF1/BRLF1 activation of the Epstein-Barr virus early promoter, BMRF1. Nucleic Acids Res 21: 1999-2007.
192. Chang LK, Liu ST, Kuo CW, Wang WH, Chuang JY, et al. (2008) Enhancement of transactivation activity of Rta of Epstein-Barr virus by RanBPM. J Mol Biol 379: 231-242.
193. Zacny VL, Wilson J, Pagano JS (1998) The Epstein-Barr virus immediate-early gene product, BRLF1, interacts with the retinoblastoma protein during the viral lytic cycle. J Virol 72: 8043-8051.
194. Swenson JJ, Holley-Guthrie E, Kenney SC (2001) Epstein-Barr virus immediate-early protein BRLF1 interacts with CBP, promoting enhanced BRLF1 transactivation. J Virol 75: 6228-6234.

195. Chang LK, Chuang JY, Nakao M, Liu ST (2010) MCAF1 and synergistic activation of the transcription of Epstein-Barr virus lytic genes by Rta and Zta. Nucleic Acids Res 38: 4687-4700.
196. Robinson AR, Kwek SS, Hagemeier SR, Wille CK, Kenney SC (2011) Cellular transcription factor Oct-1 interacts with the Epstein-Barr virus BRLF1 protein to promote disruption of viral latency. J Virol 85: 8940-8953.
197. Hall KT, Stevenson AJ, Goodwin DJ, Gibson PC, Markham AF, et al. (1999) The activation domain of herpesvirus saimiri R protein interacts with the TATA-binding protein. J Virol 73: 9756-9763.
198. Xuan Y, Gong D, Qi J, Han C, Deng H, et al. (2013) ZAP inhibits murine gammaherpesvirus 68 ORF64 expression and is antagonized by RTA. J Virol 87: 2735-2743.
199. Hong Y, Qi J, Gong D, Han C, Deng H (2011) Replication and transcription activator (RTA) of murine gammaherpesvirus 68 binds to an RTA-responsive element and activates the expression of ORF18. J Virol 85: 11338-11350.
200. Wedzicha JA (2004) Role of viruses in exacerbations of chronic obstructive pulmonary disease. Proc Am Thorac Soc 1: 115-120.
201. Pelletier M, Micheletti A, Cassatella MA (2010) Modulation of human neutrophil survival and antigen expression by activated CD4+ and CD8+ T cells. J Leukoc Biol 88: 1163-1170.
202. Wells AU, Lorimer S, Majumdar S, Harrison NK, Corrin B, et al. (1995) Fibrosing alveolitis in systemic sclerosis: increase in memory T-cells in lung interstitium. Eur Respir J 8: 266-271.
203. Marchal-Somme J, Uzunhan Y, Marchand-Adam S, Valeyre D, Soumelis V, et al. (2006) Cutting edge: nonproliferating mature immune cells form a novel type of organized lymphoid structure in idiopathic pulmonary fibrosis. J Immunol 176: 5735-5739.
204. Moore BB, Fry C, Zhou Y, Murray S, Han MK, et al. (2014) Inflammatory leukocyte phenotypes correlate with disease progression in idiopathic pulmonary fibrosis. Front Med 1.